NOVA IMS Information Management School

MGI

Mestrado em Gestão de Informação
Master Program in Information Management

Evolution of Cooperation in Multilayer Networks

Paulo Barreto Valeriano de Albuquerque Sardinha

Dissertation presented as partial requirement for obtaining the Master's degree in Information Management

NOVA Information Management School
Instituto Superior de Estatística e Gestão de Informação
Universidade Nova de Lisboa

Management School

Instituto Superior de Estatística e Gestão de Informação
Universidade Nova de Lisboa

EVOLUTION OF COOPERATION IN MULTILAYER SOCIAL NETWORKS

by

Paulo Barreto Valeriano de Albuquerque Sardinha

Dissertation presented as partial requirement for obtaining the Master's degree in Information Management, with a specialization in Information Systems and Technologies Management

Advisor: prof. Doutor Flávio L. Pinheiro (NOVA IMS)
Co Advisor: prof. Doutor Francisco C. Santos (INESC-ID/Instituto Superior Técnico)

July 2020

To my parents, Eulália and Francisco,
with love and gratitude

ACKNOWLEDGEMENTS

I would like to thank my supervisor, Dr Flávio Pinheiro, for his optimism, for the opportunity created and for providing me guidance and feedback throughout this project. Without his support I would not have been able to complete this research.

I would also like to thank my co-supervisor Dr Francisco Santos for his insightful comments on this research.

The papers I had the chance to read from them were inspiring and decisive in my decision to undertake this research.

I would also like to thank Margarida for her constant encouragement, interest and help in the subjects I studied during the master's curricular component leading to this thesis.

Last but not least I want to thank my family and friends for their incentive and for putting up with the time I invested in this master program depriving me of social gatherings.

ABSTRACT

Individuals take part in multiple layers of networks of interactions simultaneously. These interdependent networks account for the different sort of social ties individuals maintain per layer. In each layer individuals participate in N-Player Public Goods Games where benefits collected increase with amounts invested. It is, however, tempting to be a free-rider, i.e., to take advantage of the common pool without contributing to it, a situation from which a social dilemma results. This thesis offers new insights on how cooperation dynamics is shaped by multiple layers of social interactions and diversity of contributions invested per game. To this end, we resort to Evolutionary Game Theory and Network Science to provide a convenient framework to address the most important prototypical social conflicts and/or dilemmas in large networked populations. In particular, we propose a novel mean-field approach capable of tracking the self-organization of Cooperators when co-evolving with Defectors in a multilayer environment. We show that the emerging collective dynamics, which depends (i) on the underlying layer networks of interactions and (ii) on the criteria to share a finite investment across all games, often does not bear any resemblance with the local processes supporting them. Our findings suggest that, whenever individual investments are distributed among games or layers, resilience of cooperation against free-riders increases with the number of layers, and that cooperation emerges from a non-trivial organization of cooperation across the layers. In opposition, under constant, non-distributed investments, the level of cooperation shows little sensibility to variations in the number of layers. These findings put in evidence the importance of asymmetric contributions across games and social contexts in the emergence of human cooperation.

KEYWORDS

Evolutionary Game Theory, Networks, Evolution, Cooperation, Public Goods Games, Multilayer, Average Gradient of Selection

INDEX

LIST OF FIGURES

LIST OF TABLES

LIST OF ABBREVIATIONS AND ACRONYMS

AGoS	Average Gradient of Selection
ALLC	Always Cooperate
ALLD	Always Defect
BA	Barabási and Albert
CPU	Central Processing Unit
DPD	Distributed Prisoner's Dilemma
EGT	Evolutionary Game Theory
ESS	Evolutionary Stable Strategy
EXP	Exponential Networks
HeSW	Heterogeneous Small-World
HoSW	Homogeneous Small-World
NE	Nash Equilibrium
PD	Prisoner's Dilemma
PGG	Public Goods Games
SF	Scale-free network
SG	Snowdrift Game
SH	Stag-Hunt
SIR	Susceptible-Infected-Recovered
TFT	Tit-for-Tat
VM	Voter's Model

1. INTRODUCTION

> *Every individual... neither intends to promote the public interest, nor knows how much he is promoting it... he intends only his own security; and by directing that industry in such a manner as its produce may be of the greatest value, he intends only his own gain, and he is in this, as in many other cases, led by an invisible hand to promote an end which was no part of his intention.*
>
> − Adam Smith, The Wealth of Nations

The problem of cooperation revolves around the study of scenarios in which there is a clash between individual and collective interests. Consider the following prototype scenario from Game Theory (GT): two individuals need to make, independent and simultaneously, a decision on either to pay a cost c and offer a benefit b to their peers or not. Four possible outcomes ensue: if both pay the cost then both ripen the benefit and attain a payoff of $b - c$ each; if neither pays the cost then the payoff will be 0 for each; when one pays the cost but the other refuses then the former attains a payoff of $-c$ while the latter obtains b. Whenever $b > c$ individuals are said to be playing the Prisoner's Dilemma. In that context, the best course of action for a rational individual looking to optimize his/her rewards is to not pay the cost. However, such action from both players clashes with the best common outcome, in that if both pay the cost then the total aggregated payoff is of $2(b - c)$. In such scenarios, individuals are said to face a social dilemma of cooperation, in that the best outcome of the collective clashes with action that they would choose when looking to optimize their rewards.

Game Theory provides an exceptional framework to reason over individuals' strategic decision making when facing abstract scenarios. In the case of the Prisoner's Dilemma (PD), individuals have to decide between Cooperating (C) or Defecting (D), that is, between paying or not the cost associated with pro-social behaviour. The payoff structure of the scenario described in the above paragraph can be summarized in the so called Payoff Matrix (see table 1), where rows and columns identify strategies (actions) and Π_{ij} represents the outcome for the row player following strategy i against column player who chooses strategy j.

Table 1 – Payoff Matrix of Donation Game ($b > c > 0$)

Π	C	D
C	b-c	-c
D	b	0

Since a player does not know beforehand the action of the other, it can only assume that the other payer will do the best for himself. It is common to extend the payoff matrix into a more general parameterization, such as the one represented in table 2, which allows covering all possible two-person and two-strategy games. In such matrix the payoffs of each outcome are associated with parameters R, T, S, and P that stem from the following rationale: when both players decide to cooperate, each receives a reward R for mutual cooperation; Mutual defection results in a punishment P of both players; when they choose different strategies, the one offering cooperation receives the Sucker's Payoff S, whereas the Defector obtains the Temptation payoff, T, for taking the opportunity value of exploiting a Cooperator. Different scenarios, or dilemmas, result from different orderings of these payoffs, leading to different expected rational decisions.

Table 2 – Payoff Matrix of a 2-Player, 2-Strategy Game

Π	C	D
C	R	S
D	T	P

More generally, a game represents a social dilemma whenever the payoff for mutual cooperation is larger than the payoff for mutual defection ($R > P$) and still there is an incentive to defect. Such incentive is present when $T > R$, because defection is preferable when playing against a Cooperator; when $P > S$, because defection is the best strategy in an encounter with a Defector, and when $T > S$, as a Defector is better in an interaction with a Cooperator (Nowak M. , 2012).

Game Theory thus provides the mathematical framework to create the perfect abstract formulation of complex decision making scenarios, allowing for the exploration of the resulting outcomes when conflicting interests are at stake. The formal representation of a game specifies (i) a set of individuals that have to make a strategic decision; (ii) the available strategies; and (iii) the payoff structure of the possible outcomes individuals face through combination of actions available to the players. The mathematics of GT provides a unified framework of abstract models and metaphors, together with a consistent methodology, in which these problems can be recast and analysed (Szabo & Fath, 2007).

The framework discussed so far concerns one shot interaction situations, that is, individuals do not have memory of past interactions nor do they have information about their opponent until their strategy/action is revealed. However, these scenarios arguably fall short on capturing the full complexity of real world decision making scenarios. In that sense, Game

Theory literature has explored and extended scenarios as the above case in time (considering the repeated interaction between individuals); in strategy space (more complex scenarios involving more than two strategies), and in participants dimensions (when decisions have to be made in interactions that involve more than two individuals).

In particular, situations that involve N individuals have been particularly researched in the context of Public Goods Games. In such scenarios, individuals are given the chance to invest towards a common pool concerning a collective endeavour. The amount collected from all individuals' contributions is then multiplied by an enhancement factor, a proportionality constant reflecting how much bigger is the whole due to the synergies created compared to the sum of the parts. The final amount in the pool is then equally distributed among all individuals. It is up to each player to decide whether to contribute to the common pool. Being the yield from the game equally distributed among all participants irrespective of their investment decision, another social dilemma ensues: free-riding strategy, that is defecting, becomes the most rational decision for each individual although the best collective outcome is achieved when all participants cooperate. Interestingly, when we consider a Public Goods Game involving only two participants we obtain the same payoff structure of the Prisoner Dilemma. Indeed, the Public Goods Games is in many ways the group decision-making extension of the two player Prisoner's Dilemma. In this simplified description, the optional contributions to the pool were binary, zero or a positive fixed amount. With no impact on the social dilemma inherent to the game, this constraint will soon be dropped and variable non-negative values for individual contributions will be accepted.

Interactions can be unstructured or structured by a network. In the former alternative, a player can potentially encounter any other player, as if all players were connected together. In the structured alternative, modelling real life scenarios, an underlying network has to be considered with players located at its nodes. The notion of neighbourhood emerges. Networks can be of various sorts, regular with patterns as a lattice or a ring, irregular, etc. and their links dictate who plays against whom. Exemplifying for a social network, individuals may be positioned as nodes of a single-layer representing his/her family relationships. However, along his/her day an individual has other arenas of intervention, as he/she is also present on many other networks, professional, friendship, etc. A single layer network turns out to be insufficient to reflect all interactions an individual participates in along its day. Therefore, other networks in space have to be considered and now one has a network of networks or a multilayer. From the moment a structure governing interactions steps in, collective dynamics emerge which are difficult to anticipate from the games played at individual layers.

In order to allow populations to evolve along time and to identify under which particular circumstances what strategies reveal better than others, operating mechanisms of natural selection in Evolutionary Games Theory must be introduced to allow individuals to updates their strategies. These mechanisms can rely, e.g., on a Moran birth-death process or on a pairwise comparison of payoffs collected between neighbours (Traulsen & Hauert, 2008). Networks introduce an additional challenge on the definition of an individual payoff, because now it results from interactions with each of his/her multiple neighbours.

In this thesis, we explore the scenario in which individuals' resources are finite when individuals participate in multiple social networks. Hence, we evaluate how different resource investment criteria impact the evolution of cooperation. Each criterion will govern how each player will distribute a limited investment among all games he/she participates in. For the social network example just described, the finite resource to be shared across games, i.e., interactions, may correspond to time.

Along this quest to understand cooperation dynamics in multilayer networks, we pose 4 main questions:

1. What's the impact of different resource investment criteria in the evolution of cooperation in populations interacting through a multilayer network?
2. How do multilayer global dynamics relate with microscopic dynamics locally defined at individual level? E.g., will there be fractal-like cooperation patterns of "self-similarity" at different scales?
3. Cooperation level is expected to vary with simulation parameters such as the number of layers, underlying network types and others to be defined. How sensitive will the overall multilayer behaviour to simulation parameters be?
4. Are there conditions more relevant than others in dictating the cooperative performance of the multilayer? Particularly, is there any subset of parameters such that they can define a configuration subdomain in parameter space determining the evolution of the system irrespective of the values other parameters may assume?

1.1. THESIS STRUCTURE

In Chapter 2, a literature review is conducted for setting the stage for the experimentations performed. Firstly, the general problem of cooperation is addressed, what it is, why it matters and how it is mathematically tackled via Game Theory and Evolutionary Game Theory. In social dilemmas, like the Prisoner's Dilemma or Public Goods Games, selfish behaviours are

favoured. Yet, cooperation is observed on many levels of biological and social organizations. The next section attempts to explain mechanisms that may be put in place for natural selection to favour cooperation and how they offset the costs of cooperation by causing Cooperators to also be on the receiving end more often. An overview of the most relevant concepts from the novel field of Network Science to be used throughout the text follows with a characterization of the networks that support the experimentations. Game dynamics, whether unfolding over continuous or discrete time, governed at the microscopic-agent level by stochastic rules or following deterministic rules modelling the direction and intensity of selection as a function of relative population concentrations is focused next. For the sake of completeness, chapter 2 finishes with a survey on publications related to the topics pursued in this thesis.

Experiments were conducted via computer simulations that run on a framework built *ad hoc*, implementing multiple instances of agents with behaviours governed by stochastic processes. Chapter 3 aims to explain this framework, to detail the models constructed, to discuss the implementation options available and the rational beyond the options taken. Independent parameters, both topological and behavioural, and metrics to collect (outputs) as well as the methodologies followed are identified.

Chapter 4 presents the main results collected from the simulations, highlighting the individual influence of the parameters on the cooperation levels attained by the system. In particular, it shows how the combination of topology and the criteria for deciding on how to share a finite investment among all games each individual participates in impacts the cooperation level achieved, leading, in extreme circumstances, to an enslavement in which the level of cooperation attained becomes insensitive to other environment parameters. A limited set of parameters dictate the enslavement condition. When this condition sets in, changes in other parameters have a marginal effect on the levels of cooperation attained which is preserved since multilayer initialization time. Mathematical explanations for enslavement to occur and for its consequences are explored. In order to better understand the dynamics unleashed on complex systems often unrelated to the stochastic rules programmed at agent-level the former are built upon, one has resorted to Average Gradient of Selection (AGoS), a time and context independent metric, because of being averaged across time and the population, but dependent on parameters such as the networks supporting the interactions among individuals that reflects a trend for the evolution of the number of Cooperators over time. The use of AGoS initially conceived to a single layer is generalized to a multilayer case. AGoS results are interpreted and correlated with enslavement. Finally, in chapter 5, we draw concluding remarks and discuss future steps.

The thesis includes a number of appendixes complementing the results shown in chapter 4. Appendix A complements chapter 3 in presenting the algorithm conceived in order to minimize the duration of the simulations executed. In appendix B, we discuss the effects of degree-degree correlation and overlapping on the evolution of cooperation levels reached by the multilayer are explored. In appendix C, a mathematical analysis explaining the topological and investment criteria enslavement is developed. With conditions for enslavement met and taking a mean field approach, expected AGoS is anticipated via a mathematical path pursued in appendix D. Finally, in appendix E, we present results concerning cooperation levels and AGoS attained in multilayers with different types of networks are presented.

2. LITERATURE REVIEW

In this section we motivate the study of the problem of cooperation. A literature review is undertaken from seminal papers towards a general objective of assessing the current state of knowledge on the subject. The literature review allowed us to identify directions of research and unexplored questions. It also helped in adopting a consistent terminology and on building up the foundations for a theoretical framework. Along this chapter, the literature review is presented with an emphasis on a number of concepts that are the cornerstone to the research conducted and presented in this thesis and that served as the ground/baseline for the extensive computer simulations conducted.

Important keywords that summarize the topics researched in this section include Cooperation; Game Theory; Complex Networks; Evolutionary Dynamics; Public Goods Games; Multilayer Networks, and Gradient of Selection.

2.1. THE PROBLEM OF COOPERATION

All great human achievements and the emergence of human culture are results of cooperative enterprises. Genes cooperate to form a genome, cells cooperate to produce multicellular organisms, individuals cooperate to form groups and societies. Language and human culture are just examples of results from cooperative enterprises.

Cooperation relates to altruism, which opposes to competition, a cornerstone of evolution in Biology. Cooperation can be viewed as an outcome of a game that, despite potential costs incurred by participating individuals, is “good” (measured by some appropriated fitness measure) for them and that requires some sort of collective action. In this sense, to cooperate means to behave cooperatively, to bring something to the table.

The problem with cooperation is that frequently it is costly, weighs on individual wellbeing and prosperity and is, thus, always vulnerable to exploitation by Defectors. Individuals are, thus, divided between acting selfishly and sacrificing part of their self interest in exchange for bringing value to society.

The theoretical framework used most frequently to study cooperation among selfish individuals is Evolutionary Game Theory (Nowak M. , 2006), where the concept of a social dilemma captures the essence of the problem.

Social dilemmas or collective action problems are situations where there is a conflict between individual and group interests so that if the individuals try to maximize their own payoff the whole group ends up with less than if they had acted in another-regarding way.

This tension between rational choice and successful cooperation is the topic of a vast literature spread over disciplines of social science (Eriksson & Strimling, 2012).

Because cooperation is beneficial to society, understanding the mechanisms and conditions that encourage it and identifying the tuning parameters that may influence and catalyse its emergence is of utmost importance.

2.1.1. Two Person Games, the Prisoner's Dilemma

Classic game theory is based on two key assumptions. One is that players act rationally, they are fully aware of their and their opponent's strategy options and payoff values. They are capable of correctly assessing missing information (if applicable) and process new information revealed by the play of opponents (in dynamic games) in terms of probability distributions.

The second assumption is one of common knowledge, i.e., that each player knows not only that all others act rationally but also that others are aware that he/she knows they know, and so on recursively (Szabo & Fath, 2007).

Players' rationality assumption has been relaxed over time in order to push further the limits of classic game theory. Players have well defined and consistent goals and preferences, which can be described by a utility function. A utility function measures the satisfaction resulting from a certain outcome of the game, and players' goal is to maximize their utility. It must be stressed here that the maximization problem of game theory differs from a general one of physics. In physics, one generally has a single parametrized function whose extreme condition characterizes the whole system. In game theory, it is common to have instead a set of functions to optimize as many as the number of interacting players, as they continuously restructure the landscape for each other in pursuit of their selfish individual goals (optimum).

Players need to have at least two strategies to choose from. The combination of strategies chosen by each player, called strategy profiles, yields a result. In classic game theory, the payoff corresponds to the players' evaluations of this result. A static one-shot 2-player game can be represented as in table 3 by N times M matrices (normal form) with $\pi_{1_{ij}} = u_1(S_{1i}, S_{2j})$ representing the utility function for player 1, when player 1 and 2 apply S_{1i} and S_{2j} strategies, respectively. Reciprocally, $\pi^T_{2_{ij}} = u_2(S_{1i}, S_{2j})$, where u_2 represents the utility function for player 2 in the same circumstances.

Roles of the players define the game (a)symmetry. In a symmetric game players' roles are identical and interchangeable, which implies that they possess the same strategy options and payoffs, N = M and $\pi_{1_{ij}} = \pi_{2_{ij}}$.

Table 3 – Generalized Payoff Matrix of a 2-Player, 2-Strategy Game

		Player 2		
	Π	S_{21}	$\cdots$	S_{2M}
Player 1	S_{11}	$(\pi_{1_{11}}, \pi^T_{2_{11}})$	$\cdots$	$(\pi_{1_{1M}}, \pi^T_{2_{1M}})$
	$\vdots$	$\vdots$	$\ddots$	$\vdots$
	S_{1N}	$(\pi_{1_{N1}}, \pi^T_{2_{N1}})$	$\cdots$	$(\pi_{1_{NM}}, \pi^T_{2_{NM}})$

A particular group of a symmetric two-player games, the only ones to be the subject of this thesis, happen when the number of pure strategies is 2, C (Cooperation) and D (Defection), with payoff matrix as in table 2.

In order to better chart and normalize territories of fear and greed in the playground of 2-Person games and as proposed in (Santos, Pacheco, & Lenaerts, 2006; Santos F. C., Pinheiro, Lenaerts, & Pacheco, 2012) payoff matrix is linearly transformed in order for and R and P to value 1 and 0, respectively.

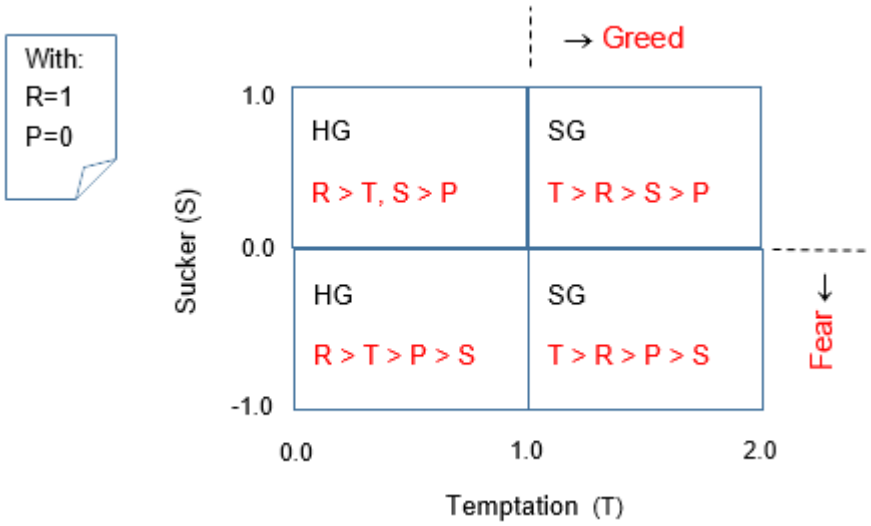

Figure 1- T-S Quadrants for 2-Player Games

Having applied this transformation and as depicted in figure 1, the Stag–Hunt (SH) also known as the Coordination Dilemma emerges with $R > T > P > S$ and unfolds in the lower left quadrant, when the fear of being cheated by D ($P > S$) may justify defection instead of cooperation.

In an isolated environment, each player may decide to behave as a C or a D. When both players decide to cooperate, each receives a reward R. Mutual defection results in a punishment of P. If they choose different strategies, the one offering cooperation receives S,

Sucker's payoff, whereas the Defector collects T, interpreted as the Temptation to defect. Different dilemmas result from different ordering of these payoffs.

Whenever $T > R$, greed emerges and defection is tempting as it is the best strategy against a Cooperator. In the absence of fear ($P < S$), greed leads to Chicken, Hawk-Dove or Snowdrift (SG) game with $T > R > S > P$. With both greed and fear present, $T > R > P > S$, the game obtained is Prisoner Dilemma (PD) (Santos F. C., Pinheiro, Lenaerts, & Pacheco, 2012).

More generally, a game is a cooperative dilemma when two Cooperators get a higher payoff than two Defectors, $R > P$, and still there is an incentive to defect. This incentive must exists when at least one of the following conditions hold true: (i) if $T > R$ then it is better to defect when playing against a Cooperator; (ii) if $P > S$ then it is better to defect when playing against a Defector; and (iii) if $T > S$ then it is better to be the Defector in an encounter between a Cooperator and a Defector (Nowak M. , 2012).

This sort of dilemma is present in anyone's everyday life, when one has to decide between committing or being lazy, being selfish or altruistic, etc.

A game is in a Nash equilibrium (NE) if, for each player, the strategy applied is the one that brings him the highest payoff considering the strategies chosen by other players, with is the same to say that the strategy followed by each player is the one he/she has no interest to deviate from, as it maximizes his/her payoff, taking into account the strategies chosen by his/her peers. The dilemma underlying prisoner's game is that acting rationally unable to anticipate opponent's strategy, players will defect and NE occurs with mutual defection, although both players would be better off if they cooperated.

NE is insensitive to payoff matrix scaling or an addition of arbitrary constants to payoff columns (Szabo & Fath, 2007). Thus, offsetting the matrix in order to get a null payoff when Defectors meet each other and further scaling it in order for a 1 unit payoff to result between Cooperators interaction as was performed in figure 1, is a linear transformation from which no loss of generality in game dynamics results (Broom, 2005). The offset is irrelevant in replicator dynamics based on payoff differential. As to the positive multiplicative factor, it only rescales the time.

Along the text the concept of Evolutionary Stable Strategy related to the probability of a homogenous population to be immune against the invasion of a minority of intruders or mutants will emerge. A strategy S is considered to be an Evolutionary Stable Strategy (ESS) if a population composed only by S individuals is resilient to the invasion from a minority of invaders with any other strategy. Being a refinement of a NE, not all NE are necessarily ESS.

2.1.2. Public Goods Games

There are many socially and economically important examples with a number of decision makers involved greater than two. Although sometimes these situations can be modelled as repeated play of simple pair interactions, there are many cases where the most fundamental unit of the game is irreducibly of multi-player nature. These games cannot be cast in a matrix or bi-matrix form. Still the basic solution concept is the same: when played by rational agents the outcome should be a Nash equilibrium where no player has an incentive to deviate unilaterally.

One example of Public Goods Games (PGG) is the Tragedy of the Commons, an abstract game that exemplifies what has been one of the major concerns of political philosophy and economic thinking since the 19th century (Hardin, 1968) and is now part of the mainstream economic theory, assuming that the selfish and rational human nature will lead to the depletion of essential and common resources, e.g. water, soil, etc., in the absence of well-defined property rights, formal, top-down management institutions, rules of access and exploitation.

In order to quantitatively better illustrate how the Tragedy of Commons unfolds, one can assume a common finite resource, e.g. a village green, and N players, farmers. The cost of taking one goat grazing in the green is c. It is up to each player i to decide on how many goats g_i he/she will take grazing. In total there will be $G = g_1 + \cdots + g_N$ goats grazing. u(G) is an utility function that returns the individual benefit from taking a goat grazing as a function of green utilization. As the green suffers from overgrazing, not only will $u(G)$ decrease with G, which means $\frac{du}{dG} < 0$, as this decrease will be sharper for higher G, which means $\frac{d^2u}{dG^2} < 0$. The payoff of each player will be of

$$p_i = (u(G) - c)g_i \tag{1}$$

At a Nash equilibrium, famers' decision on the number of goats grazing will be $(g_1^*, \dots, g_N^*)$ as no farmer will be better of if he changes his/her chosen number of goats in the green. Thus, at Nash equilibrium $\frac{\partial p_i}{\partial g_i} = 0$, i.e.,

$$\frac{\partial p_i}{\partial g_i} = u(G^*) + \frac{du(G^*)}{dG}\frac{\partial G}{\partial g_i}g_i^* - c = u(G^*) + \frac{du(G^*)}{dG}g_i^* - c = 0 \tag{2}$$

Summing up left identity of rightmost equation for all players, one gets

$$u(G^*) + \frac{G^*}{N}\frac{du(G^*)}{dG} - c = 0 \tag{3}$$

If $u(G)$ is known, the optimum G^* can be found. However, were there a central management entity in place, the social welfare would take place at G^{**}which maximizes total payoff $p = (u(G) - c)G$. This implies

$$u(G^{**}) + G^{**}\frac{du(G^{**})}{dG} - c = 0 \quad (4)$$

Comparing both equations and taking into account the fact of $u(G)$ and its derivate decreasing with G, one concludes that $G^{**} < G^*$, which means that at Nash equilibrium compared with social welfare optimum the common resource is over utilized. This makes the game a social dilemma (Szabo & Fath, 2007).

In another variation of PGG (Kleineberg & Helbing, 2018; Battiston, Matjaz, & Latora, 2017; Li, Shen, & Jiang, 2016; Pacheco, Pinheiro, & Santos, 2009; Santos, Santos, & Pacheco, 2008) each player i in a total of N makes a contribution c_i to a common pool, topped arbitrarily by 1. The total collected, $\sum_i c_i$ is multiplied by an enhancement factor $F, 1 < F < N$, a synergy factor reflecting how much the whole is greater than the sum of the parcels, to be equally divided among all participating players, no matter the amount of individual contributions,. Being a Defector in this game means contributing with $c_i = 0$. Those who contribute with $c_i > 0$ are Cooperators.

Maximum total income is achieved if all players contribute maximally. In this case each player receives Fc, resulting in a final payoff is $(F - 1)c$. Players are faced with the temptation of being free-riders, i.e., to take advantage of the common pool without contributing to it, as any individual investment is a loss for the player because only the fraction $\frac{F}{N} < 1$ will be repaid. Consequently, rational players invest nothing and one ends up with another Tragedy of Commons, Free Rider problem, Social Dilemma on N-Player PD (Szabo & Fath, 2007).

If the number of players is 2 and players' choices are binary, i.e., they are constrained to not invest or to invest a fixed amount, then the game becomes a Prisoner's Dilemma. With due tuning of parameters, a N-person round robin PD game can simulate a PGG.

As it will be hereafter discussed in Network section individuals are located as nodes in a network. Each PGG instance makes use of a focal node such that the focal node has all its direct neighbours, i.e., all nodes directly linked to the focal node, constitute the N players of the game.

While it is common to assume that in every game individuals can contribute/invest a fixed amount c to the public good, a broader scenario inspired in the 2-Player Distributed Prisoner Dilemma (DPD) from (Pacheco, Pinheiro, & Santos, 2009) is explored. Hence, a PGG

involving two individuals that participate in multiple games is considered, investment values being distinct per players. In the distributed scenario, individuals have to split their investment across a set of games they participate (that can be all of them, or part of them). In that case, the possible outcomes of each player actions can be summarized in a payoff matrix as in table 4 with C_1 and C_2 representing, respectively, the investments of players 1 and 2.

Table 4 - Payoff matrix for Public Goods Games in the 2-Player Distributed
(Version in Player1's Perspective)

	π (Payoff)	Player 2 C	Player 2 D
Player1	C	$(\frac{F}{2}-1)C_1+\frac{F}{2}C_2$	$(\frac{F}{2}-1)C_1$
Player1	D	$\frac{F}{2}C_2$	0

Depending on the assumptions of the DPD the values of C_1 and C_2 may be computed differently. The single N+1-Player game is substituted by N 2-Person games, one per each of the N neighbours the focal node can play with.

2.1.3. Evolutionary dynamics in finite populations

The evolutionary game dynamics of a finite population can be described by a stochastic process, an approach well suited for computer simulation that models the microscopic mechanisms underlying strategy transference between individuals. Once the evolutionary path is traced, one will force both (i) population size to tend to infinity and (ii) time intervals between system updates to tend to zero, looking for a convergence with the solution that would have been reached had the population been considered infinite and dynamical rules defined at population level.

As a mechanism for strategy transference, some alternatives can be considered from which the following are highlighted:

- **Pairwise comparison**- Along this alternative, a focal individual f available to update his strategy is randomly selected. A second distinct individual r is also randomly selected. All individuals have an equal probability of being chosen in any selection.

The first individual copies a strategy of a second individual with a probability that increases with the fitness differential between them. The reference probability can be

$$\text{Prob} = \frac{1}{2} + \frac{w}{2}\frac{\pi_r - \pi_f}{\triangle \pi} \quad (5)$$

with $\triangle \pi$ representing the maximum payoff difference that can be found between individuals, the numerator of the fraction standing for the difference between r and f individuals' payoff and $0 \leq w \leq 1$. w measures the relative importance of selection compared to neutral drift.

An alternative for not having to anticipate $\triangle \pi$ is to rely on Fermi distribution and have (Traulsen, Nowak, & Pacheco, 2006)

$$\text{Prob} = \frac{1}{1 + e^{-w(n_r - n_f)}} \quad (6)$$

In both pairwise comparisons, for $w = 0$ the decision to update a strategy has 0.5 probability and does not take into account payoff differences. For $0 < w \ll 1$, the two reference probabilities become similar because $\frac{1}{1+e^{-w(n_r-n_f)}} = \frac{1}{2} + \frac{w}{2}(n_r - n_f) + O(w^2)$. Specifically for the Fermi case, if $w \to \infty$ the process becomes deterministic: an individual switches strategy if and whenever the one he compares to has an higher payoff (Traulsen & Hauert, 2008).

Pairwise comparison models a process of cultural evolution by learning and imitation.

- **Moran birth-death process**- Firstly a focal individual f is randomly selected for reproduction with a probability proportional to its fitness. His/Her offspring inherits ancestor's strategy. Another r distinct individual is selected randomly with uniform probability. In order to preserve the size of the population, the r individual is replaced by the offspring. The Moran birth-death process (Moran, 1958) originated in genetics provides a mechanism for most fit individuals to spread across the population. Fitness of an individual as proxyed by its payoff can be given by $1 - w + w\pi$, with $0 \leq w \leq 1$ standing for the balance between selection and neutral drift.

  The Moran birth-death process maps to the traditional interpretation of evolutionary game dynamics in which strategies are encoded in genomes and spread throughout the population as a function of its relative fitness.

In order to better illustrate how finiteness impacts evolution, one starts considering a well-mixed population with N individuals and with two strategies, A and B, available for individuals to choose from with a generic payoff matrix π_{ij} as in table 5.

Table 5- Generic Payoff Matrix

π	A	B
A	a	b
B	c	d

The population being well-mixed means that one can assume that each individual can potentially encounter and interact with any other.

The dynamics of the game will be formulated via a pairwise comparison strategy transference mechanism of imitation type, the one to consider along the thesis. The rational to apply with no loss of generality is extensible to the birth-death Moran process via minor tweaks to point out in due time.

Being the population well-mixed, the identity of individuals following each strategy loses relevance and instead knowing the total number of followers of each strategy is what matters. The evolutionary dynamics of such population corresponds to a Stochastic Markov Birth-Death process whose dynamics becomes fully described upon the computation of all transition probabilities between available configurations. Each state of the Markov chain reflects the number of followers of each strategy.

Considering the fitness to coincide with the payoff and the mean-field hypothesis that individuals interact with all others, but not with themselves, and being i the number of individuals with strategy A, the fitness of individuals of both strategies is given by

$$f_{Ai} = a\frac{i-1}{N-1} + b\frac{N-i}{N-1}, 1 \leq i \leq N \tag{7}$$

$$f_{A0} = 0 \tag{8}$$

$$f_{Bi} = c\frac{i}{N-1} + d\frac{N-i-1}{N-1}, 0 \leq i \leq N-1 \tag{9}$$

$$f_{BN} = 0 \tag{10}$$

where $f_{Ai}(f_{Bi})$ stands for the expected fitness of one in a set of i individuals following strategy A(B) at a particular moment in time. With i followers of strategy A, one of them can interact with $i-1$ of the followers of the same strategy from which an a payoff is collected or with $N-i$ followers of B strategy obtaining a b payoff. The fractions affecting a, b, c and d are just the probabilities of collecting these payoffs from randomly chosing a peer to play with. Because of the underlying Moran process, only transitions between consecutive states are allowed. They are as follows:

$$P_{i\to i+1} = \frac{N-i}{N}\frac{i}{N-1}\frac{1}{1+e^{-w(f_{Ai}-f_{Bi})}}, 1 \leq i \leq N-1 \tag{11}$$

$$P_{i\to i-1} = \frac{i}{N}\frac{N-i}{N-1}\frac{1}{1+e^{-w(f_{Bi}-f_{Ai})}} \quad , 1 \leq i \leq N-1 \tag{12}$$

$$P_{i\to i} = 1 - P_{i\to i+1} - P_{i\to i-1} \quad , 1 \leq i \leq N-1 \tag{13}$$

$$P_{0\to 1} = P_{N\to N-1} = 0 \tag{14}$$

$$P_{0\to 0} = P_{N\to N} = 1 \tag{15}$$

The probability of selection of a B individual with uniform probability as a focal individual coincides with the proportion of these individuals in the population. This corresponds to the first fraction in equation 11. Second fraction reflects the probability of finding an A individual to copy the strategy from. Third fraction represents the Fermi probability of a strategy transference. Equation 12 has an analogous rational. Were the strategy transference based on a Moran process, only equations 11 and 12 would be updated: their first factor would now stand for the proportion of B(A) individuals in the population duly weighted by their relative fitness whereas third term would simply be removed.

The process has two absorbing states, $i = 0$ and $i = N$: when the population reaches either one of these states, it will stay there forever. In an absorbing Markov chain, the probability that the process will be absorbed is 1 (Grinstead & Snell, 1997). This is reflected in equations 14 and 15. This Markov chain is represented in figure 2.

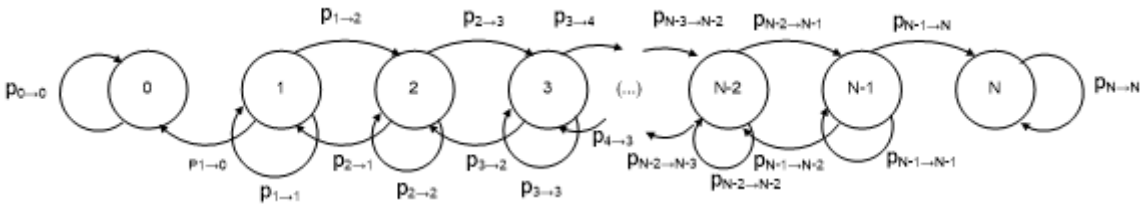

Figure 2- Markov Chain for a Layer with State reflecting the Number of Cooperators

The corresponding Markov transition matrix can be described as matrix P

$$P = \begin{array}{c|ccccccc} & \mathbf{0} & \mathbf{1} & \mathbf{2} & \mathbf{\dots} & \mathbf{N\text{-}2} & \mathbf{N\text{-}1} & \mathbf{N} \\ \mathbf{0} & 1 & 0 & 0 & \dots & 0 & 0 & 0 \\ \mathbf{1} & p_{1,0} & p_{1,1} & p_{1,2} & \dots & 0 & 0 & 0 \\ \mathbf{2} & 0 & p_{2,1} & p_{2,2} & \dots & 0 & 0 & 0 \\ \mathbf{\dots} & \dots & \dots & \dots & \dots & \dots & \dots & \dots \\ \mathbf{N\text{-}2} & 0 & 0 & 0 & \dots & p_{N-2,N-2} & p_{N-2,N-1} & 0 \\ \mathbf{N\text{-}1} & 0 & 0 & 0 & \dots & p_{N-1,N-2} & p_{N-1,N-1} & p_{N-1,N} \\ \mathbf{N} & 0 & 0 & 0 & \dots & 0 & 0 & 1 \end{array}$$

where $p_{ij} = P_{i \to j}$. The Markov transition matrix presented mixes absorbing and transient states. Its canonical form results from the original one with lines and columns interchanged coherently such that first lines/columns correspond to transient states and last ones to absorbing ones as in

$$P = \begin{array}{c|cc} & \text{Trans.} & \text{Abs.} \\ \text{Trans.} & \text{Q} & \text{R} \\ \hline \text{Abs.} & 0 & \text{I} \end{array} \qquad P^n = \begin{array}{c|cc} & \text{Trans.} & \text{Abs.} \\ \text{Trans.} & Q^n & \left(\sum_{i=0}^{n-1} Q^i\right)\text{R} \\ \hline \text{Abs.} & 0 & \text{I} \end{array}$$

Rearranging the lines and columns in order to have P in the canonical form, we obtain

$$\begin{array}{cc|cccccc|cc} & & \multicolumn{6}{c|}{\textbf{Transient States}} & \multicolumn{2}{c}{\textbf{Absorbing States}} \\ & & 1 & 2 & 3 & \dots & \text{N-2} & \text{N-1} & 0 & \text{N} \\ & 1 & p_{1,1} & p_{1,2} & 0 & \dots & 0 & 0 & p_{1,0} & 0 \\ & 2 & p_{2,1} & p_{2,2} & p_{2,3} & \dots & 0 & 0 & 0 & 0 \\ \textbf{Trans. Stat} & 3 & 0 & p_{3,2} & p_{3,3} & \dots & 0 & 0 & 0 & 0 \\ & \dots & \dots & \dots & \dots & \dots & \dots & \dots & \dots & \dots \\ & \text{N-2} & 0 & 0 & 0 & \dots & p_{N-2,N-2} & p_{N-2,N-1} & 0 & 0 \\ & \text{N-1} & 0 & 0 & 0 & \dots & p_{N-1,N-2} & p_{N-1,N-1} & 0 & p_{N-1,N} \\ \hline \textbf{Abs. States} & 0 & 0 & 0 & 0 & \dots & 0 & 0 & 1 & 0 \\ & \text{N} & 0 & 0 & 0 & \dots & 0 & 0 & 0 & 1 \end{array}$$

For an absorbing Markov chain P in canonical form, the matrix $\text{N} = \sum_{k=0}^{+\infty} Q^k = (I - Q)^{-1}$ is called the fundamental matrix for P. The entry n_{ij} of N reflects the expected number of

times the process visits the transient state s_j starting in the transient state s_i and before ending up in an absorbing state. Thus,

$$Prob\ (state\ =\ s_j \mid start\ state = s_i)\ =\ \frac{n_{ij}}{\sum_j n_{ij}} \tag{16}$$

reflects the probability distribution of next transient states to visit until one of the two absorbing states is reached, given that at present the system is in transient state s_i.

Because of ephemeral character of transient states, equally interesting as calculating the probability of visiting them, particularly for biology applications, is to calculate the probability of fixation of a strategy, i.e., the probability of the population reaching a state N (or 0), i.e., all individuals with the same strategy, starting from state s_i (Nowak M. , 2006).

As matrix P is stochastic, i.e., $\sum_j p_{ij} = 1$, the absorbing probabilities are given by the right-hand side eigenvector associated with the largest eigenvalue, which is 1. So one can write $u = Pu$, with $u\ =\ \{u_0, u_1, \dots, u_N\}^T$. If u_i denotes the probability for the system to end up in state N when starting in state s_i, the following recursive relation hold

$$u_i = P_{i\to i-1}u_{i-1} + P_{i\to i}u_i + P_{i\to i+1}u_{i+1} = \tag{17}$$

$$P_{i\to i-1}u_{i-1} + (1 - P_{i\to i-1} - P_{i\to i+1})u_i + P_{i\to i+1}u_{i+1} \tag{18}$$

$$u_0 = 0 \tag{19}$$

$$u_N = 1 \tag{20}$$

Recalling equations 11 and 12, if one considers

$$\alpha_i = \frac{P_{i\to i-1}}{P_{i\to i+1}} = e^{-w(f_{Ai} - f_{Bi})} \tag{21}$$

equations 17 and 18 can be simplified to

$$u_{i+1} - u_i = \alpha_i\ (u_i - u_{i-1}) \tag{22}$$

As na aside, if one considers a strategy transference based on a Moran process, equation 22 still applies, but in equation 21 α_i would value f_{Bi}/f_{Ai}, as a result of the aforementioned adaptation of equations 11 and 12 to a Moran process.

$1 - u_i$ represents the probability of reaching state 0 stating from state s_i, because there are only two absorbing states and the system must end up in one of them. Introducing

$$y_i = u_i - u_{i-1} \qquad , 1\ \le i\ \le N \tag{23}$$

results in

$$\sum_{i=1}^{N} y_i = u_1 - u_0 + u_2 - u_1 + \cdots + u_N - u_{N-1} = u_N - u_0 = 1 \tag{24}$$

$$y_{i+1} = \alpha_i y_i \tag{25}$$

Additionally,

$$\begin{aligned} y_1 &= u_1 \\ y_2 &= \alpha_i y_1 = \alpha_i u_1 \\ y_3 &= \alpha_2 y_2 = \alpha_2 \alpha_i u_1 \\ &(\ldots) \\ y_n &= \prod_{k=1}^{n-1} \alpha_k u_1 \end{aligned} \tag{26}$$

Considering that all y_i sum 1, one is left with

$$\begin{aligned} u_1 &= \frac{1}{1 + \sum_{j=1}^{N-1} \prod_{k=1}^{j} \alpha_k} = \frac{1}{1+\sum_{j=1}^{N-1} \prod_{k=1}^{j} e^{-w(f_{Ak}-f_{Bk})}} \\ &= \frac{1}{1+\sum_{j=1}^{N-1} e^{-w \sum_{k=1}^{j}(f_{Ak}-f_{Bk})}} \end{aligned} \tag{27}$$

and then, the probability of reaching state s_N departing from state s_i resumes to:

$$\begin{aligned} u_i &= \sum_{k=1}^{i} y_k = u_1 \left(1 + \sum_{j=1}^{i-1} \prod_{k=1}^{j} \alpha_k\right) \\ &= \frac{1 + \sum_{j=1}^{i-1} e^{-w \sum_{k=1}^{j}(f_{Ak}-f_{Bk})}}{1 + \sum_{j=1}^{N-1} e^{-w \sum_{k=1}^{j}(f_{Ak}-f_{Bk})}} \end{aligned} \tag{28}$$

The fixation probability for population A is the probability of a single A individual in a population of $N-1$ others following strategy B taking over the all population and values

$$\rho_A = u_1 \tag{29}$$

Reciprocally, the fixation for population B, i.e., the probability of a single B individual in a population of $N-1$ A individuals, values

$$\rho_B = 1 - u_{N-1} \tag{30}$$

The Replicator Equation

Equations 17 and 18 relate the probability of states with probabilities of transitions in a discrete system at any instant of time because of system stationarity. If time is introduced the master equation describing the evolution of process with τ discrete (Traulsen & Hauert, 2008) is given by

$$p(i, \tau + 1) = p(i-1, \tau)T^{+}(i-1) + p(i+1, \tau)T^{-}(i+1) + \tag{31}$$

$$p(i,\tau)(1 - T^{+}(i) - T^{-}(i))$$

with $p(i,\tau)$ representing the probability of a stochastic process being found at time τ in state i. $T^{\pm}(i)$, a shortcut to $p_{i\to i\pm1}$, represents the probability of a population with i followers of strategy A to increase/reduce its number by 1 unit. This quantity is invariant with time. Basically equation 31 states that the probability of the system being found in state i at the next birth-death occurrence equals to the probability of system being in same state i with no change in the numbers of strategy followers plus the probability of being in a neighbour state and the system evolving to state i. Only neighbour states of i are considered as in each evolutionary step of the birth-death process considered the number of Cooperators in the system can change up to 1 unit.

Time taken into account evolves by fixed steps. In what follows and in order to perform a macroscopic approach as the limit of microscopic one with well-mixed populations, the size of population increases unboundly, $N \gg 1$, in such a way that instead of counting the number of followers of a strategy its frequency will be accounted for. Moreover, time steps are reduced in order for time to appear to flow continuously. With the change of variables $x = \frac{i}{N}$, $t = \frac{\tau}{N}$ and $\rho(x,t)$ transformed into $p(i,\tau)$, equation 31 becomes

$$\begin{aligned}\rho\left(x, t + \frac{1}{N}\right) - \rho(x,t) = {} & \rho\left(x - \frac{1}{N}, t\right) T^{+}\left(x - \frac{1}{N}\right) + \\ & \rho\left(x + \tfrac{1}{N}, t\right) T^{-}\left(x + \tfrac{1}{N}\right) - \\ & \rho(x,t)(T^{+}(x) + T^{-}(x))\end{aligned} \tag{32}$$

x stands now for the proportion over the entire population of individuals with A strategy. Considering second order Taylor series expansion at x and t of a generic $f(x,t)$ function of class C^2, i.e., twice continuously differentiable, with t fixed

$$f(x + dx, t) = f(x,t) + \frac{\partial}{\partial x} f(x,t)dx + \frac{1}{2!}\frac{\partial}{\partial x^2} f(x,t)dx^2 \tag{33}$$

individual terms on right hand side of equation 32 are transformed into

$$\rho\left(x \pm \frac{1}{N}, t\right) = \rho(x,t) \pm \frac{1}{N}\frac{\partial}{\partial x}\rho(x_0,t)dx + \frac{1}{2!\,N^2}\frac{\partial}{\partial x^2}\rho(x_0,t) \tag{34}$$

$$T^{\pm}\left(x \pm \frac{1}{N}\right) = T^{\pm}(x) \pm \frac{1}{N}\frac{d}{dx}T^{\pm}(x_0,t)dx + \frac{1}{2!\,N^2}\frac{d}{dx^2}T^{\pm}(x_0,t) \tag{35}$$

with x_0 lying within interval $]x, x + \frac{1}{N}[$.

Substituting the last two expansions in right hand side of equation 32 and on the other side applying mean value theorem one gets a Fokker-Planck equation

$$\frac{\partial}{\partial t}\rho(x,t_0) = -\frac{\partial}{\partial x}\left[\left(T^+(x_0) - T^-(x_0)\right)\rho(x_0,t_0)\right] + \frac{1}{2}\frac{\partial^2}{\partial x^2}\frac{\left[\left(T^+(x_0)+T^-(x)\right)\rho(x_0,t_0)\right]}{N} + O(N^{-2}) \quad (36)$$

x_0 and t_0 are points within intervals $]x, x+\frac{1}{N}[$ and $]t, t+\frac{1}{N}[$, respectively, with N tending to infinity. In order to solve this equation, a parenthesis is opened to derive the same equation via a Stochastic Differential equation of the form

$$dX_t = \mu(x,t)dt + \sigma(x,t)dB_t \quad (37)$$

X_t is a stochastic process with a drift over time of $\mu(x,t)$ and a local volatility given by $\sigma(x,t)$. Both μ and σ functions are deterministic. B_t is a Brownian process, also known as Wiener process, resulting from the integration of white noise. It is characterized by being stationary with $Prob(B_0 = 0) = 1$ and $B_t - B_s \sim N(0, |t-s|)$. Differential calculus will be of no use here as B_t, although continuous, is not differentiable. However, Itô lemma can be applied. Further calculating density probability $p(x,t)$ of process X, one gets a similar Fokker-Planck equation (Oksendal, 2003)

$$\frac{\partial}{\partial t}p(x,t) = -\frac{\partial}{\partial x}(\mu(x,t)p(x,t)) + \frac{1}{2}\frac{\partial^2}{\partial x^2}(\sigma^2(x,t)p(x,t)) \quad (38)$$

Comparing equation 36 to 38 and considering process X as defined in 37 to be a solution for equation 38, a solution for equation 36 is

$$\frac{dx(t)}{dt} = \left(T^+(x) - T^-(x)\right) + \sqrt{\frac{T^+(x)+T^-(x)}{N}}\eta(t) \quad (39)$$

Second term on the right hand side, which includes a white noise component $\eta(t)$ derivate of the Brownian process can be discarded, because of $\eta(t)$ having a normalized Gaussian amplitude probability and the population size N tending to infinity. Payoff of followers of A and B strategy from a Stochastic Markov Birth-Death process as in equations 7 and 9 adapted to the continuous case and still considering payoff as a proxy to fitness results in

$$f_A(x) = ax + (1-x)b \quad (40)$$

$$f_B(x) = cx + (1-x)d \quad (41)$$

$T^{\pm}(x)$ for the Fermi distribution pairwise comparison, the one to be explored along the thesis, values

$$T^{\pm}(x) = x(1-x)\frac{1}{1+e^{\pm\beta(f_B(x)-f_A(x))}} \quad (42)$$

For $T^+(x)$, $1-x$ stands for the probability of first individual to be randomly selected from B population, x for the probability of second selected individual to be from population A and

finally the fraction represents the Fermi probability of first individual to copy strategy from second one.

Introducing equalities from equation 40 to 42 into equation 39 and considering in this last equation only the first term from right side, as second one is discardable when N tends to infinity, one gets

$$\frac{dx(t)}{dt} = x(1-x)\left(\frac{1}{1+e^{\beta(f_B(x)-f_A(x))}} - \frac{1}{1+e^{-\beta(f_B(x)-f_A(x))}}\right) = x(1-x)\tanh\left(\frac{\beta}{2}(f_A(x)-f_B(x))\right) \quad (43)$$

which for for $\beta \ll 1$ simplifies to

$$\frac{dx(t)}{dt} = \frac{\beta}{2}x(1-x)\big(f_A(x)-f_B(x)\big) = \frac{\beta}{2}x(f_A(x)-\langle f(x)\rangle) \quad (44)$$

with $\langle f(x)\rangle$ standing for the average payoff of the population, equal to $xf_A(x) + (1-x)f_B(x)$.

This is the replicator equation, a deterministic equation for infinite populations to be introduced in the following chapter stating that the relative growth rate of a population $(\frac{1}{x}\frac{dx(t)}{dx})$ is proportional to the differential of its fitness to average fitness. It assumes individuals are equally likely to interact with any others. (Traulsen, Claussen, & Hauert, 2006; Traulsen & Hauert, 2008) show that the replicator equation is also the limit of equation 36 for infinite populations for Moran birth-death process.

2.1.4. The Replicator Dynamics

On a large unstructured population tending to infinity, the rules describing the selection among a limited number of strategies is defined at macroscopic level. They assume the form of nonlinear differential equations coined as the replicator dynamics that take into consideration the selection mechanism applicable, modelling the evolution of the populations' frequency by means of fitness comparisons. The replicator equation provides a mean-field deterministic description of a population evolutionary dynamics, which means considering an infinite and well-mixed population driven by a continuous time dynamical process.

Concretizing, by taking a dynamic perspective in Evolutionary Game Theory and by interpreting the rate of reproduction of a population as its fitness, a population with x(t) individuals at time t without environment constraints against its growth and reproducing at a rate of r per individual and unit of time has an evolution over time that can be described by the differential equation

$$\frac{dx}{dt} = \text{rx} \tag{45}$$

with the solution

$$\text{x(t)} = x_0 e^{rt} \tag{46}$$

where x_0 represents the size of the population at $t = 0$. If r is positive, the population growths to infinity. If population death is to be considered, the differential equation is to be replaced by

$$\frac{dx}{dt} = (r - d)x \tag{47}$$

with d representing the death rate per individual and unit of time.

If one considers additionally a maximum environment carrying capacity K, growth rate can be topped by a $\left(1 - \frac{x}{K}\right)$ factor as in

$$\frac{dx}{dt} = (r - d)x\left(1 - \frac{x}{K}\right) \tag{48}$$

with solution

$$x(t) = \frac{Kx_0 e^{(r-d)t}}{K + x_0(e^{(r-d)t} - 1)} \tag{49}$$

So far, a single population of individuals was considered. When second population is introduced, natural selection gets in the play because it is a key mechanism of evolution that operates whenever different types of individuals reproduce at different rates.

With more than one population and considering a scenario in which the total population is held constant, e.g. due to the ecosystem having a maximum constant carrying capacity, on the macroscopic level the replicator dynamics can be postulated directly with the reasonable assumption that the per capita growth rate of a population, $\frac{1}{x}\frac{dx}{dt}$, is proportional to the population fitness to average fitness differential (Szabo & Fath, 2007; Nowak M. , 2006),. The fitness measures the individual's evolutionary success, i.e., the payoff of the game in this game theory context.

Along this rational, let x and y represent the ratio of individuals over total population and let a and b stand for reproduction ratios for X and Y populations, respectively. Obviously $x + y = 1$. Let also $\emptyset = \text{ax} + \text{by}$ stand for the average fitness of the all population. Then, according to assumptions about populations' growth, one has

$$\frac{dx}{dt} = x(a - \emptyset) \tag{50}$$

$$\tag{51}$$

$$\frac{dy}{dt} = y(b - \emptyset)$$

Because the sum of x and y proportions is fixed, the sum of their derivate equals 0. So, if right sides of both equations are added one gets $(ax + by) - (x + y)\emptyset$, which equals zero as expected. Previous system of equations is redundant, so replacing y by $1 - x$ in first equation (or vice-versa) one gets

$$\frac{dx}{dt} = x(1 - x)(a - b) \tag{52}$$

Equilibrium is reached when $\frac{dx}{dt} = 0$, i.e., when $x = 0$ or $x = 1$. This makes sense, because it corresponds of all population consisting only of X or Y individuals. The equation highlights another aspect. If $a > b$, $\frac{dx}{dt} > 0$, which implies that X population will dominate and Y be extinct. If $a < b$ it is Y time to dominate. If $a = b$, whatever the initial relative proportions of X and Y population, they are preserved.

The evolutionary scenario analysed is an example of the survival of the fittest, but other scenarios can be anticipated in which both population can co-exist. Such scenarios can be represented by more general evolutionary equations such as

$$\frac{dx}{dt} = ax^c - \emptyset x \tag{53}$$

$$\frac{dy}{dt} = bx^c - \emptyset y \tag{54}$$

where x, y, a, and b maintain their previous meaning. There is now a new variable, c. If $c = 1$, the previous scenario is recovered. In order to keep total population constant, i.e., for the sum of variations in X and Y populations to be zero, $\emptyset$ is updated to $\emptyset = ax^c + by^c$. Substituting $\emptyset$ in first system of equations one gets

$$\begin{aligned} \frac{dx}{dt} &= ax^c - (ax^c + by^c)x = \\ & x(ax^{c-1} - ax^c - by^c) = \\ & x((1 - x)ax^{c-1} - b(1 - x)^{c-1} = \\ & x(1 - x)(ax^{c-1} - b(1 - x)^{c-1}) \end{aligned} \tag{55}$$

The derivate of X population frequency is zero for $x = 0$ or $x = 1$, as in previous scenario. There is however a new root for this derivate that values

$$x^* = \frac{1}{1 + \sqrt[c-1]{\frac{a}{b}}} \tag{56}$$

Depending on the combination of a, b and c parameters, this root can be stable or unstable.

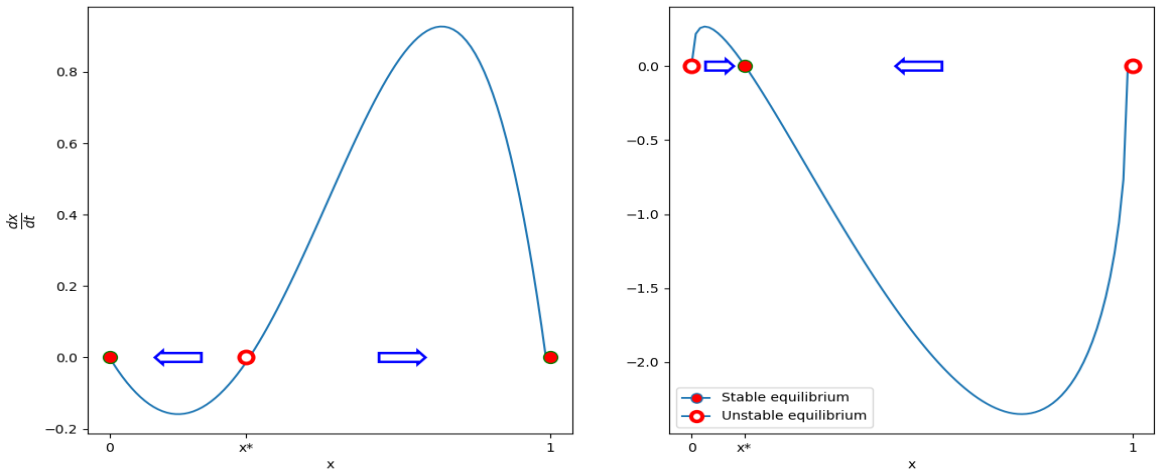

Figure 3- Examples of superexponential and subexponential growths. Growth is governed by $\frac{dx}{dt} = x(1-x)(ax^{c-1} - b(1-x)^{c-1})$ equation. Left panel obtained with $a = 9$, $b = 2$, $c = 3$ has an unstable root. In right panel, the combination $a = 3$, $b = 8$, $c = 0.5$ leads to a stable root.

Figure 3 presents examples of both sorts of roots. The root x^* naturally belongs to interval]0,1[. However, depending on $c - 1$ signal, the behaviour of the system changes. If $c > 1$, the derivate of X population frequency will be negative in interval $]0, x^*[$, positive in $]x^*, 1[$. If the derivate is positive, the trend of the population is to grow. Thus, in first interval the population shrinks, to grow on the second one.

No matter how small the perturbation is, if x surpasses x^*, because of $\frac{dx}{dt}$ being positive, x keeps increasing until $x = 1$. The reciprocal happens if a perturbation makes x smaller than x^*, with x darting to 0. This makes x^* is an unstable equilibrium point.

The remarkable aspect to stress is that this conclusion is irrespective of the rates of growth of X and Y populations. Even if Y has a higher reproduction rate, if at a certain point in time frequency of population X goes beyond x^*, population Y is doomed.

If $c < 1$, $x = 0$ and $x = 1$ are still equilibrium points but unstable. The introduction of a minimum number of individuals from X or Y population in a population of all Y or all X individuals, respectively, drives the system to a co-existence scenario with x^* and $y^* = 1 - x^*$ as the relative frequencies for X and Y populations, respectively. Again, irrespective of the reproduction rates of both populations. The relative reproduction rates of the populations only determines where x* is located.

Because starting relative frequency dictates the stable equilibrium point to converge to, superexponential growth ($c > 1$) favours whoever was there first (survival of the first), whereas subexponential growth ($c < 1$) leads to the survival of all. This is illustrated in figure 3.

2.2. THE MECHANISMS OF COOPERATION

Cooperation problems emerge as a result from a misalignment between individual motivations and collective goals. This tension is best captured by the prisoner's dilemma a 2-Player game with $T > R > P > S$, played in both territories of greed, as it is tempting to defect against a Cooperator because $T > R$, and fear as with $P > S$ defection arises as the best strategy against a Defector (see figure 1). Thus, no matter the strategy followed by the opponent, the best option for a rational player is always to defect. By seeking selfishly to maximize his/her own profits, rational players end up in a less desirable collective outcome, instead of $2R$ they get $2P$.

Natural selection is a key mechanism of evolution that operates whenever different types of individuals reproduce at different rates (Nowak M. , 2006) which leads one to expect that every individual should be designed to promote its own evolutionary success at the expense of its competitors. This is why, in the absence of any other assumption and in a well-mixed population, Defectors always have a higher expected payoff than Cooperators, and therefore natural selection rewards selfish behaviour and favours Defectors.

In opposition, cooperation is an altruistic act that is costly to perform, because it means individuals giving up part of their (reproductive) potential in order to benefits others and in favour of a common good

Besides, cooperation is always vulnerable to exploitation by Defectors. Thus, this stated, cooperation future does not look promising.

Yet cooperation is observed on many levels of biological organization, from bacteria and cellular organisms to animals (Nowak M. , 2007). Cooperation is the decisive organizing principle of human society. Many great achievements of humankind were accomplished via cooperation. Additionally, populations of Defectors have a lower fitness than if they played the cooperation role.

So, besides relying on individual social value orientation (Bogaert, Boone, & Declerck, 2007), a concept from social psychology attempting to reflect how much weight a person attaches to the welfare of others in relation to its own, for justifying cooperation, explaining the

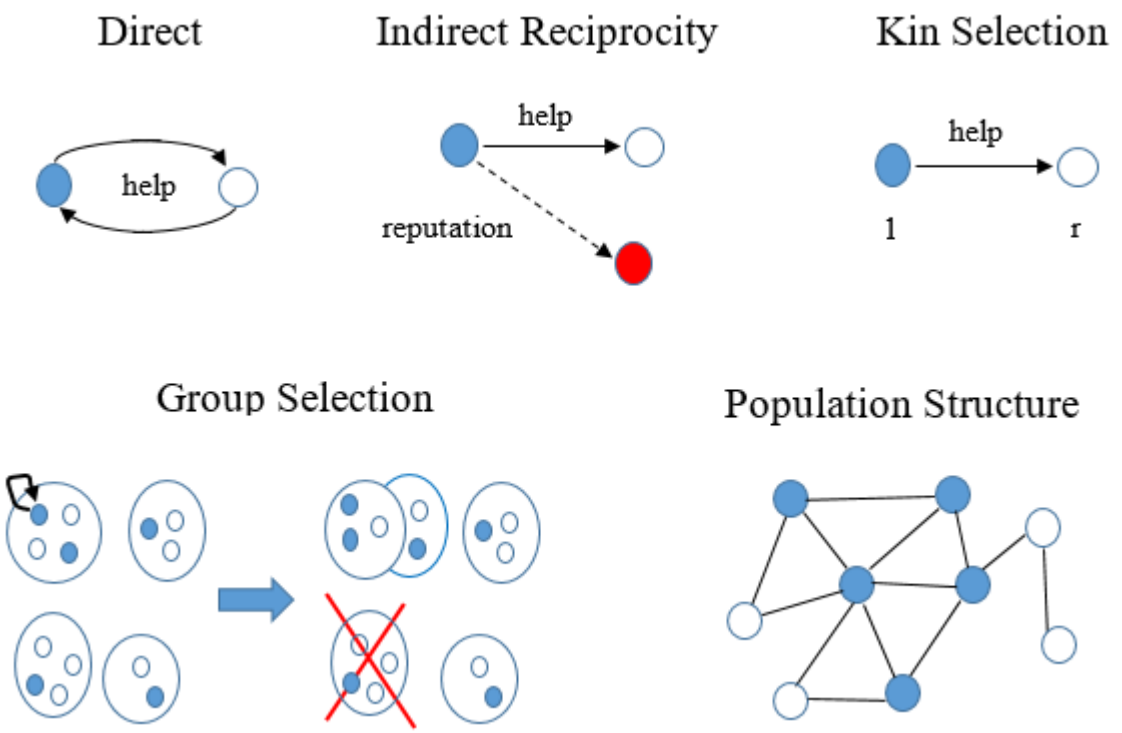

Figure 4- Mechanisms of Cooperation. Clockwise from top left corner direct reciprocity mechanism is presented with individuals repeatedly interacting and helping each other. Indirect reciprocity follows. By helping a peer an individual builds on his reputation. In kin selection the level of help depends on peer relatedness. In group selection when a an individual reproduces in a group already at its maximum capacity the group splits in two and another already existing group is chosen for extinction. Population structure dictates who interacts with whom allowing the formation of cluster

emergence of cooperation requires certain mechanisms in place for natural selection to favour cooperation over defection and to prevent Cooperators from losing ground to Defectors. Such mechanisms will have for sure to offset the costs of cooperation by causing Cooperators to also be on the receiving end more often.

In (Nowak M. , 2007) 5 such mechanisms are identified: kin selection, direct reciprocity, indirect reciprocity, group selection and network reciprocity, which are schematically represented in figure 4. For each mechanism, the authors start from a PD payoff matrix duly adapted with new parameters in order for it to correctly reflect the interaction between two basic strategies with the mechanism in action. In doing so rewards from choosing a cooperation strategy get more appealing. Conditions are even created for cooperation to become an evolutionary stable strategy. A sixth mechanism of punishment was also considered as studied in (Fehr & Gächter, 2002; Fowler & Harpending, 2005).

These mechanisms can be briefly summarized as follows:

- **Kin Selection**- Kin selection operates whenever interactions occur among genetic relatives, i.e., among individuals who are more probable to share a common ancestor

than if they were randomly sampled from the whole population. Relatedness of individuals is defined as the probability of them sharing a gene. The coefficient of relatedness between two individuals, r, a value in the interval [0,1] equals 1/2 for two brothers, 1/8 for cousins (Nowak M. , 2007).

- **Direct Reciprocity**- In nature cooperation between unrelated individuals is noticeable, so kin selection fails short to explain cooperation in more general circumstances. In order to tackle this limitation, (Trivers, 1971) proposed direct reciprocity as another mechanism for the evolution of cooperation based upon the principle of "I will help you if you help me later". The fact of encounters between the same players been repeated turns cooperation more inviting.
- **Indirect Reciprocity**- Direct reciprocity relies on repeated encounters between the same two individuals. Help provided by the donor is less costly than beneficial for the recipient. However, particularly in human relations, interactions are asymmetric and unbalanced. Indirect reciprocity relies on reputation and applies mostly to human relationships. "For direct reciprocity one needs a face, but for indirect reciprocity a name is needed instead". Indirect reciprocity is build out of direct reciprocity witnessed by an interested audience. Encounters are observed by others and information spreads through communication channels, allowing individuals to adopt conditional strategies depending on the reputation of the peer in the game. Direct reciprocity relies on a player's own experience with someone, while indirect reciprocity uses the experience of other players. In indirect reciprocity the help provided may never be returned by the beneficiary, or by individuals who in turn have been helped by the beneficiary (Nowak M. S., 1998).
- **Group Selection**- Group selection also known as multilevel selection is based on the assumption that competition occurs not only between individuals but also between groups. (Traulsen & Nowak, 2006) propose a minimalist stochastic model of group selection where the population is subdivided into n_g groups, which grow in size as individuals within them reproduce. In any one time step, a single individual from the entire population is chosen for (genetic) reproduction with a probability proportional to its payoff. The offspring is added to the same group. When a group reaches a threshold size N, it either divides into two child groups with probability q (in which case a random group from the population is eliminated), or it does not divide (with complementary probability $1 - q$), in which case a random individual in the group is

eliminated so that groups do not get over populated. Social interactions occur only among members of the same group and individuals bearing a mutant allele, a particular form of a gene, help others by decreasing their payoff by c as the counterpart of generating a benefit b to be shared by all other group members. As a result, selfish individuals tend to replicate faster than helpers within groups, but groups comprising helpers grow faster and have a greater chance of dividing before risking extinction.

- **Network Reciprocity** - With no mechanisms to catalyse cooperation, natural selection favours defection because a well-mixed population is assumed where a player potentially can play any other with equal probability. This approximation is used by all standard approaches to evolutionary game dynamics (Nowak M. , 2007). However, in reality populations are not well-mixed and it is not equally likely that a player meets any other. In fact individuals tend to interact with a limited number of peer per geographic reasons or any others. Thus, with network reciprocity populations are supported in networks with individuals at their nodes, links represent interactions and determine who can interact with whom. In this context, it has been shown that cooperation may emerge (or not) depending on the topology of the interaction graph (Santos & Pacheco, 2005; Santos, Pacheco, & Lenaerts, 2006). As discussed in more detail below, the network structure changes the effective game played at a population-wide level, even if, locally, individuals continue to face the same dilemma (Pinheiro, Pacheco, & Santos, 2012). The network reciprocity mechanism relies on two factors. The first is a limitation in the number of game opponents, that is, "depressing anonymity," rather than having an infinite and well-mixed population (Ohtsuki, Hauert, Lieberman, & Nowak, 2006). Second one is a local adaptation mechanism, in which a player can only copy a strategy from a directly linked neighbour as determined by underlying network (Tanimoto, 2015).
- **Punishment**- From an evolutionary perspective, cooperation is a double-edged sword. On the one hand, it brings an edge advantage to a community, since some tasks can only be achieved through cooperation. On the other hand, since punishment involves additional costs (Fehr & Gächter, 2002; Fowler & Harpending, 2005) from an individual's perspective it becomes tempting to enjoy the results of cooperation, without investing in it. This is the typical free-rider problem that characterizes social dilemmas and if allowed to proliferate can break down cooperation. Since selection in evolution takes place on the level of the individual, Cooperators are replaced by free-riders, putting cooperation to an end. In order to discourage free-riders behaviour, a

mechanism of punishment is considered with two main objectives: first one is to expel from the group free-rider members, from which decision a payoff per capita increase results; second one is to account for the costs of a group exclusion in defection strategy, which ends up as a dissuasive measure.

A more exhaustive list of supporting mechanisms for the evolution of cooperation can be found in (Zaggi, 2013).
Of all these cooperation mechanisms considered, this thesis focus on network reciprocity.

2.3. THE SCIENCE OF NETWORKS

A network in its simplest form is a collection of points joined together in pairs by lines. Points are referred to as nodes or vertices (V) and represent the elements in a system, e.g. stations in subway map, and the lines, referred to as links or edges, represent a direct relation between the nodes they connect, e.g. a line connection between two stations.

Many objects of interest in the physical, biological, and social sciences can be thought of as networks. From a modelling standpoint, a network is a relatively simple object, consisting of only nodes and links formally described by $G = (V, E)$ where V represents the set of nodes and $E \subseteq V \, x \, V$ the set of links considered as pairs of nodes linked together.

Social networks is a recent jargon referring to the mesh of social relationships between individuals in a group, community or population. The type of relationships dictates the type of network, be it scientific collaboration, professional, hobby-oriented, etc. The ubiquity of networks far extend social domain, to enter those of transportation /subway, airlines), power grid, telecommunications, health care and others (Kim, Olave-Rojas, Álvarez-Miranda, & Seung-Woo, 2018).

In general, not only are networks shaped from individuals' actions as reciprocally individuals' traits and behaviour are largely influenced by the network (Girard, Hett, & Schunk, 2014). In the particular case of social networks, this individual versus collective behaviour had already been addressed decades ago in Sociology with Structuration theories which emerged as an attempt to dispel division within the social sciences between those who considered social phenomena to be determined by objective social structures (determinism) and others who saw social phenomena as the outcome of human agents subjectively interpreting the world (voluntarism) (Timbrell, Delaney, Chan, Yue, & Gable, 2005).

Most networks being dealt with do not have the regularity of a crystal lattice or the predictable architecture found in throughout biology, e.g. in a flour or in an orange slice. Instead, at first inspection they look as if they were drawn randomly. Identified the nodes, the challenge is to decide where to place links between which nodes in order for the complexity of a real system to be well modelled.

A network as in figure 5 can be completely described by means of the so-called adjacency matrix, A, a squared V x V matrix whose entry a_{ij} values 1 if nodes i and j are connected by a link; 0, otherwise. The matrix is symmetric, i.e., $a_{ij} = a_{ji}$ if links are bidirectional. In some situations, it may be useful to represent links as having a strength, weight or value assigned, usually a real number. This value can represent a bandwidth in an internet link, the electrical tension between two power stations or the travel time between two subway stations. In these circumstances, a_{ij} is no more binary and stores these weights. The diagonal, a_{ii}, concerns loops, i.e., links that start and terminate in the same node.

Along this thesis, only undirected and unweighted networks with no loops will be addressed.

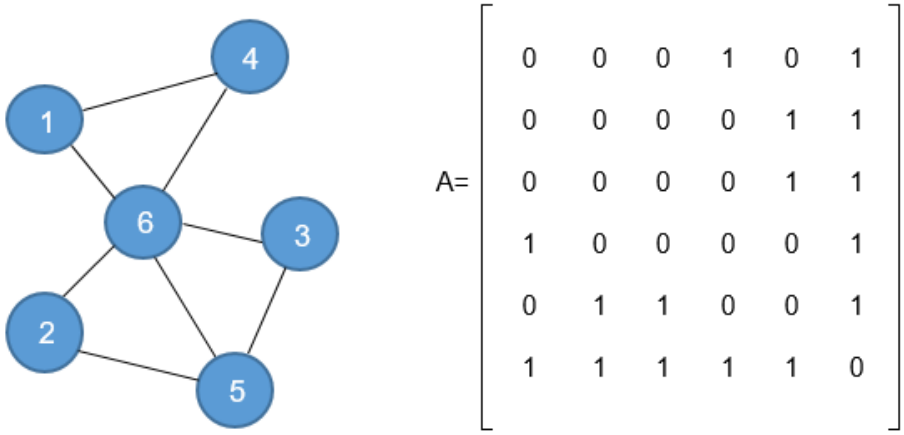

Figure 5- Network Adjacency Matrix

Since the adjacency matrix is not handy to deal with, because its size raises with the square of the number of nodes, and above all is inefficient for sparse networks, a number of concise statistical indicators of centrality are defined in an attempt to capture the essence of the network and allow the generation of a new ones with similar properties. In that sense, it is relevant to revise some of the most important metrics.

Let us consider a network with N nodes and L links. The density of such network is given by the ratio between the effective number of links and the potential number of links the network can accommodate.

$$\text{Density} = \frac{L}{C_2^N} = \frac{2L}{N(N-1)} \tag{57}$$

The number of links that a node i participates can be readly computed from the adjacency matrix as

$$k_i = \sum_j a_{ij} \tag{58}$$

and corresponds to the degree of node i. The degree distribution, D(k), reflects the probability of a node in the network randomly chosen having degree k. The average of D(K) is given by

$$E(k) = \langle k \rangle = \sum_{k=1}^{\max(k)} kD(k) = \frac{2}{N} \sum_{i>j} a_{ij} = 2\frac{L}{N} \tag{59}$$

The second moment of D(k) is given by

$$\sigma_k^2 = E(k^2) - E^2(k) = \langle k^2 \rangle - \langle k \rangle^2 \tag{60}$$

The degree distribution is perhaps the simplest and most frequent property used to characterize networks, as real world networks often exhibit different degree distribution signatures at fixed instants of time and evolving over time.

D(*k*) describes individual nodes' degree distribution regardless of any degree-degree correlation, which are characteristics of many real networks. Thus, in order to address degree-degree correlation, $D(k|k')$ should be calculated. Degree correlations capture the relationship between the degrees of nodes that link to each other. One way to quantify their magnitude is to consider for each particular node i the average degree of its k_i neighbours

$$k_{nn}(k_i) = \frac{1}{k_i} \sum_{j=1}^{N} a_{ij} k_j \tag{61}$$

The average degree of the neighbours of all degree-k nodes is given by

$$k_{nn}(k) = \frac{1}{ND(k)} \sum_{i=1}^{N} \delta_{kk_i} k_{nn}(k_i) \tag{62}$$

where δ_{kk_i} values 1 only for those nodes with degree k. This apparently complex formula boils down to firstly identify all k-degree nodes. Secondly, for each of k-degree nodes, average degree of their neighbours is calculated. Lastly, the average of average degree of k-degree nodes' neighbours is calculated.

In accordance to $k_{nn}(k)$ dependency on k, networks can be classified as:

- **Assortative**, In this networks, as $k_{nn}(k)$ increases with k, the higher the degree *k* of a node, the higher is the average degree of its nearest neighbours

- **Neutral**, $k_{nn}(k)$ has no dependency on k.
- **Disassortative**, $k_{nn}(k)$ decreases with k, so higher degree nodes tend to link with lower ones and vice-versa.

The networks that will be experimented along the thesis, Horand and Scale-free BA to be described in next sections, are neutral. Examples of assortive and disassortive networks are illustrated in figure 6.

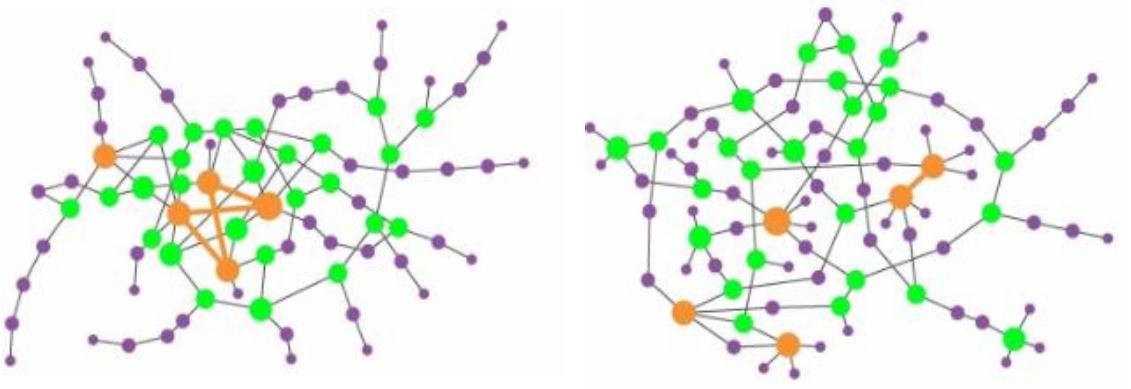

Figure 6- Examples of Network Assortativity and Disassortativity. Source: (Barabási & Pósfai, Network Science, 2016)

Left network concerns an assortative network, where nodes with higher/lower degree connect preferentially with nodes with higher/lower degree. The reciprocal takes place on the right side for a disassortative network. Node colour reflect their degree.

The degree of a node contains no information about the relationship between node's neighbours. For any two neighbours of a node, two patterns can be anticipated: either these nodes are directly connected or they are not. Clustering coefficient captures the degree to which the neighbours of a given node link to each other. As in (Watts & Strogatz, 1998), for a node i with degree k_i, the local clustering coefficient measuring the density of links in node i's immediate neighbourhood is defined as

$$C_i = \frac{L_i}{C_2^{k_i}} = \frac{2L_i}{k_i(k_i - 1)} \tag{63}$$

where Li represents the number of links between the k_i neighbours of node i. C_i values:

- 0, if none of the neighbours of node i link to each other
- 1, if all neighbours of node i link to each other

In general, C_i measures the network's local link density and represents the probability of two randomly chosen neighbours of node i having a common link. The more densely interconnected the neighbourhood of node i are, the higher is its local clustering coefficient.

The clustering of a whole network is captured by the average clustering coefficient, $E(C) = \langle C \rangle$, representing the average of C_i over all nodes

$$\langle C \rangle = \frac{1}{N} \sum_{i=1}^{N} C_i \tag{64}$$

The clustering coefficient is particularly meaningful in social networks where nodes represent individual and links social relations, e.g. friendship. A node having a high clustering means that its related friends are also friendship and that "my friends' friends tend to be my friends". Figure 7 illustrates the calculation of the clustering coefficient.

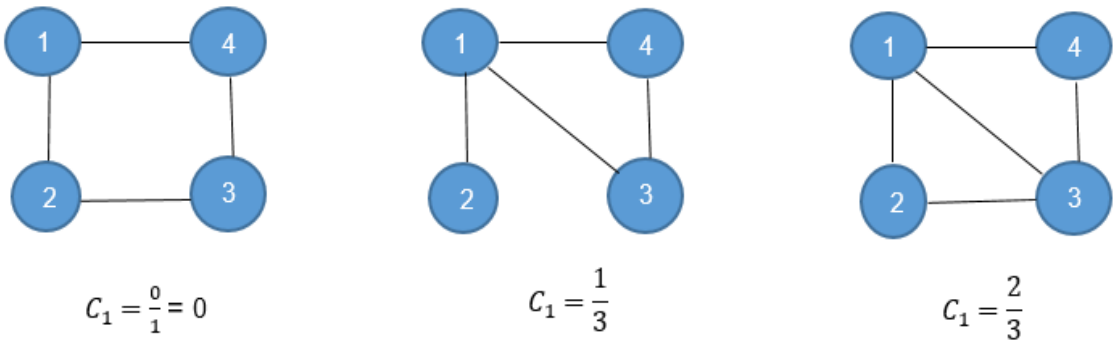

Figure 7- Examples of Clustering Coefficient Calculations for 3 Networks. From left to right panel, node 1 has 2, 3 and 3 neighbours. This means potentially there could be $C_2^2 = 1$, $C_2^3 = 3$ and $C_2^3 = 3$ distinct triangles with node 1 on one of its vertices and two of its neighbours on the other vertices. These values are the denominators of fractions in the figure. Effectively, the numbers of such triangles found in networks from left to right are 0, 1 and 2. On the right panel, triangle 1-2-4 is missing for clustering coefficient to reach value 1.

In networks, physical distance is replaced by path length. A path is a route that runs along the links of the network. A path's length represents the number of links the path contains (Barabási & Pósfai, Network Science, 2016). The shortest path between nodes i and j is the path with the fewest number of links. By definition, the shortest path can never intersect itself, which means it cannot contain loops. The shortest path is often called the distance between nodes i and j, and is denoted by d_{ij}. Multiple shortest paths of the same length d between a pair of nodes can exist.

The average shortest path length of a network, $\langle d \rangle$, is given by

$$\langle d \rangle = \frac{1}{C_2^N} \sum_{i=j=1, i<j}^{N} d_{ij} = \frac{2}{N(N-1)} \sum_{i,j=1, i<j}^{N} d_{ij} \tag{65}$$

where $\langle d \rangle$ is only meaningful for single connected network, i.e., for networks with at least a path connecting any pair of nodes. The average path length, $\langle d \rangle$, gives the expected distance between two randomly chosen different nodes.

The notion of distance can be extended to take into account the weight of each link reflecting space or time separation between nodes. E.g. the algorithms of Dijkstra and Floyd used in navigation applications calculate shortest paths using weighted links (Buescu, 2018).

2.3.1. Models of Networks

It is common to use the terms network and graph interchangeably, however there is a subtle difference. Network refers to real systems with nodes representing entities and links standing for their relationships. Graph is used for the mathematical representation of these networks (Barabási & Pósfai, Network Science, 2016). Network theory by studying graphs as representations of relationships between entities, which can be unidirectional or bidirectional, has applications is diverse areas, both technological and social, such as physics, computer science, engineering, biology, sociology or social networks.

In order to better understand the phenomena modelled by a network, it needs to be characterized by indexes such as the ones presented hereinabove.

These indexes, however, only provide a model of the reality, like a blur photograph. However, and for some applications, having a faithful but static representation of reality only allows anyone to recognize it but an understanding of the process leading to that reality is still lacking. This is exactly what evolving network models attempts to achieve. They capture the way networks are built up by reproducing the steps followed by nature or society when they created the complex systems

Thus, the goal is shifted from simply describing the topology of a network to understanding the mechanisms that shape its evolution allowing its reproduction in laboratory or simulation.

2.3.1.1. Random Networks

A random network, also known as Erdős-Rényi, can be created from a set of N nodes as follows: for each possible pair of nodes in a total of $C_2^N = \frac{N(N-1)}{2}$, a link is traced between the node pair with a probability p.

This implies that the degree of a node follows a binomial distribution. From the N-1 possible links that converge to a node k are activated with probability

$$D(k) = C_2^{N-1} p^k (1-p)^k \quad (66)$$

First moments are:

$$\mu_k = \langle k \rangle = (N-1)p \quad (67)$$

$$\sigma_k^2 = p(1-p)(N-1) \quad (68)$$

Most real networks are sparse, meaning that for them $\langle k \rangle \ll N$. Keeping $\langle k \rangle = (N-1)p$ constant, $\langle k \rangle \ll N$ is equivalent to make N tend to infinity. Under these circumstances, the binomial distribution tends to a Poisson one

$$D(K) = \frac{e^{-\langle k \rangle} \langle k \rangle^k}{k!} \tag{69}$$

with

$$\mu_k = \langle k \rangle \tag{70}$$

$$\sigma_k^2 = \langle k \rangle \tag{71}$$

For most random networks, $\langle d \rangle \approx \frac{\ln(N)}{\ln(\langle k \rangle)}$ offers a good approximation to the average distance between nodes (Barabási, 2013).

This dependency of $\langle d \rangle$ on ln(N) on random network and not on any power of N as in lattice cases is relevant because in many real networks the average distance between two nodes depends logarithmically on N. A network is classified as small-world if the average distance between nodes or the network diameter, i.e., maximum distance between any two nodes, depends logarithmically on the system size.

Apart from all its simplicity, random networks lack two important properties observed in many real-world networks:

- They do not generate local clustering. Because they have a constant and independent probability of two nodes being connected, random networks tend to have a low clustering coefficient.

  The cluster coefficient for a general node in a random network is given by the ratio between the number of triangles formed by a focal node and any two of its neighbours and the total potential number of such triangles. Thus,

  $$C_i = \frac{pC_2^{k_i}}{C_2^{k_i}} = p = \frac{<k>}{N-1} \tag{72}$$

  a number tending to zero for sparse networks.
- Random networks do not lead to the formation of hubs. Additionally, they are characterized by a degree distribution converging to a Poisson distribution, rather than to a power law observed in many real-world networks.

In order to tackle the first of these limitations, the Watts-Strogatz model was conceived, which attempts to reconcile two observations:

- Small-World Property

  In real networks, the average distance between two nodes depends logarithmically on

N (see 2.3.1.1), rather than following a polynomial expected for regular lattices.

- High Clustering

  The average clustering coefficient of real networks is much higher than the one expected for a random network of similar number of nodes and links.

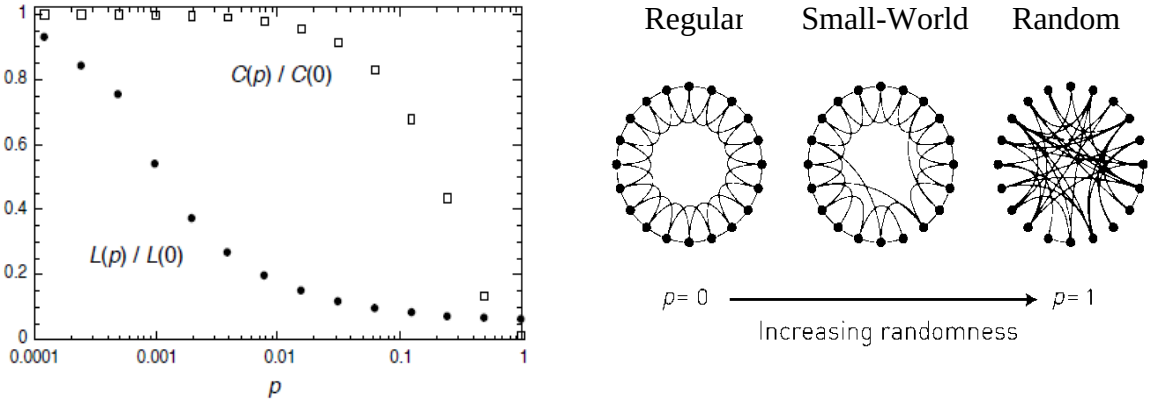

Figure 8- From Regular to Random Neworks. (source: (Watts & Strogatz, 1998)). L is defined as the number of edges in the shortest path between two vertices, averaged over all pairs of nodes. C measures clustering coefficient averaged over all nodes. A probability of $10^{-3}$is enough for making average distance in the network to decay around 45%. A probability of 10^{-2}already makes average distance to decay 80% with almost no degradation of clustering index.

As in figure 8, one starts with a regular ring lattice where nodes are positioned. Each node is connected to $\frac{<k>}{2}$ neighbours on each side, with $\langle k \rangle$ denoting the intended average degree. If $\langle k \rangle$ is odd it is arbitrated which side has regularly minus one neighbours.

In a second step, for each node n_1, the connection to each of its n_2 right side neighbours is considered for rewiring with probability p, a parameter of the algorithm. In case of rewiring, a node n_3 is randomly chosen with uniform probability among those with which n_1 has not yet a connection and excluding n_1. Rewiring consists of n_1 connecting to n_3 and disconnecting from n_2.

The Watts-Strogatz network interpolates between a regular lattice, which has high clustering but lacks the small-world phenomenon, and a random network, which has low clustering, but displays the small-world property.

Because of the small-world character inherited from random network influence via the rewiring mechanism activated, Watts-Strogatz networks are also known as small-world networks .

This small-world effect had already been identified by Stanley Milgram in an experiment conducted in the late sixties that was later coined as six degrees of separation. Surprising

results showed that despite society huge size of 6 billion individuals, by following social links any pair of nodes is on average six links apart, requiring each person to have an average degree lesser than 2 (Barabási & Frangos, Linked, 2002).

2.3.1.2. Horand Networks

In a homogeneous networks such as lattices, all nodes share the same degree implying degree distribution to be a delta function exhibiting a single peak at $\langle k \rangle$.

This useful feature is combined with the small-world one in Horand networks (Santos, Rodrigues, & Pacheco, 2005; Santos F. C., Pinheiro, Lenaerts, & Pacheco, 2012). The construction of a Horand network as in Watts-Strogatz model starts with a regular ring lattice where nodes are positioned. Being $\langle k \rangle$ the intended degree of the network, each node connects to the closest $\frac{<k>}{2}$ nodes on its left and right side. Up to now, the network exhibits the intended degree, has maximum clustering coefficient but lacks small-world feature. Second step of Watts-Strogatz algorithm provides the small-world character but at expenses of degree variation among nodes. To acquire the small-world feature without sacrificing degree homogeneity a pair of links is chosen randomly. Subject to a certain probability p, one node of one link is exchanged with one node in the other link, ensuring no duplication of links among the same pair of nodes. The process is repeated iteratively until a fraction p of all links has been rewired.

The appearance of a Horand network is similar to a Watts-Strogatz one but with a fixed degree distribution.

2.3.1.3. Scale-Free Networks

The degree distribution of a random network is of Poisson form, which means that most nodes have a degree that is close to its average. It implies additionally that there are extremely few nodes highly connected, because the curve falls away from its peak faster than exponentially.

The random model of Erdős-Rényi rests on two simple and often disregarded assumptions. The first one is that the set of nodes if fixed, remains unchanged throughout the network lifetime and is known upfront from the beginning of network conception. The second one is that all nodes are equal. Unable to distinguish between the nodes, they link randomly to each other (Barabási & Frangos, 2002).

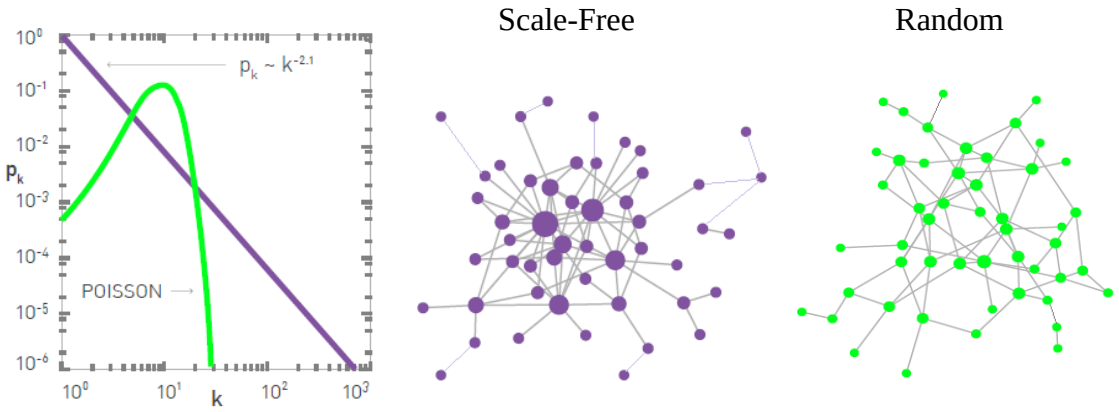

Figure 9- Poisson versus Power-law Distributions. (Source: (Barabási & Pósfai, Network Science, 2016))

On the left panel of figure 9 a Poisson distribution for the probability of finding a node with degree k (p_k) from random networks is compared to a power-law distribution (γ= 2.1) from Scale-free networks on a log-log plot. Both distributions have ⟨k⟩= 11.
On the central and right panel a random and a scale-free networks are plot. Both networks have 50 nodes and $\langle k \rangle = 3$. The size of each node is proportional to its degree.

(Reka, Jeong, & Barabasi, 1999) studied the World Wide Web and found out that degree distribution follows a power law, where the probability of a node having degree k is proportional to $k^{-\gamma}$ with $\gamma \geq 2$. The same conclusion was drawn for other networks analysed as power-grid, Hollywood network of actors or IBM chip wiring diagram. A Scale-Free (SF) network is a network whose degree distribution follows a power law as in figure 9. The SF qualifier derives from the fractal-like character of the network, namely that the distribution of the nodes' degree is preserved no matter the scale of analysis. Thus, for populations tending to infinity, the distribution of the node degree in interval [a, b], apart from a multiplicative factor, is invariant whenever interval boundaries are multiplied by another positive factor.

The second and higher moments of the degree distribution goes to infinity when γ < 3. For many SF networks, γ is located between 2 and 3.

This type of dependency on k, which is not exclusive to the technology field or online communities but also characterizes other networks in the natural world and social fields, is not fortuitous but derives instead from the process conducting to network growth over time.

In (Barabási, 2013) four organizing principles are identified for networks such as web and social networks to be held together. SF is the first organizing principle, which implies that hubs are not only tolerated, but expected. Small-world is the second principle, which states that two nodes are likely to be connected by a relatively short path of nodes, even in a very

large and sparse SF network as the Web. The third principle is of preferential attachment by which newcomers to the network preferably connect to nodes with higher degree. The forth principle is related to the notion of fitness and allows merit to prevailed over seniority and provide competition. Network growth develops over time, new links are stablished between old nodes, but the rate of growth is controlled by the fitness and the nodes with a greater fitness will tend to 'win out' and become very highly connected. This explains why Google or Facebook arrived late to the web but became winners. By viewing networks as dynamical systems that change continuously over time, the SF model embodies a new modelling philosophy.

SF topology is the result of organizing principles acting at each stage of the network formation process. Growth and preferential attachment explain the basic features of many of the networks seen in nature, social networks included. As long as these ingredients are present, it will maintain its hub-dominated SF topology.

One important property of SF networks is resilience against random error. If nodes are removed at random from most types of networks they will eventually fragment into a set of smaller networks or individual nodes, but instead a SF network will remains robust against random decay; it may shrink but not fall apart. It even remains connected indefinitely if $\gamma < 3$ as in the case of World Wide Web. The Achilles' heel of a SF network is an intentional attack targeting the most connected nodes (Barabási, 2013).

(Barabási, 1999) propose an algorithm to generate a SF network with $\gamma = 3$ used extensively along the simulations in this thesis. It starts with m_0 nodes fully connected. Then iteratively nodes are added. Each new node is connected to m distinct nodes ($m \leq m_0$) already part of the network. A new node choses randomly a node in the network to connect to with a probability proportional to its degree. This mechanism favours seniority and creates hubs. In order to avoid a correlation between the index of the nodes and its degree, a final step once the network is constructed consists of scrambling the indexes of the nodes. The average degree of created network tends to $\langle k \rangle = 2m$. SF networks with $\gamma = 3$ are called Barabási-Albert. Barabási-Albert stresses the small-world characteristic of the network by having

$$\langle d \rangle \sim \frac{\ln(N)}{ln(\ln(N))} \tag{73}$$

2.3.1.4. Multilayers

Networks consisting of a set of nodes or vertices connected by links or edges have been typically used to describe for example traffic in a city, interactions between individuals, the

trade among markets or the World Wide Web. Information in the form of news, messages, or digital viruses can be transmitted through networks, as well as infectious diseases or general goods. Several algorithms have been proposed to generate and replicate the most important structural properties of real-world networks from which examples were presented in previous chapters.

In spite of the progress achieved in network science during recent decades, traditionally one has assumed that nodes are connected to each other within the same, isolated infrastructure, the so-called single-layer network.

This assumption, however, may in some circumstances be an oversimplification, considering that some nodes can simultaneously be the building blocks of more than just one network. This important consideration applies to natural as well as to social systems. Many complex systems demand manifold resources to be supplied from distinct channels to function properly, such as water, gas, and electricity for a city (De Domenico, et al., 2013).

As major cities are interconnected not just by means of roads, but also by means of rails, as well as by means of air transportation, similarly, people interact face-to-face, via phone, on online social networks, in their work environment, and so on (Min, 2014). It is thus often justified to abandon the traditional assumption of a single-layer network and replace it with a multilayer network formalism. Not surprisingly then, the multilayer network, defined as a combination class of networks that are interrelated in a nontrivial way, has recently emerged as a fundamental concept to quantitatively describe the interactions not just within, but also among different networks.

Networks of networks have been brought to the spotlight by the discovery that even small and seemingly irrelevant changes in one network can have catastrophic and very much unexpected consequence in another network (Buldyrev, Parshani, Paul, Stanley, & Havlin, 2010).

What sets a multilayer network apart from the traditional single-layer network is that a multilayer network typically consists of M ($M > 1$) networks (or layers), where the nodes in each network (layer) are connected via intra-layer links, but there may be also inter-layer links that connect together nodes from other networks. Sometimes the inter-layer links do not serve to connect the nodes, but merely serve to communicate information or some other form of influence between the nodes forming the M networks.

The same node may appear in more than one network and sometimes all the nodes pertain to all M networks with the difference between them being the intra-layer links. Depending on these particularities, the terminology that is used also varies.

One of the challenges in network theory is therefore to treat together ties of different kind preserving existing differences. The multilayer metaphor, which allows to distinguish the different kinds of relationships among a set of nodes, constitutes a promising framework to study and model multilayer systems.

If evolutionary games are played on multiplex networks, strategy imitation and payoff accumulation can take place either in the local neighbourhood of a particular layer or across the layers, since all nodes exist in all layer.

2.3.1.5. Definition of a Multilayer Network

When nodes are connected to each other in a single infrastructure one has a single-layer network or graph formally described by G = (V, E) where V represents the set of nodes and E $\subseteq$ V x V the set of links considered as pairs of nodes linked together.

However, a single-layer can be an oversimplification, e.g. if nodes represent airports and the links the different airline companies flights. Airlines have their own set of connections linking the airports, constituting a layer of coverage independent from the ones corresponding to other companies. Whenever there are different infrastructures to consider and there are costs flowing between them, it is preferable to consider a multilayer formally described as $G_M = (V_M, E_M)$ where M represents the number of layers, $V_M = \ U_{\alpha=1}^{M} \ V_\alpha \ with \ V_\alpha = \{V_1^\alpha, \dots, V_{N_\alpha}^\alpha\}$ and N_α equal to the number of nodes in layer α. V_α and V_M represent, respectively, the set of nodes in layer α and in the all multilayer.

In what concerns multilayer edges one has $E_M = \{E_\alpha \ U \ E_{\alpha\beta} : \alpha, \beta \epsilon \{1, \dots, M\}, \alpha \neq \beta\}$ with $E_\alpha \subseteq \ V_\alpha x \ V_\alpha$ and $E_{\alpha\beta} \subseteq \ V_\alpha x \ V_\beta$.

According to (Wang, Wang, Szolnoki, & Perc, 2015) and as in figure 10 multilayers can be classified into three broad categories:

- **Multiplex Networks**

  In a multiplex network all the layers contain the same set of nodes or share at least some fraction of the nodes. The difference between the layers is the way the nodes are connected with each other in each particular layer.

  The network of airports can be translated into a multiplex form with different layers consisting of the routes of different airplane carriers. The collaboration and the citation networks constitute another example of layers of a multiplex.

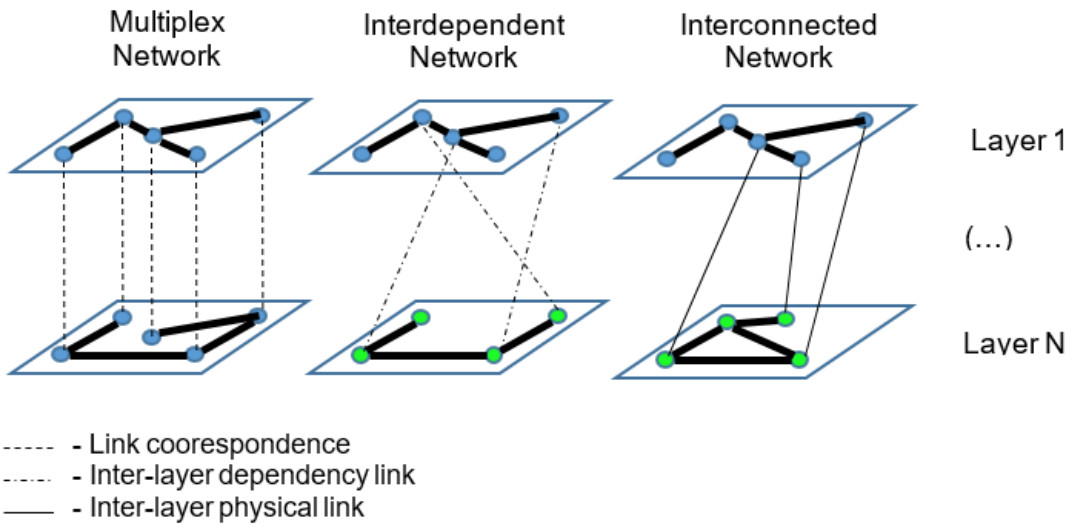

Figure 10- Multilayer Networks. Multiplex network have the same nodes across all layers. Interdependent networks typically have different nodes in different layers. Additionally well-being of nodes in one layer may depend of the well-being of other nodes in other layers. Interconnected network are like interdependent ones but with physical connections inter-layer. In all the three types of multilayers intra-layer connections are independent across layers.

All layers having the same nodes and no inter-layer links can be formally expressed as $V_\alpha \cap V_\beta = V_M = V, \forall\, \alpha \neq \beta$. Additionally, $E_{\alpha\beta} = \emptyset, \forall\, \alpha \neq \beta$, i.e., no links between layers.

- **Interdependent Networks**

  An interdependent network is typical made up of two or more different networks, such that there is little or no overlap between the nodes in the different layers. The performance of nodes in a particular layer depend on the performance of nodes in a different layer, and vice versa. Thus, there exists the so-called dependency links between the nodes that are part of different layers. These links are not actual physical links, but rather imaginary links that denote the co-dependence; hence the name interdependent networks.

  The concept of interdependent networks is referred to in (Buldyrev, Parshani, Paul, Stanley, & Havlin, 2010) where cascading failures between an electrical grid network and a computer network are studied. Airports and seaport networks can be interpreted as interdependent networks, because the proper functioning of a seaport may depend on goods delivered by air.

Each layer having different types of nodes and there being no dependency links (not physical connections) between the nodes can be formalized as $V_\alpha \cap V_\beta = \emptyset \, \forall \, \alpha \neq \beta$.

- **Interconnected networks**

  An interconnected network is similar to an interdependent network in that it is typical made up of two or more different networks, such that there is little or no overlap between the nodes in the different layers. In the interconnected network, however, there are actual physical links that connect together the nodes from different layers. Interconnected networks can thus be regarded as interconnected communities or clusters within a single larger network.

  The climate network can be decomposed into different network interconnected layers in exploiting the stratification and circulation of the terrestrial atmosphere.

  Each layer having different types of nodes and there being actual physical links between the nodes in different layers can be formalized as $\exists \alpha, \beta \in \{1, \dots, M\} \, V_\alpha \cap V_\beta \neq \emptyset \, \wedge \alpha \neq \beta$.

Real multiplex networks are far from random superposition of their constituent layer topologies. Instead, the degrees of the same nodes in different layers may be correlated, as they may tend to connect to similar nodes in different layers creating overlapping edges.

In this thesis only multiplex networks will be addressed. Whenever hereafter multilayer social network are referred to, it is its multiplex variant to be assumed.

2.3.1.6. Degree-Degree Correlation

An interesting property observed in real multiplex networks is the presence of correlations between the degrees of the same node at different layers. This is normally signalled by the fact that the probability $P(k^\alpha = k_1 1, k^\beta = k_2)$ to find a node with degree k_1 on layer α and degree k_2 on layer β does not factorize in the product $P^\alpha(k)P^\beta(k)$ of the degree distributions of the two layers.

Within a layer, degree correlation captures the relationship between the degrees of nodes linking to each other. Layers can be assortative, if nodes with a higher (lower) degree tend to link to nodes with a higher (lower) degree, disassortative if the trend is the other way around or neutral if no trend is identified.

Multiplex networks, because of having the same nodes in all layers, allow the extension of intra-layer degree correlation concept to multiplex scope. This is the rationale behind degree-

degree correlation index designed to quantify assortative (disassortative) mixing pattern between layers. The degree-degree correlation is evident in social networks. If a famous individual like a singer or a sportsman is famous in one network, e.g. Facebook or Twitter, probability he/she will also be famous in another one. Degree-degree correlation is supposed to reflect this assortative pattern.

(Nicosia & Latora, 2015) propose several methods to calculate degree-degree correlations. One possibility is the Pearson's linear correlation coefficient. If $k_i^{\alpha}$and k_i^{β} denote respectively de degree of node i in layer α and β, Pearson's correlation coefficient of the two-degree sequences is defined as:

$$r_{\alpha\beta} = \frac{\frac{1}{N}\sum_{i=1}^{N} k_i^{\alpha}k_i^{\beta} - \frac{1}{N^2}\sum_{i=1}^{N} k_i^{\alpha}\sum_{i=1}^{N} k_i^{\beta}}{\sqrt{\frac{1}{N}\sum_{i=1}^{N}(k_i^{\alpha})^2 - (\frac{1}{N}\sum_{i=1}^{N} k_i^{\alpha})^2}\sqrt{\frac{1}{N}\sum_{i=1}^{N}(k_i^{\beta})^2 - (\frac{1}{N}\sum_{i=1}^{N} k_i^{\beta})^2}} \tag{74}$$

which can succinctly be stated as

$$r_{\alpha\beta} = \frac{<k_i^{\alpha}k_i^{\beta}> - <k_i^{\alpha}><k_i^{\beta}>}{\sigma_{k^{\alpha}}\sigma_{k^{\beta}}} \tag{75}$$

Another possibility is to use the Spearman's rank correlation coefficient, which for the two R_i^{α} and R_i^{β} rank sequences of degree in layer α and β, respectively, is given by:

$$\rho^{\alpha,\beta} = \frac{\sum_i (R_i^{\alpha} - \overline{R^{\alpha}})(R_i^{\beta} - \overline{R^{\beta}})}{\sqrt{\sum_i (R_i^{\alpha} - \overline{R^{\alpha}})^2 \sum_j (R_j^{\beta} - \overline{R^{\beta}})^2}} \tag{76}$$

where R_i^{α} and $R_i^{\beta}$are the ranks of node i due to its degree in layers α and β, respectively, and $\overline{R^{\alpha}}$ and $\overline{R^{\beta}}$ are the average ranks of nodes in the same layers[1].

A third alternative would be to use Kendall's τ rank correlation coefficient.

(Nicosia & Latora, 2015) calculate the 3 correlation coefficients for American Physical Society co-authorship network with 10 layers each one assigned to subfields or research area. The procedure is repeated for IMDb network of collaboration between actors with layers defined according to movie genre. In both networks, the 3 correlation coefficients provide a consistent indication about assortativeness between layers.

(Nicosia & Latora, 2015) provide two algorithms based on simulated annealing to construct multiplex networks with controllable inter-layer degree-degree correlation, useful for

[1] Within layer α, node i having rank R_i^{α} means that in this layer nodes with an higher degree than i's have $R_i^{\alpha} - 1$ distinct values of degree. E.g., nodes with second greater degree in a layer have rank 2 in that layer.

simulations in order to better understand how degree correlations across layers influence multiplex performance.

2.3.1.7. Overlapping

In multiplexes, networks nodes take part in all layers of networks simultaneously. Social networks where each individual node has different kind of social ties, one for family ones, another for friendship, for professional, etc., or transportation systems where each location is connected to another location by different types of transport, one per layer, are just examples of multiplex characterized by a significant overlap of the links in different layers (Bianconi, 2013).

Overlapping between two layers α and β provides an indicator on how probable it is for an arbitrary pair of nodes to be linked in both layers. It is defined according to (Battiston, Matjaz, & Latora, 2017) as

$$\text{overlapping}^{\alpha\beta} = \frac{\sum_{i<j} a_{ij}^{\alpha} a_{ij}^{\beta}}{\sum_{i<j} a_{ij}^{\alpha} + \sum_{i<j} a_{ij}^{\beta} - \sum_{i<j} a_{ij}^{\alpha} a_{ij}^{\beta}} \tag{77}$$

with a_{ij}^{α} and a_{ij}^{β} representing, respectively, the adjacency matrixes in layers α and β and

$$a_{ij}^{\alpha} = \begin{cases} 1, \text{ if nodes } i \text{ and } j \text{ are linked in layer } \alpha \\ 0, \text{ otherwise} \end{cases} \tag{78}$$

Overlap between two layers falls in the interval $[0,1]$. Minimum value is achieved if layers have no links in common. Maximum value reflects the case of both layers coinciding. Degree-degree correlation is a more relaxed measure of the similarity between layers, because a correlation of 1 does not imply layers' coincidence. It only concerns the same node on different layers having the same number of neighbours no matter if they differ between layers.

The overlapping of the whole multiplex can be defined as the average of the overlap for every pair of layers:

$$\begin{aligned} \text{overlapping} \; = \; & \frac{1}{C_2^M} \sum_{\alpha=1,\beta=1,\alpha<\beta}^{M} \text{overlapping}^{\alpha\beta} = \\ & \frac{2}{M(M-1)} \sum_{\alpha=1,\beta=1,\alpha<\beta}^{M} \text{overlapping}^{\alpha\beta} \end{aligned} \tag{79}$$

2.4. Evolutionary Games on Structured Populations

Evolutionary Game Theory is a mathematical approach aiming to describe the competition of species in an ecosystem, the interaction between individuals of distinct populations, whether they are molecules, living organisms or humans ideas and behaviours. The mechanism that leads to the evolution of cooperation in these settings could be called 'spatial

selection': Cooperators prevail against Defectors by clustering in physical or other spaces (Nowak, Tarnita, & Antal, 2010; Szabo & Fath, 2007).

Mean-field-type behaviour occurs for two drastically different graph structures with N, the number of nodes, tending to infinity. Mean-field approximation is exact by definition for those systems where all pairs are linked, i.e., the corresponding graph is complete. A similar mean-field behaviour arises if each player's payoff derive from games with only a finite number of players chosen randomly in every evolutionary step, as long as choice of a peer in one step is memoryless, i.e., with no correlation with previous choices (Szabo & Fath, 2007).

In the mean-field approach, a macroscopic population-level aggregated description of the state of the population expressed as a frequency is adequate. However, when mean-field conditions do not apply, a more detailed, lower-level analysis is required. Such a lower-level approach is usually termed "agent-based", since on this level individual agents are the basic units of the model. The agent-level dynamics of the system are usually defined by strategy update rules, which describe how the agents perceive their surrounding environment, what information they acquire, what believes and expectations they build from experience, and how this all maps to strategy updates during the game. These rules can genetically code Darwinian selection or boundedly rational human learning.

In real-world systems players do not interact with all other players but instead are located as nodes of a network, which determines who interacts with whom (Santos & Pacheco, 2005), but also who may be imitated. (Ohtsuki, Pacheco, & Nowak, 2007) propose a model with two networks, one determining the peers playing the game from which payoff is collected and fitness calculated; another one specifying the geometry of evolutionary competition and updating. Latter one can potentially have weights on the links characterizing the strength of influence among neighbours and have them unidirectional if asymmetry in the teaching-learning activity between the connected players is relevant (Szolnoki & Szabo, 2007). Along this thesis, both the game interactions and the learning mechanisms will be based on the same network of undirected connectivity and with unitary link's weight.

The effects of population structure on the outcome of evolutionary games is sensitive to a number of factors: population dynamics (Zukewich, Kurella, Doebeli, & Hauert, 2013), translation of payoffs into fitness, the diversity of players (Pacheco, Pinheiro, & Santos, 2009), and the type of game played. For example, spatial structure tends to support cooperation in the PD but conversely, in the snowdrift game, spatial structure may be detrimental (Hauert & Doebeli, 2004). Global dynamic features of the evolutionary process experimented at population level, such as the frequency and distribution of Cooperators, are

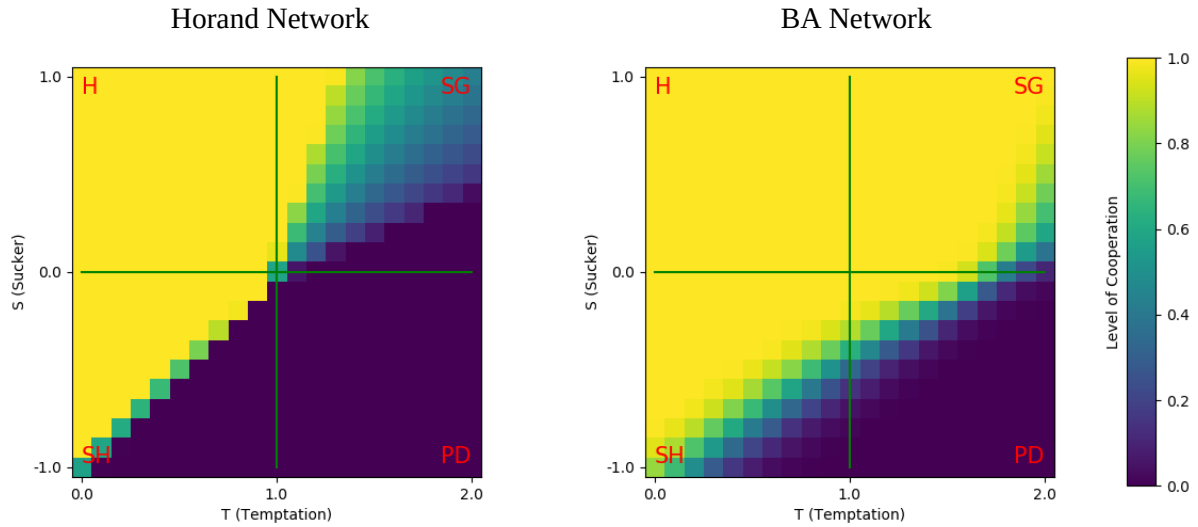

Figure 11-Effects of Population Structure on 2-Player Games. On the left panel, population was supported on a Horand network with $\beta = 1, \langle k \rangle = 4$. Left panel concerns a BA network with $\beta = 0.1, \langle k \rangle = 4$. For both panels $R = 1, P = 0$. Cooperation territory is larger in left panel. Yellow areas in Prisoner Dilemma Game quadrant correspond to a global coordination dynamic. This heat map reproduces results already obtained in (Pinheiro, Pacheco, & Santos, 2012)

determined by local mechanisms at individual level, such as the way payoffs are calculated and the rate at which interactions take place (Maciejewski, Fu, & Hauert, 2014).

Figure 11 compares two network structures illustrating how underlying network affects cooperation.

2.4.1. Accumulated versus Average Payoffs

Individuals collect payoffs, a proxy for fitness, from interaction with their neighbours. For homogeneous network, accumulated versus average payoffs is an issue of minor relevance. However, things are different for heterogeneous networks. If payoffs are accumulated, heterogeneous structures further promote the evolution of cooperation (Santos & Pacheco, 2006); in contrast, averaging the game payoffs can remove the ability for SF graphs to sustain higher levels of cooperation.

In heterogeneous populations, the range of payoffs depends on the payoff accounting: if payoffs are averaged, the range is determined by the maximum and minimum values in the payoff matrix but if payoffs are accumulated the range additionally depends on the size and structure of the population. The frontier in T-S plan (see figure 11) between the cooperative and defective regions get blurred, wider besides moving South-Eastwards (Maciejewski, Fu, & Hauert, 2014).

When accumulated payoff is adopted and considering payoff matrix from table 2, partial payoffs collected by individual i are

$$p_i^C = k_i^C R + k_i^D S \quad (80)$$

$$p_i^D = k_i^C T + k_i^D P \quad (81)$$

where k_i^C and k_i^D represent, respectively, the number of Cooperators and Defectors neighbours of individual i. Were average payoffs considered instead and the sum of previous partial payoffs would have to be divided by $k_i^C + k_i^D$.

These calculations are extendable to multiplex scenarios. Accumulated payoffs for an individual are the sum of all payoffs acquired with all neighbours in all layers. Average payoff is the average across layers of the accumulated payoff in each layer (Kleineberg & Helbing, 2018).

The intrinsic advantage of some vertices in a graph over others can be further enhanced through game interactions leading to differences in fitness that depend on an individual's strategy as well as its position on the graph. For example, a Cooperator occupying a favourable vertex can more easily establish a cluster of Cooperators, which creates a positive feedback through mutual increases in fitness. Conversely, a favourable vertex also supports the formation of a cluster of Defectors but this results in a negative feedback and lowers the fitness of the Defector in the favourable vertex. The fact that heterogeneity can promote cooperation was first observed for the PD and snowdrift games (Santos & Pacheco, 2005; Santos, Pacheco, & Lenaerts, 2006; Santos F. C., Pinheiro, Lenaerts, & Pacheco, 2012) and was subsequently confirmed for PGG (Santos, Santos, & Pacheco, 2008; Santos M. , Pinheiro, Santos, & Pacheco, 2012). However, the detailed effects not only crucially depend on the dynamics but also on how fitness is determined. For example, heterogeneous population structures favour cooperation if payoffs from game interactions are accumulated but that advantage disappears if payoffs are averaged (Szolnoki, Perc, & Danku, 2007).

2.4.2. Update Rules

Strategy revision opportunities can happen synchronously or asynchronously. In synchronous update, the whole population updates simultaneously in discrete time steps, resulting in a discrete-time dynamics at the macro level. Synchronous update is typical of biological models when generations are discernible in time or with seasonal character.

In many real social systems, the players modify their strategies independently of each other. For these systems, random sequential (asynchronous) update provides a more appropriate description.

Asynchronous update is the option taken along the thesis. Time is discrete and an opportunity for a strategy update occurs at every time step.

Defined the timing for strategy update, the attention is now turned to the underlying population dynamics. In heterogeneous graphs, nodes vary in their degree and have therefore a different number of interactions contributing to their fitness. Because of this, with accumulated payoff, some node positions become more advantageous to occupy than others. Which sites are favoured depends on the type of population dynamics. E.g., for the Moran process in structured populations it is important to distinguish between birth-death and death-birth updating. In the former case, a node is randomly selected for reproduction with a probability proportional to its fitness and then the cloned offspring replaces a uniformly random selected neighbour. In the latter case, firstly an individual is selected at random to die and then the vacant site is repopulated with the offspring of a neighbouring node with a probability proportional to its fitness. Even in homogenous populations the sequence of events is of crucial importance but becomes even more pronounced in heterogeneous structures (Ohtsuki, Hauert, Lieberman, & Nowak, 2006). Because of its dynamics, in death-birth updating, all nodes share the same expected life time, but highly-connected nodes will get more frequently a chance to produce offspring, since they have more dying neighbours and are thus more favoured than vertices with few neighbours.

In social networks, reproduction assumes the form of a cultural process of learning and imitation. Imitation constitutes a wide class of microscopic update rules. The essence of imitation is that an individual having the chance to revise his strategy copies the one from a neighbour with a certain probability. The neighbour's strategy is preserved, it only plays a catalysing role. Imitation is non-innovative because it may never introduce a strategy which is not already present in the population. Two variables are relevant in an imitation processes: whom to imitate and with what probability. A node with a strategy to be copied can be identified by randomly choosing among neighbours with a probability uniform or proportional to node fitness. The imitation probability may depend on the information available for the copying node, depending whether only the strategy used by neighbours is known or if both strategies and payoffs are available.

Along this thesis, at each time step a node A is chosen with uniform probability to revise its strategy. Afterwards, a reference node B candidate to have its strategy copied is randomly chosen with uniform probability from the set of A neighbours. If nodes have different strategies, node A will copy node B strategy with a probability given by Fermi distribution (Traulsen, Nowak, & Pacheco, 2006)

$$\text{Prob}(S_B \rightarrow S_A) = \frac{1}{1 + e^{-\beta(P_B - P_A)}} \tag{82}$$

β, a positive amount, stands for the intensity of selection, also known as selection pressure, a factor amplifying payoff differential. P_A and P_B represent the payoffs accomplished so far by nodes A and B. Two extreme cases are to be considered depending on the argument of the exponential. If node A has a much higher payoff than node B, then the exponential tends to positive infinity, and with probability tending to zero node A will copy node B strategy. In the opposite extreme, node B being the one to have a much higher payoff, then with a probability close to 1 node A will copy node B strategy. In an intermediate scenario where both nodes have equal probabilities, there is a 50% chance of node A copying the strategy from node B.

For the multiplex case, there is a previous additional action in each time step: choosing a layer with uniform probability. With a layer chosen, the algorithm for the identification of nodes A and B just presented applies but circumscribed to the chosen layer. Node A and node B payoffs to consider in Fermi distribution encompass all layers. More precisely, as stated in previous section, the payoff of each individual to be compared in equation 82 accounts for the sum of payoffs collected by the individual in each game played against his/her neighbours across all layers.

Firstly a layer, layer l, is selected with uniform probability. Within this chosen layer l, a node is selected with uniform probability: node A. Next, with uniform probability one of the neighbours of node A in selected layer l is chosen: node B.

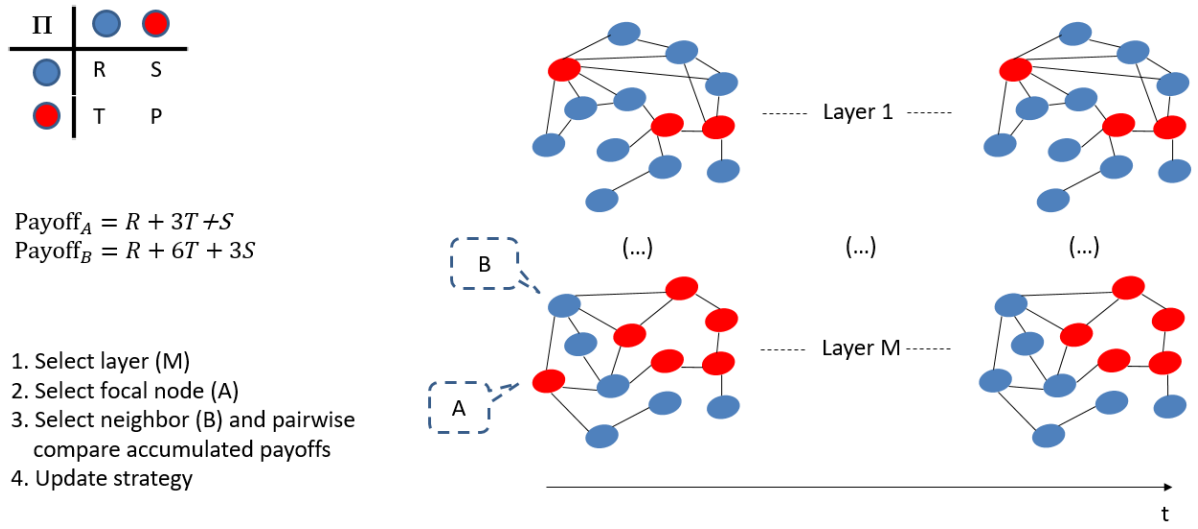

Figure 12 depicts the application of this update rule on a multiplex with last layer being the chosen one.

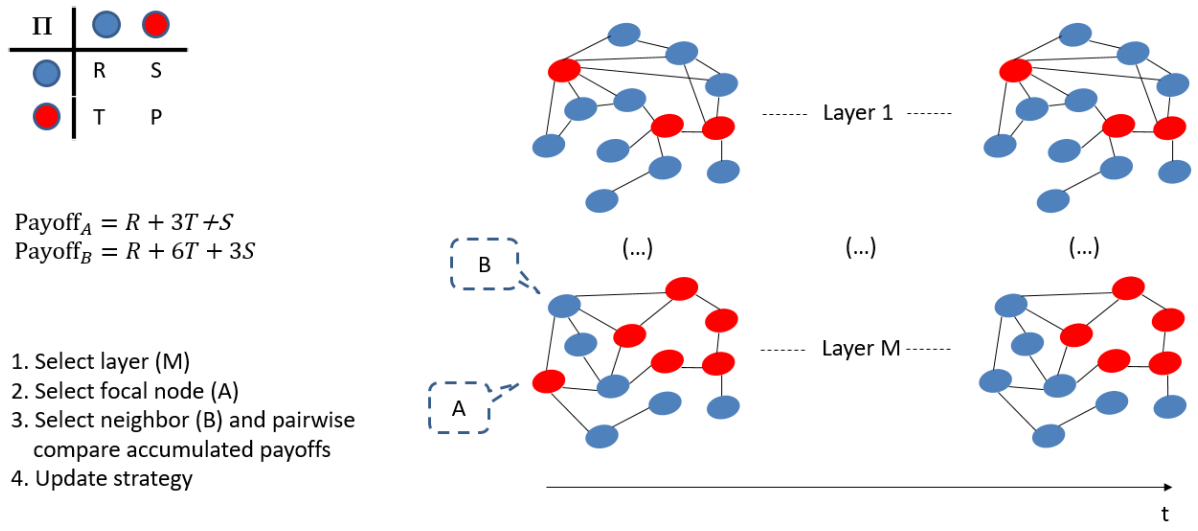

Figure 12- Application of Update Rule in a Multiplex

Considering only the two layers presented in the figure, i.e., $M = 2$, and according to payoff matrix recovered from table 2, node A has an accumulated payoff of $R + 3T + S$. Node B has an accumulated payoff of $R + 6T + 3S$. Were averaged payoff considered and the calculated payoffs would have to be divided by M. With the probability given by Fermi distribution applied to payoffs differential, node A copies strategy from node B. Even if node B is performing poorly in the chosen layer, $R + 3S$, it may have a good global payoff, becoming appealing for strategy copy. Moreover, it is node B's strategy in the chosen layer to be copied, although it may differ from strategies in other layers, which may have contributed the most to overall node payoff. In the example, the blue strategy of node B is appealing to be copied in layer M, although its payoff is mostly due to red strategy followed in first layer.

2.4.3. Gradient of Selection

Dynamical processes involving populations of individuals constitute challenging examples of complex systems, in which the behaviour of the whole is difficult to predict from behaviours at individual level.

Studies developed to understand the global dynamics of cooperative scenarios promoted by network topologies and how they relate to local self-regarding actions result either from numerical simulations and analysis of equilibrium, e.g. (Santos & Pacheco, 2005; Santos, Santos, & Pacheco, 2008; Szabo & Fath, 2007; Szabo & Tőke, 1998), or from an analytical determination of the conditions for fixation of strategies in the population, e.g. (Ohtsuki &

Nowak, 2006; Traulsen, Shoresh, & Nowak, 2008), failing to explain how a strategy co-exists or outcompetes another. The weakness of analytical studies stem from their validity scope, often requiring unrealistic population structures or other extreme conditions such as weak-selection for Moran processes, which means having $w \ll 1$ when fitness (f) is related to payoff (π) as in

$$f = (1 - w) + w\pi \tag{83}$$

Besides, these studies target on fixation probabilities, a concept specific to biology, missing the nexus between the network topology and the evolutionary dynamics created. Until (Pinheiro, Pacheco, & Santos, 2012), network studies failed to characterize the self-organizing process by which one strategy co-exists with or displaces the other.

In order to shed some light on the topological mechanism that departing from networked individuals engaged in a local game leads to a global, population wide, behavioural dynamics which deviates strongly from the original one, (Pinheiro, Pacheco, & Santos, 2012) define an average gradient of selection (AGoS) to track the self-organization of Cooperators when interacting with Defectors under network reciprocity. At any point in time, AGoS reflects the expected increase in the number of Cooperators in the population. In arbitrary network populations, it is not possible to derive a closed form expression for the AGoS, but it can be numerically calculated. It allows assessing the role of population structure in the evolutionary dynamics since it is by design similar to the replicator equation in an infinite well-mixed population.

For AGoS calculation, evolution is modelled via a stochastic birth-death process where each individual i with payoff p_i adopts the strategy of a randomly selected neighbour j with payoff p_j with probability given by the Fermi function

$$p = \frac{1}{1 + e^{-\beta(p_j - p_i)}} \tag{84}$$

For each individual i, the probability of imitating the behaviour of any of its neighbours at time t, $T_i(t)$, is given by

$$T_i(t) = \frac{1}{k_i} \sum_{j=1}^{n_i} \frac{1}{1 + e^{-\beta(p_j - p_i)}} \tag{85}$$

with k_i and n_i representing, respectively, the degree of i and the number of its neighbours with a different strategy then the one from i.

If $T_i(t)$ is averaged across all Cooperators or Defectors, one obtains the probability for the population at time t to decrement or increment by 1 the number of Cooperators, respectively, $T_A^-(c,t)$ and $T_A^+(c,t)$, given by

$$T_A^{\pm}(c,t) = \frac{1}{N} \sum_{\substack{j=1,AllDs \\ j=1,AllCs}}^{N} T_j(t) \tag{86}$$

The first parameter in $T_A^{\pm}(c,t)$ was added to make explicit the dependency of this variable on the number of Cooperators in the population.

During the course of simulation s at time t, the expected increase in the number of Cooperators in the population already with c Cooperators is given by

$$G_s(c,t) = T_A^+(c,t) - T_A^-(c,t) \tag{87}$$

a quantity with an absolute value no greater than 1.

Trusting on the ergodicity of the process, which means that averages over probability space and over time coincide, AGoS is obtained by averaging $G_s(c,t)$ across the time of a large number of samples:

$$\text{AGoS(c)} = \frac{1}{\Lambda\Omega} \sum_{s \in \Lambda} \sum_{t \in \Omega} G_s(c,t) \tag{88}$$

where Λ represents the space dimension of all network evolutionary simulations. Ω represents the number of time steps per simulation.

In a network with N nodes, there are $C_c^N = \frac{N!}{(N-c)!c!}$ distinct configurations with c Cooperators. Along the evolution simulations, some strategy configurations will be more likely than others, e.g. movements from uncorrelated assortments to correlated ones should be more probable than the other way round, which will make the probabilities of the various configurations with c Cooperators unequal.

In order for AGoS to be drawn for all possible c number of Cooperators and for a maximum number of distinct configurations with c Cooperators to be evaluated, each simulation in the Λ space is to be initialized with Cooperators randomly positioned in the network in a number given by a uniformly distributed variable in the interval [0, N], in order to prevent lack of observations in the state space.

AGoS being a topology dependent mean-field descriptor for a structured population can be computed for arbitrary population structure and arbitrary game parameterization.

Figure 13 exemplifies possible shapes for AGoS.

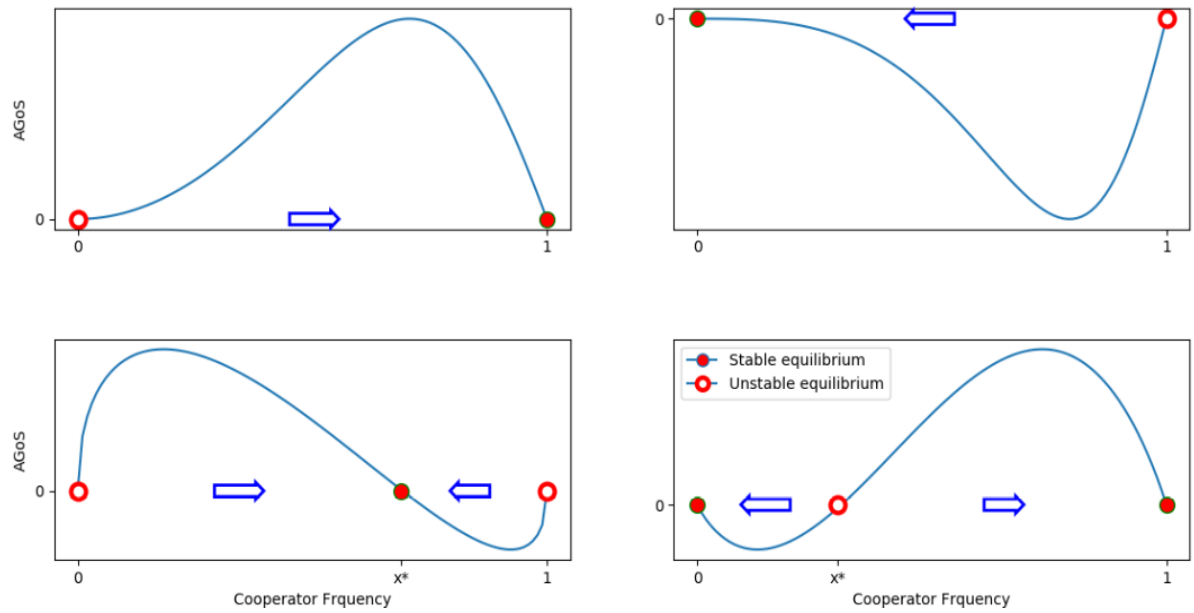

Figure 13-Average Gradient of Selection

Average Gradient of Selection in structured populations are measured across networks randomly sampled from a set of networks of the same type, e.g. Horand vrs BA, degree, assortativity, etc.

Clockwise, starting in top left corner in first panel, the network will evolve towards Full Cooperation. In next panel the evolution is toward Full Defection. In next panel, the network is bound to either Full Cooperation or Full Defection, final destination depending on initial Cooperator frequency in relation to critical frequency x*. One has a Coordination Game. In last panel, the system converges to a strategy co-existence scenario. The type of network or the relative values of payoff matrix contribute to dictate the type of AGoS applicable.

2.4.4. The Structure of Social Graphs

The connectivity structure can be characterized by a number of topological properties presented in section 2.3. The graphs to consider along the thesis are all connected, meaning there is at least one path along links between any pair of nodes.

Networks co-exist in different layers of a multiplex. All layers share the same set of nodes, but with a layer specific link set. Nodes in different layers may have degree-degree correlation or links have a certain amount of overlapping between layers.

Square lattices are one of the simplest networks. They can be a lattice with von Neumann neighbourhood, 4 connections between nearest neighbour nodes, or Moore neighbourhood with connections between nearest and next-nearest neighbours, in a total of 8, etc. It may be the case that regular lattice only provides an initial structure for the creation of more realistic

social networks where a portion of players and/or interactions are randomly removed (Nowak M. , 2006).

Lattices lack the small-world typical characteristic of real-networks. Along the thesis, Horand networks will be considered. Due to their construction process not only do they exhibit the small-world characteristics but also a fixed degree, useful when trying to understand analytically certain phenomena or the role of another property, without degree variation. Homogenous networks, in which category Horand networks fit in, allow the creation of clusters of Cooperators that interact and maximize payoff in order to better resist Defectors exploitation, although with an high sensitivity on the intensity of selection (Pinheiro, Pacheco, & Santos, 2012).

A pattern observed in numerical simulations is that for games played on networks, at the beginning the number of Cooperators decreases, as a Defector playing against a Cooperator gets a higher payoff. However, on the long run, small clusters of Cooperators form on the lattice, because Cooperators playing against each other perform better than Defectors against Defectors. The initial decrease in cooperation is the price to pay for Cooperators to reorganize and assemble (Perc, 2013).

For Moran process of death-birth type in a donation game with weak selection (see equation 83), (Ohtsuki, Hauert, Lieberman, & Nowak, 2006) state that cooperation is favoured whenever $\frac{b}{c} > \langle k \rangle$, with b standing for the benefit of an altruistic act, c for its cost and $\langle k \rangle$ for the degree of the networks. The authors also concluded that the aforementioned condition leads Cooperators (Defectors) to a fixation probability $\rho_A(\rho_D)$, such that $\rho_A > \frac{1}{N} > \rho_D$, with $\frac{1}{N}$ standing for the fixation of a single Cooperator with neutral drift, i.e. w=0 in equation 83. These results holds for large populations with $N \gg \langle k \rangle$.

Real networks that evolved by adding nodes, such that new nodes attach randomly to existing nodes with a probability proportional to the degree of the latter are better described by a SF network. Aged nodes tend to have greater degree. Along the thesis, the BA model, a SF network with $\gamma = 3$, is adopted. These heterogeneous networks provide not only an adequate topology for Cooperators to gather, interact and reinforce mutual payoffs, but also function as a reference landmark of cooperation strategy influence over the neighbourhood due to the high payoff achieved.

The impact of heterogeneous networks on cooperation reflected in the right panel of figure 11 is pointed out in (Santos & Pacheco, 2005) for 2-Players games and later on extended for PGG in (Santos, Santos, & Pacheco, 2008). Initially Defectors perform well interacting with

high-degree nodes, but soon are victims of their own success as their neighbours cease being Cooperators. This allows a Cooperator to invade the hub, seed a cluster and avoid exploitation by other Defectors.

(Gómez-Gardeñes, Campillo, Floría, & Moreno, 2007) show that a more heterogeneous degree distributions results in increased cooperation by measuring the frequency or proportion of players that consistently play either cooperation or defection after the system reaching equilibrium. In SF networks, there is a single large core of pure Cooperators difficult to invade organized in hubs. The smaller number of hubs on random network is the reason for the lower level of cooperation in these networks.

2.5. Other Relevant Bibliography for the Thesis

If previous sections targeted to establish a common ground of consistent terminology and to build up the foundations for a theoretical framework, this sections accounts for bibliography more specific to the subjects of multilayer networks, modelling and structural measures, support for evolutionary dynamics and the sort of Public Goods Games (PGG) that can be played in these structures.

(Santos, Santos, & Pacheco, 2008) focus on PGG in a single layer. Each node with k degree participates in $k + 1$ games with a start topology, centered on each of its k neighbours and itself.

The only two strategies considered are cooperation and defection. The fitness of a player is associated with the accumulated payoff resulting from all PGG in which he/she participates. Strategy evolution is implemented via replicator dynamics: at each time step, each individual adopts the strategy of a randomly chosen neighbour with a probability proportional to the payoff (fitness) difference.

The two parameter variables considered are the type of network, either regular graphs or SF, and the investment to apply per player in each game. Per Cooperator player, either there is a fixed investment to be applied per game, or there is a fixed investment per player to be equally divided among the k+1 games he/she plays. Simulation results show that network heterogeneity favours cooperation. Additionally, sharing a fixed investment across all games, i.e., having fixed investment by player, lowers the synergy factor normalized by $k + 1$ threshold beyond which cooperation becomes viable.

A mathematical analysis to the results presented in (Santos, Santos, & Pacheco, 2008) is developed by (Pacheco, Pinheiro, & Santos, 2009) in order to explain why diversity on contribution and on network favour cooperation. Conditions for a Cooperator to invade a

Defector hub are presented for both cases of fixed investment per player or per game. Condition for latter alternative is less stringent that its counterpart for the former one. As in (Santos F. C., Pinheiro, Lenaerts, & Pacheco, 2012) the AGoS reflecting the variation (increase or decrease) in the number of Cooperators as a function of Cooperators frequency is plot. The plots unveils that the underlying structure effectively transforms a local cooperative dilemma into a global coordination game. For fixed investment per game with underlying SF networks, there is a critical initial level of cooperation, function of applicable synergy factor, below (above) which the level of cooperation tends to an All-Defectors (Cooperators) network.

Moreover, changing the contributive scheme from fixed investment per game to fixed investment per player in a SF network population structures changes a PD effectively into a Harmony Game where cooperation become advantageous irrespectively of their concentration, which means evolution moved to an ALL-Cooperators network.

2.5.1. Multilayer networks

A formalism to deal with systems composed of several layers, either with binary or weighted links, is proposed by (Battiston, Nicosia, & Latora, 2014). Different perspectives of description of a multiplex network are introduced: the aggregated topological matrix, the overlapping and the weighted overlapping matrix, which are simpler and more compact structures, but not so rich as the adjacency matrix A_{ij} per layer. Basic metrics to characterize the structural properties of a single layer network such as degree distribution, node clustering, shortest paths, betweenness or closeness are extended to a multiplex scenario. New measures as multiplex degree entropy emerge. There is a focus on the quantification of the participation of single nodes to the structure of each layer, and on its importance for the overall efficiency of the multiplex network, in terms of node reachability and clustering. Proposed measures are tested and validated on a genuine multiplex real-world dataset, the one of Top Noordin Terrorist Network (Battiston, Nicosia, & Latora, 2014).

2.5.2. Cooperation in Multilayer Networks

(Li, Wang, & Sheng, 2017) study in a single layer representing a 2D space the evolution of cooperation on networks that incorporate geographical costs into the payoff function of evolutionary games. The longer the distance between a pair of players, the higher the spatial cost incorporated into the payoff matrix of the game.

Nodes have weights standing for its relevance, e.g. population of a city. Networks are fully connected with structures geographically induced, as both nodes' relevance and their distance

are taken into account in a gravity alike function, used in cost-benefit analysis when deciding which links to incorporate in the network.

Nodes have 2D coordinates and each link is characterized by the Euclidean distance between the nodes it connects. PGG are played but the amount invested by a player in each game is now proportional to a cost function given by a Fermi distribution applied to the Euclidean distance to each of his neighbours.

A relevant result is that a polarized distribution of geographical costs can significantly lower the threshold value of the synergy factor for cooperation in networked PGG to succeed. In other words, the geographical mechanism, which polarizes cooperative costs is able to lower the threshold value of the synergy factor for cooperation in PGG. On the other hand, more uniform alike distribution of geographical costs hinders the evolution of cooperation.

(Nakamur, Nagashim, & Yasutak, 2015) study a two layer multiplex with random networks, small-world networks, following Watts-Strogatz model, and SF graphs, based on Barabási-Albert model. Nodes appear in all layers with no inter-layer links and have a single strategy across layers. 3 network types in 2 independent layers, in a total of 3^2 combinations are simulated. In each layer, PD is played taking into account payoffs acquired exclusively in that layer. Each nodes updates its strategy by copying it from a neighbour with a probability linearly proportional to their layer payoff difference normalized by the maximum degree between them. Once a node updates its strategy on one layer, it assumes it in all other layers so that a node's strategy is coherent across layers. In this model, cooperation only has a chance if both layers are SF.

(Battiston, Matjaz, & Latora, 2017) explore multiplexes with layers formed by regular random graphs, nodes with independent strategies per layer. Player's playoff is accumulated across layers. For a common synergy factor across all layers, the more overlapping are links across layers, the lesser is the critical synergy factor for cooperation to set in. Moreover, for a given positive average node overlapping, the bigger the number of layers the smaller the critical synergy factor for cooperation to prevail. In a two layer multiplex case, having different synergy factors in the layers allows new absorbing states with Full Cooperation on one layer and Full Defection on the other.

(Li, Shen, & Jiang, 2016) tackle a scenario of players having limited resources available to be spent in PGG played across all multiplex layers. An agent is represented by a tuple of nodes, one per layer. The synergy factor is common to all layers. Layers have homogeneous networks, Erdős–Rényi or small-world models, or SF heterogeneous models. Each agent has

an investment allocation, an array of investments, one element per layer, such that the investment per layer is non-negative and the total investment per agent is topped. Agent payoffs are calculated per layer.

Agents have variable contributions across layers with null contributions allowed. An Agent behaves as a Cooperator or a Defector when his/her contribution is positive or null, respectively. Per iteration, an agent is randomly selected. Selected agent payoffs across layers are compared and based on Fermi distribution, a layer is selected. In the chosen layer, the focal node adopts the allocation strategy of a random neighbour in the same layer with Fermi probability distribution applied to focal and neighbour nodes' payoffs in that layer. In case allocation strategy is copied, further normalization of the new investment allocation of the focal agent is required in order to keep its total topped.

Greedy-first mechanism was coined for the scenario when an agent in choosing the layer to play prefers to update the allocation strategy in the higher payoff layer as determined by Fermi distribution.

Simulations for 2-layer multiplex reveal that greedy-first agents can perform cooperative behaviours in multiplex networks when one layer is SF network and degree differences between peer nodes increase. An additional conclusion is that degree diversity and greedy-first mechanism can defeat temptation of defective behaviours and avoid the extremely biased cooperation in a certain layer.

A critic to the paper from the author of this thesis is that parts of the formalism introduced, in particular the greedy-first mechanism, lacked generalization to multiplexes of more than 2 layers.

(Hayashi, Suzuki, & Arita, 2016) address a multiplex scenario where an agent cannot afford to play PGG in more than 1 layer at any instant of time. Thus, an agent can have a node in any layer, but exclusively, i.e., in any point in time an agent will have a single node that will be positioned in only one layer, although this presence layer can dynamically evolve over time. Cooperation and defection are the applicable strategies. Game evolution allows an agent to change the layer where its single node lays.

All layers, independent, are defined as Erdös–Rényi random graph with the same constant degree.

The game roughly evolves as follows. For each agent the payoff of its representative node is calculated in its layer of presence by playing PGG with its neighbours as dictated by layer network who are necessarily present in that layer. With payoffs calculated, for each agent a

potential neighbour, not necessarily present in the same layer, is identified. A reference value function of node's payoffs dictates the probabilities with which strategy and layer of presence is copied from focal agent to its neighbour or the other way around.

With arbitrary probabilities mutations hit agents: layer of presence of its single node updates to a randomly chosen new one and strategy of its node changes.

As the number of layers increase, other things being equal, cooperation frequency increases, so does the normalized entropy of the distribution of the presence of agents per layer, resulting this increase from the cyclic coevolution processes of game strategies and layer selection strategies.

Departing from a scenario with the same Erdös–Rényi random graph across all layers and then randomly rewiring them in each layer, it was also showed that heterogeneity among layers is a catalyst in multiplex networks to facilitate the evolution of cooperation. In a way, this result is a reminiscence of the results obtained by (Santos F. C., Pinheiro, Lenaerts, & Pacheco, 2012) in a single layer case.

(Kleineberg & Helbing, 2018) study multiplexes with independent SF networks. Nodes have independent strategies per layer. Evolution of the system is governed by imitation dynamics, which means individuals tend to adopt the strategy of more successful neighbours. In each round of the game, firstly each node chooses one layer randomly and then, within this layer, one neighbour at random. Neighbour's strategy for that layer is copied with a probability given by Fermi distribution applied to the differential of nodes payoff. The payoff of a node is calculated as the average payoff accomplished across all layers.

If PD is the game played and there is no degree correlation between layers, increasing the number of layers only leads to minimum changes in final level of cooperation from a single layer scenario. However, if degree correlations are present and the number of layers is large enough, an average level of cooperation of 0.5 dominates the whole T-S parameter space and justifies the 'topological enslavement' title of the article. Topological enslavement emerges and highlights payoff irrelevance as both the number of layers and the strength of degree correlations are increased.

Topological enslavement is also observed with the Harmony game ($S = T = 0.5$) and PD with $S = -0.5, T = 1.5$. In a single layer, former game tends to All Cooperators; latter one to All Defectors. However, the same games with a sufficient large number of layers and strong degree correlation among layers converge to a Cooperator concentration of 0.5.

Topological enslavement implies also that the initial multiplex level of cooperation determines the final distribution of the level of cooperation across layers, almost irrespective

of T-S parameter combination supporting the game played, subject to the condition of existing a strong degree correlation across layers.

Topological enslavement is not exclusive to 2-Player games like the PD or the Harmony game. It also occurs in PGG. PGG are played independently in different layers, and the total payoffs are aggregated and averaged per node. There is a fixed investment per player per layer. Cooperators' frequency gets larger in the absence of degree correlations, but if this correlation is present and the number of layers increases, Cooperators' frequency drops to a fixed value around 50%. These results are independent of similarity correlation or overlapping, a trend nodes may have to connect to the same neighbours in different layers.

3. MODEL AND METHODS

In this section we briefly describe the model and methods used in chapter 4 to analyse how distributed investments in multilayer social networks impact the evolution of cooperation.

3.1. MODEL

Population Structure

Interactions between individuals in the population are captured by a multiplex, a particular subclass of a multilayer social network with only intra-layer links, no inter-layer links, and the same individuals present in all layers. Layers are supported in distinct networks. In that sense, we will use either Scale Free Barabási-Albert (BA) networks or Homogeneous Random Networks (Horand) as the two main models for the networks of each layer. The former is best suited to model social networks, while the latter is used as a benchmark. We will consider in all scenarios that networks have an average degree of four links ($\langle k \rangle = 4$) and a size Z of 1000 nodes.

Networks also define the paths of strategy spreading via imitation processes. Unless explicitly stated, networks supporting each layer of the multilayer result from independent instantiations of a single type of network, leading to an expected zero degree-degree correlation between layers. Having no inter-layer links in addition to layers built from the same network type being statistically indistinguishable implies to not exist a notion of layer neighbouring.

Game

The Distributed Prisoner's Dilemma (DPD) is a 2-Person version of a Public Goods Games, where individuals have to choose between investing an amount to a common pool (Cooperating) or not (Defecting). When Player1 (Player2) cooperates he/she invests an amount of C_1 (C_2). Defectors invest zero. Total investment is then multiplied by an enhancement factor F and the result is equally distributed between the two players no matter the strategy they followed or the amount they invested, in case they played as Cooperators.
The game is deemed asymmetrical because, although the template of the payoff matrix is symmetrical, each of its instances for a particular pair of players will be in general asymmetrical, as investments from players can be distinct. From Player1's perspective the payoff matrix is as

π (Payoff)		Player 2	
		C	D
Player1	C	$(\frac{F}{2}-1)C_1+\frac{F}{2}\,C_2$	$(\frac{F}{2}-1)C_1$
	D	$\frac{F}{2}C_2$	0

Investment Criteria

With each individual involved in many pairwise DPD interactions, there is room for criteria decisions on how to calculate C_1 and C_2 to apply in each game. Three formulations for C_1 and C_2 are explored along this work:

- **Baseline (1 unit per game)**

  In every layer an individual plays as a Cooperator, he/she invests 1 unit per game. So the total investment of an individual in the multilayer amounts to $\sum_{i\in\{layer\ where\ node\ is\ C\}} k_i$ with k_i representing the degree of the individual in layer i.

  All individuals invest the same amount in any game in any layer where they cooperate: 1 unit. Thus, $C_1 = C_2$.

- **Distributed per Layer (1 unit to divide per cooperative layer)**

  A total of 1 unit of investment is equally divided among all layers where an individual plays as a Cooperator. The quantity assigned to a layer i is then equally applied to each of the k_i links of an individual in that layer.

  So the total investment of an individual in the multilayer values $\frac{\sum_{i\in\{layer\ where\ node\ is\ C\}} k_i}{\sum_{i\in\{layer\ where\ node\ is\ C\}} 1}$. For a particular individual, all games in any layer where he/she cooperates benefit from an equal investment. Distinct individuals apply different investments per layer, if they cooperate in a different number of layers.

- **Distributed per Game (1 unit to divide per all distinct games as a Cooperator)**

  In this alternative the investment of an individual in all games played across the multilayer and where it plays the Cooperator role is the same, this investment being equal to $\frac{1}{\sum_{i\in\{layer\ where\ node\ is\ C\}} k_i}$. Total investment of an individual in the multilayer values 1.

Whenever an individual switches to a Defector strategy in a layer, the investment he/she previously applied in that layer is equally distributed among all the other games in the multilayer where he/she still plays as a Cooperator.

The first criterion is unconstrained, the remaining two are constrained, representing scenarios where players have limited resources that have to be divided among layers or games.

3.2. COMPUTER SIMULATIONS

In order to study the evolution of behaviour/strategy abundance in the population, we resort to extensive computer simulations. Simulations are conducted in multilayer networks with a variable number of layers. All layers have the same number of nodes or individuals. Unless explicitly stated, networks are of the same type across the layers of the multilayer. For all purposes, we consider that the same individual participates in the different layers but with an independent connectivity (degree) in each layer.

The total payoff of an individual i in layer l, π_i^l, is given by the sum of the payoffs collected by this individual from playing once with each of his/her neighbours in that layer as in

$$\pi_i^l = \left(\frac{F}{2} - 1\right) k_i^l C_i^l S_i^l + \frac{F}{2} \sum_{j \in \{Neighbors\ of\ i\ in\ layer\ l\}} C_j^l S_j^l \tag{89}$$

with k_i^l representing the degree of individual i in layer l, C_i^l standing for the amount player i is willing to invest in any game he/she participates in layer l and

$$S_i^l = \begin{cases} 1, \text{ if node } i \text{ is Cooperator in layer } l \\ 0, \text{ if node } i \text{ is Defector in layer } l \end{cases} \tag{90}$$

The total payoff collected by an individual (player) i throughout the multilayer, to be mapped to his/her fitness, is given by the sum of partial payoffs acquired across all multilayer layers and is expressed as

$$\pi_{i,} = \sum_{l=1}^{M} \pi_i^l \tag{91}$$

with M representing the number of layers of the multilayer.

Metrics concerning a particular point in parameter space result from averaging metrics collected from a set of independently run simulations.

A simulation starts with the construction of the multilayer social network. Hence, and in the case of uncorrelated layers, each layer is populated by randomly sampling with replacement networks from a pre-generated pool of BA and Horand networks. Each pool contains 3.000 independently generated instances of each type of network. Any randomly chosen pair of distinct BA network instances has an expected zero degree-degree correlation.

Each simulation is supported on a set of networks, 1 per layer, chosen independently from networks used in previous simulations. Additionally, for each simulation initialization of nodes makes use of random variables independent from the ones used in previous simulations.

The simulation or the evolutionary dynamics is an iterative process with the following stopping conditions: 1) a simulation reaches $3x10^6$ times the number of layers iterations; or 2) all layers saturate, each one into a state of ALLC (All Cooperators) or ALLD (All Defectors).

At each iteration, strategy update proceeds asynchronously.

Firstly, a layer from the multilayer is randomly selected with uniform probability. Subsequently and within this layer, an individual is randomly selected with uniform probability and is given the chance to revise his/her strategy by putting in action its agent level update mechanisms. This means that each individual in each layer has on average up to 3.000 chances to revise its strategy during each simulation.

The levels of cooperation achieved to present in chapter 4 result from averages calculated across 5.000 simulations.

For AGoS related computations, 300.000 simulations are performed and averaged. Each simulation lasted until the first of the two possible events occur: 1) the number of iterations reaches the number of 150 generations; or 2) all layers saturate each one as ALLC or ALLD.

A generation equals the product of the number of individuals per layer times the number of layers[2].

Because simulations are very CPU demanding, an algorithm optimization was conceived in order to save CPU time at expenses of internal memory consumption. Along each simulation iteration, both global and individual payoffs of all individuals in every layer are kept in memory, in order to recalculate the minimum set of these indicators at each iteration.

[2] AGoS requires much computation and is noisier than level of cooperation values, i.e. for a given number of simulations, it was verified that the variations in the scalar level of Cooperation achieved was less pronounceable than variations in vector AGoS entries indexed by the number of Cooperators. In order to reduce AGoS entries variances, the number of simulations AGoS is averaged on was increased. The counterpart of this decision was to make AGoS span fewer generations so that to keep its computation time within reasonable boundaries.

The same applies to AGoS. Thus, in each iteration whenever an individual i in a layer l updates his/her strategy, the following minimum of incremental updates are performed:

- If the baseline criterion is used, the payoffs of *i* and all its neighbours in that layer are to be recalculated. If a distributed investment criterion is the option, payoffs of i and any of his/her neighbours in any layer are revised. For the baseline case, there is no need to recalculate payoffs in other layers than l, because payoffs result from investments and these ones only changed in layer l.
- Applicable to any layer and investment criteria, individuals that had his/her payoff updated plus their neighbours need to have their individual AGoS updated. Thus, whenever an individual updates his/her strategy in one layer, he/she, his/her neighbours and neighbours of his/her neighbours in any layer have to update their AGoS in all layers.

This is because within a layer a strategy update of a single individual has a payoff and AGoS impact range of 1 and 2 links, respectively. If baseline criteria is in place, payoff impact is circumscribed to the layer where strategy upgrade occurred; otherwise, this impact spreads to all layers. Whatever the criteria applicable, AGoS impacts are transversal to all layers.

The algorithm conceived for optimizing the numeric calculations is explained in chapter 3.2.1.

Update Dynamics

At the start, individuals are assigned a random initial strategy, that is, Cooperation or Defection. Depending on the simulation objectives, the number of Cooperators to initialize each layer with varies. Namely, for determining the level of cooperation layers are initialized with half the individuals as Cooperators. If instead the objective is to determine (i) the quasi-stationary distribution or the (ii) Average Gradient of Selection (AGoS), then in each simulation each layer is initialized with a random number of Cooperators uniformly distributed between 0 and Z. In either case, layers are independently initialized.

Individual payoffs and AGoS, accumulated payoff across all layers and layer AGoS are calculated. This finishes multilayer initialization. Now an iterative cycle is launched. In each iteration, an individual A (player) is randomly chosen from a layer l also randomly chosen. All layers are chosen with equal probability. So are individuals within the chosen layer. In the selected l layer, accordingly to the supporting network a B A's neighbour, with a different strategy is selected again with an uniform probability. A will copy his/her selected neighbour's

strategy with a probability proportional to individuals' accumulated payoffs differential given by Fermi distribution

$$\text{Prob}(S_A \rightarrow S_B) = \frac{1}{1 + e^{-\beta(\pi_B - \pi_A)}} \quad (92)$$

keeping its strategy with complementary probability. In Equation 92, β is the intensity of selection. It is common to define two limits according to the intensity of selection: 1) Strong selection ($\beta \rightarrow +\infty$) imply deterministic actions by individuals, i.e., given the chance an individual will always copy its neighbour's strategy if latter's payoff is minimally higher than former's; 2) weak selection ($\beta \rightarrow 0$), average payoff difference becomes less relevant in the decision-making of an individual and approaches a random walk scenario.

An individual updates his/her strategy in a layer without concern to other strategies it may follow in other layers, apart from the influences of these strategies in the individual payoff.

After an individual updates his/her strategy in a single layer, its investments are recalculated with possible impacts in all layers, depending on investment criteria. In all layers, the investment of an individual is updated, its partial layer payoff and the one of all its neighbours are updated.

For AGoS an individual strategy update is even more far reaching because of this indicator being based on the probability of individuals copying strategies from their neighbours, which is a function of a differential of accumulated payoff across layers. In all layers that an individual changed its investment, which are not confined to the one its strategy was updated, AGoS has to be recalculated for the individual, for its neighbours and for neighbours' neighbours.

Both aggregated payoffs and aggregated AGoS at layer level resulting from accumulation or averaging of parts at individual level are differentially updated in each iteration. In order to avoid the recalculation of the aggregations at each iteration, the differential between new and old values of parts are added to totals with due weighting applied. Measures were taken against cumulative numeric errors.

Summary of parameters metrics collected from computer simulations

Table 6 lists a summary of the parameters used in the computer simulation model.

Table 6- List of the Parameters used in the Computer Simulation model

List of parameters used
• Investment Criteria
• Network type, BA or Horand, common across all layers
• Number of layers (M)
• Intensity of selection (β), within the interval between 0.01 and 10.0
• Enhancement factor (F), within the interval between 1 and 2

Table 7**Error! Reference source not found.** summarises the metrics obtained from computer simulations used to conduct the discussion and support our findings.

Table 7- List of all the Metrics collected from Computer Simulations

Metrics to collect from Computer Simulations
• Level of Cooperation corresponding to the average level of cooperation over all layers snapshotted at the end of each simulation
• Distribution of the probability of the number of Cooperators per layer and aggregated, i.e., averaged across all layers, as observed during simulations period
• Distribution of the probability of the number of Cooperators per layer and aggregated as snapshotted at the end of each simulation
• Level of Cooperation corresponding to the average level of cooperation over all layers snapshotted at the end of each simulation
• Distribution of the probability of the number of Cooperators per layer and aggregated, i.e., averaged across all layers, as observed during simulations period
• Distribution of the final evolutionary outcome discriminated per layer
• Average Gradient of Selection (AGoS) per layer and averaged across all layers snapshotted at the end of regular number of generations and at the end of each simulation
• Strategy coherence or node consistency

Distribution of the final evolutionary outcome per layer is snapshotted at the end of simulations in each of the following disjoint conditions: (i) All layers saturated as ALLC; (ii) All layer saturated as ALLD; (iii) All layers saturated, at least one as ALLC and at least one as ALLD; and (iv) At least one layer not saturated as ALLC or as ALLD.

Strategy coherence or node consistency, which is computed as

$$\xi = \frac{1}{N}\sum_{node=1}^{N}\frac{1}{M}\left|\sum_{layer\ l=1}^{M} S^{*l}_{i}\right| \tag{93}$$

with

$$S^{*}{}_{i}^{l} = \begin{cases} 1, \text{ for a Cooperator} \\ -1, \text{ for a Defector} \end{cases} \quad (94)$$

is measured at the end of each simulation and averaged across all simulations. If there are M layers and the node is Cooperator in M_C of them, then consistency equals $|1 - 2p|$, with p = M_C/M. Consistency as a function of p is a v line with a minimum of 0 at $p = 0.5$.

3.2.1. Numerical Methods

Calculating AGoS is very CPU demanding. Taking into account that the consequence of an individual updating his/her strategy is that its investments across layers vary, its neighbours at distance 1 across all layers have their payoff updated and that the impact on individual contributions to AGoS at layer level is circumscribed to neighbours at distance up to 2 in any layer, an algorithm was conceived to incrementally update multilayer payoffs and AGoS at each stochastic process iteration, instead of recalculating these metric integrally from scratch.

Appendix A presents the algorithm followed to incrementally calculate AGoS and payoffs at each iteration of the stochastic process having numerical optimization in mind. The algorithm conceived results from a trade-off between a lesser burden on CPU time and an increase in memory consumption, with more auxiliary variables being considered. Although attractive because of its performance, the downside of adopted incremental updating of

Table 8- Comparison on the Number of Operations required for Payoff and AGoS Calculation with and without Numerical Optimization

Average number of Operations per a Node Strategy update in a Layer		
Operations	**Unoptimized Version**	**Optimized Version**
# of individual Payoff Calculations	NM	Baseline: $2\langle k\rangle \frac{1}{\langle k\rangle} + 1 = 3$ [(1)] Distributed criteria: $2M\langle k\rangle \frac{1}{\langle k\rangle} + M = 3M$ [(1)]
# of individual AGoS Calculations	NM	$M(\langle k\rangle + 1) + 2M\frac{1}{\langle k\rangle}\langle k\rangle^2 = M(3\langle k\rangle + 1)$ [(3)]

[(1)]From steps 2, 5 and 6 of the algoritm (see appendix A)

[(2)]From steps 1, 7 and 8 of the algoritm (see appendix A)

variables per iteration is that rounding errors due to machines finite precision accumulate. Measures to mitigate and control this consequence are also mentioned in appendix A.

The compared number of operations in optimized and non-optimized calculations for each iteration of the stochastic process on a multilayer with M layers of networks, each with N nodes and $\langle k \rangle$ average degree, is as in table 8.

In non-optimized version it is assumed that at every iteration all payoffs and AGoS are calculated from scratch.

As $N \gg \langle k \rangle$, the saving of CPU utilization in the optimized calculus of stochastic process evolution is evident. Were other operations as the calculus of layer and multilayer aggregated AGoS considered and the gain on the optimized version side would be strengthened.

4. RESULTS AND DISCUSSION

The goal of this work is to explore how different investment criteria impacts the evolution of cooperation. Given the large parameter space, our first approach was to slice it along a number of dimensions. That means, keeping some variables constant while exploring the impact of varying the remaining along a predefined domain. Hence, it made it possible to investigate the impact of different conditions graphically and derive some intuition on the underlying mechanics of cooperation promotion.

Figure 14 results from a coarse grain sweeping of the parameter space and plots levels of cooperation averaged across all layers of the multilink colour coded. It is an eagle's eye view on how the 5 parameters considered, investment criteria, network type, number of layers, intensity of selection (β) and enhancement factor (F), determine the levels of cooperation attained. In a single go it attempts both to roughly assess the impact of different resource investment criteria in the evolution of cooperation in populations interacting through a multilayer network and to assess how sensitive is the overall multilayer behaviour to environment parameters, in particular the number of layers and underlying network types.

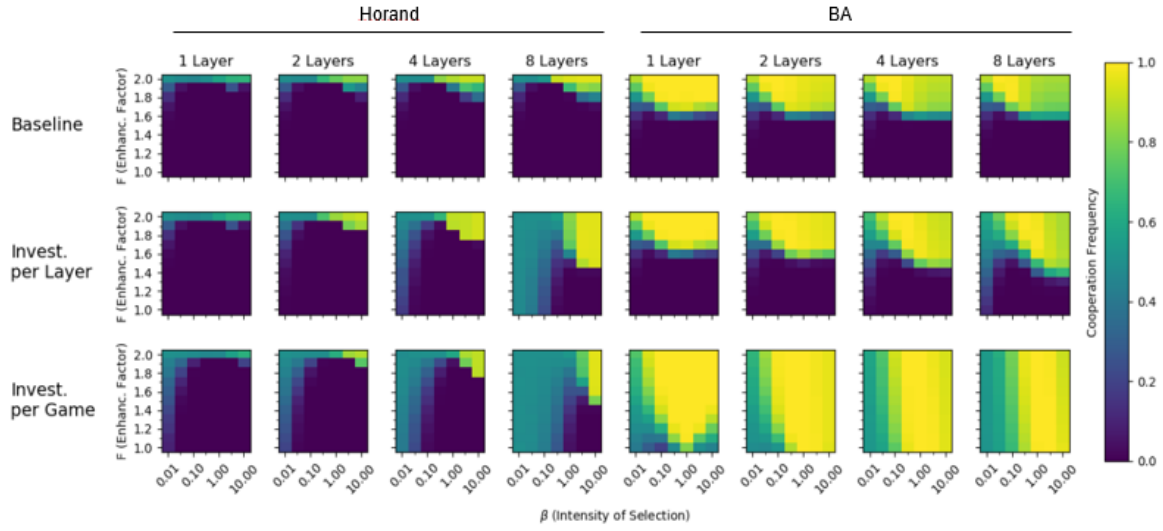

Figure 14- Level of Cooperation as a Function of Network type, Investment Criteria, Number of Layers, Intensity of Selection (β) and Enhancement Factor (F). Each layer with N=1000 individuals was initialized with half of them randomly chosen as Cooperators. There is no degree-degree correlation or overlapping.

Overall, we concluded that in the presence of distributed investment criteria, levels of cooperation increased with increasing number of layers. In opposition, for baseline criteria the level of cooperation has little sensibility to variations in the number of layers. This is because adding more layers to a multilayer with baseline criteria has a limited impact on original

layers. Partial payoff of individuals on original layers suffers no change; only the probability of copying the strategy from a neighbour changes as accumulated payoff per individual is updated. On the other hand, with distributed investment the addition of a layer completely changes the game. By forcing a fraction of the investment of each individual to flow towards the new layer, as long as the individual cooperates in the new layer, such flow of investment impacts on the payoffs of individuals' neighbours in all layers he cooperates. This creates a new dynamics by changing both individuals' partial payoffs in original layers as well as the probability of copying strategies from neighbours.

When all other variables are set as constant, cooperation improves with increasing enhancement factor (F) as expected, because a greater F implies that in the payoff matrix of DPD Cooperators' payoffs get closer to Defectors' ones, thus promoting Cooperation[3]. Additionally, BA networks lead to broader conditions for the promotion of cooperation than Horand networks.

Concerning the role of the intensity of selection (β), we observe that cooperation is favoured in strong selection regimes with large enhancement factors. When the number of layers increases, cooperation becomes dominant across the entire range of selection pressures for an intensity of selection above a critical threshold that raises with the number of layers, but in a way that is not transversal to all parameter scenarios and thus requires a segmented analysis. Noticeable in each heat map (see figure 14), under distributed investment criteria and for increasing number of layers there is a region on the left side with an uniform colour corresponding to half way the colour map considered, precisely the same level of cooperation with which layers were initialized. Noticeable also is that this region gets larger with its right frontier moving rightwards as the number of layers increases. Within this region, the cooperation level tends to become insensitive to enhancement factor (F). The formation of this region is more evident in Horand networks and with investment distributed per layer criteria, but although not experimented in the parameter subdomain underlying the figure it is extensible to the other distributed investment criteria and BA networks. The phenomenon in place is a combined topological and criteria enslavement that further on we will elaborate on and that in short boosts multilayer inertia to change, leading the multilayer to preserve

[3] In each iteration, would the choice of the layer where to play the DPD game be deterministic, e.g. by choosing the layer where an individual maximizes its local payoff, and cooperation level would not increase with enhancement factor.

throughout simulations whatever level of cooperation it was initialized with. Characteristic of this enslavement region is also that the maximum intensity of selection (β) delimiting its border varies in the same direction as the number of layers.

Under the baseline criteria and with four BA layers or more, cooperation levels are high (around 80%) in strong selection and high enhancement values (F). This trend has a different motivation than the one pointed out for distributed investment criteria cases and had already been identified in (Kleineberg & Helbing, 2018). What happens is that in the absence of correlations between layers as their number increases so do the odds of an individual being a Cooperator and a hub in at least one of the layers. As payoffs are accumulated and new layers do not change investment already applied, the contribution from new cooperative hubs helps an individual both to hold his/her ground in layers where he/she plays cooperation with few neighbours as in layers where defection was the option. We considered F = 1.7 in baseline criteria, and we observed that average cooperation level tops at around 80% with the multilayer in a stable equilibrium point with layers holding individuals with both strategies and individuals with distinct strategies across layers. Figure 15 plots the probability of finding an 8-layer baseline multilayer at a particular average level of cooperation by the end of a simulation. The expected value of this distribution corresponds precisely to the values measured in figure 14.

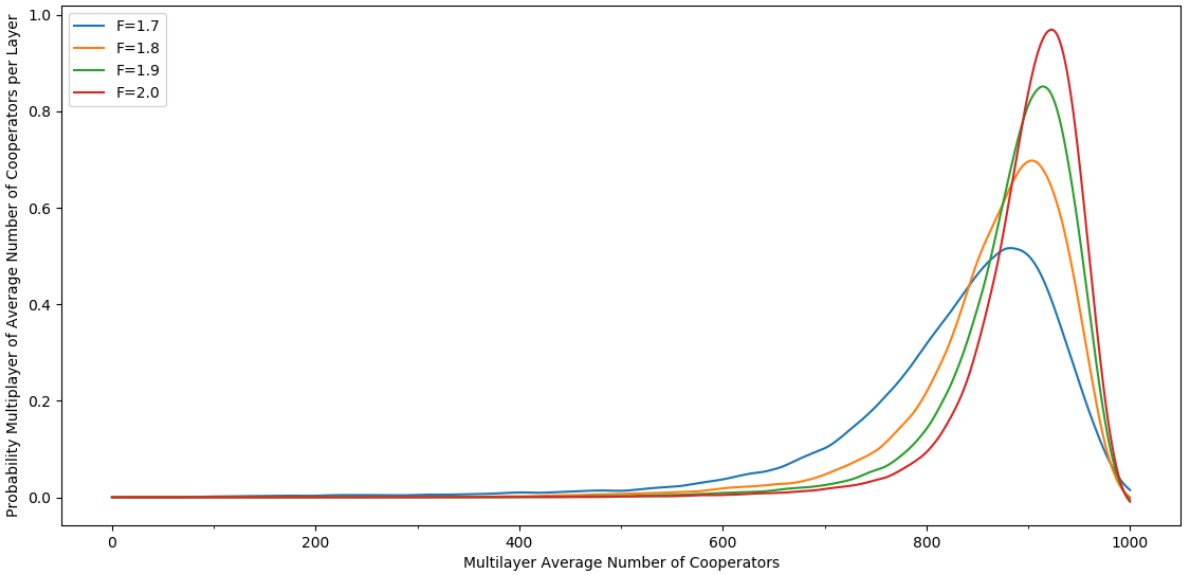

Figure 15- Quasi-Stationary Probability for an 8-Layer Multilayer with BA Networks and Baseline Investment Criteria. Intensity of Selection (β) values 1 and the number of individuals (N) per layer equals to 1000. Probabilities were calculated at the end of simulations. Each layer was initialized with half individuals randomly chosen as Cooperators. There is no degree-degree correlation or overlapping.

In order to shrink the parameter space and zoom in into different sub-domains where cooperation is experienced, reference values were identified for the intensity of selection (β). Values chosen were 1.0 and 0.1, based on the rational that multilayers with this parametrization can span the entire range of cooperation levels.

Figure 16 explores how the level of cooperation responds to different slices in parameter space defined by an intensity of selection (β); enhancement factor (F) and number of layers (M). In each column we consider scenarios where two parameters are constant and the remaining ones vary within the interval of analysis.

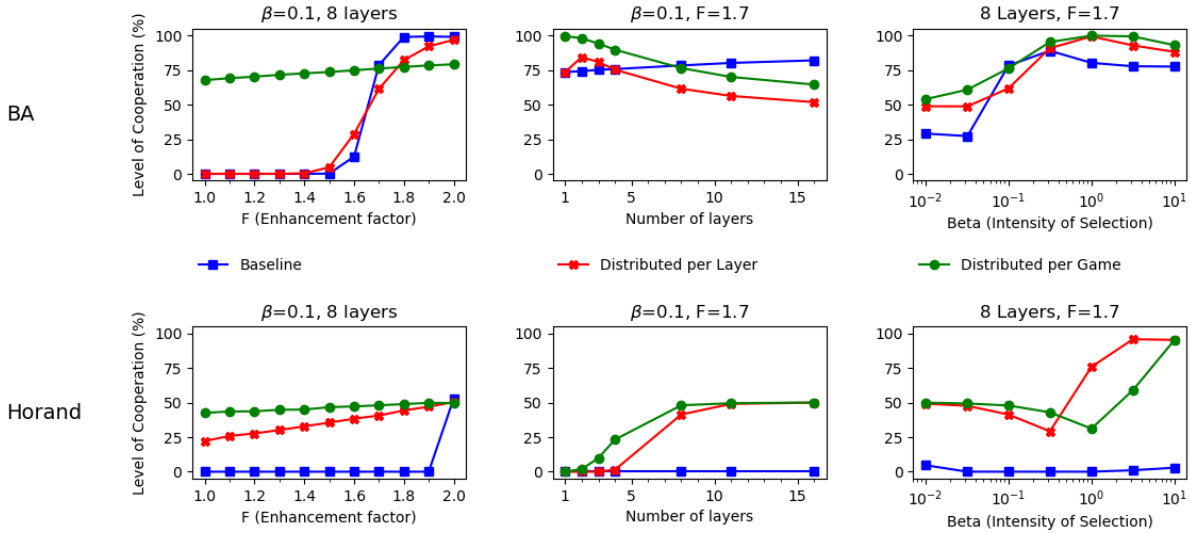

Figure 16- Level of Cooperation in Multilayer Networks in 2-Player Distributed Prisoner Dilemma (β=0.1). Level of cooperation was measured and averaged at the end of simulations. Networks in each layer have 1000 individuals (N), half random and independently initialized as Cooperators.

The upper and bottom left panels show the level of cooperation as a function of enhancement factor (F), with the number of layers set to 8 and intensity of selection $\beta = 0.1$. For BA networks, under the baseline criteria for F lower than 1.5 we observe that full defection (ALLD) is the dominant outcome, and for F greater than 1.8, population reaches a full cooperation state (ALLC). In between these values, we witness individuals changing strategy from Defection to Cooperation. The existence of a critical enhancement factor (F) beyond which cooperation levels rise had already been identified in (Pacheco, Pinheiro, & Santos, 2009) for a single layer. Although not shown, results from this article were recovered. Investment distributed per layer line has a similar trend to the one concerning baseline. If investment is distributed per game cooperation raises steadily with F, but with a low slope.

Under the baseline criteria with Horand networks the critical enhancement factor (F) is located near $F = 1.9$, meaning that it is a more stringent context for the evolution of cooperation. Only beyond this value, there is room for cooperation. Under the distributed investment criteria the level of cooperation increases monotonically with F until reaching a level of cooperation of 0.5 for $F = 2.0$. This behaviour is due to these slices cutting the parameter space almost entirely within the aforementioned regions of uniform cooperation level of 0.5 in figure 14.

The middle top and bottom panels show the evolution of cooperation while varying number of layers in the multilayer. We consider a constant enhancement factor of 1.7 and an intensity of selection of $\beta = 0.1$. The selection of the enhancement factor took into consideration the location of the level of cooperation phase transition observed on BA on top left panel.

On BA networks (upper middle) panel we observe the existence of an optimum number of layers that maximizes cooperation. This maximum can be explained by the combination of two mechanisms with opposing effects: first, as the number of layers increases the critical F beyond which cooperation is triggered decreases, as the case for investment per layer criteria is the most evident one; secondly, as the number of layers increases the cooperation level tends to reach a fixed value determined by the initial proportion of cooperation, a phenomenon known as enslavement region (see appendix C). The baseline related curve raises with the number of layers but topped by the already mentioned barrier around 80%.

On Horand networks and in the bottom middle panel we explore a scenario where the enhancement factor (F) lies in a region of full defection. Hence, a similar outcome is obtained when we increase the number of layers. However, when investment is distributed per layer, cooperation becomes feasible in networks with four or more layers. For investment distributed per game, cooperation becomes feasible for networks with two layers or more. Under distributed investment criteria, there is thus a critical number of layers for cooperation to emerge.

Relevant from middle panels is also that for both distributed investment criteria and for both types of networks, although more evident in the Horand case, the level of cooperation converges to 0.5 as the number of layers increase. Again, this is due to point $\{\beta, F\} = [0.1, 1.7\}$ for the number of layers sampled lying within the aforementioned regions of uniform level of cooperation of 0.5 in figure 14.

Finally, on the upper and bottom right panels we explore the level of cooperation as a function of the intensity of selection (β), for networks with 8 layers and an enhancement factor of 1.7. On BA networks, cooperation is sustained in the entire interval of selection pressures

investigated. Moreover, there is an optimal intensity of selection (β) that maximizes the level of cooperation. A finding that has been observed previously in single layered networks (Pinheiro, Pacheco, & Santos, 2012).

On Horand networks, since for F = 1.7 under the baseline criteria a regime of full defection is in place, there is little impact in varying the intensity of selection (β). However, for the distributed investment criteria, we observe significant gains in the level of cooperation for increasing selection pressure and in particular when investments are distributed per layer.

For both distributed investment criteria and both networks, right panels also highlight the fact that for minimal intensity of selection (β), the level of cooperation reached coincides with the one of multilayer initialization. The deviation increases as intensity of selection (β) raises. As experimentally verified, were the figure replicated with a higher number of layers and the critical β until which initial and final levels of cooperation are convergent would increase.

Although not shown here, we have repeated the case where the fitness of individuals corresponded to the averaged payoff across layers, that is, instead of the accumulated payoff. In that context, the results are similar to the ones discussed in here with a rescaled selection pressure to account for the normalization done by the number of layers.

Moreover, in appendix B we explore the impact of degree-degree correlations in multilayer social networks in the evolution of cooperation for the three investment criteria under analysis. We show that while increasing degree-degree correlations widens the range of dilemmas for which cooperation is prevalent, the region of parameters where the population is able to reach an ALLC state decreases substantially.

4.1. Topological Enslavement under Distributed Investments and Large Number of Layers

It is important to detail the limiting case of topological enslavement that emerges when the number of layers is very large. This scenario is specific to distributed investment criteria, although it can also be observed under the baseline criteria in restricted subdomains of the parameter space, eventually requiring additional conditions on the multilayer degree-degree correlation.

The prevalence of topological enslavement stems from the fact that, in opposition to baseline criteria, in distributed investment criteria when an individual becomes a Defector in one layer he/she will redistribute his/her investment towards the other layers where he/she remains a Cooperator. As a result, all individuals will have the same expected accumulated payoff with minimal variance. From this, it results that in the limit of many layers the

evolutionary dynamics recovers a random walk pattern, where the outcome is a function of the initial abundance of Cooperators and Defectors.

Quasi-Stationary Distribution for Horand Multilayer averaged across Layers ($\beta = 1, \langle k \rangle = 4, F = 1.7$)

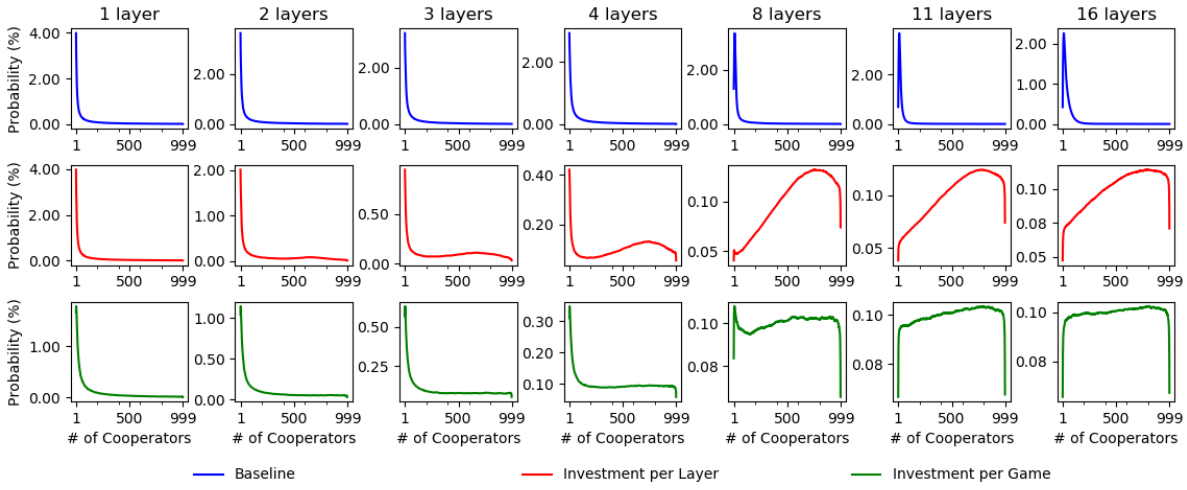

Quasi-Stationary Distribution for BA Multilayer averaged across Layers ($\beta = 0.1, \langle k \rangle = 4, F = 1.7$)

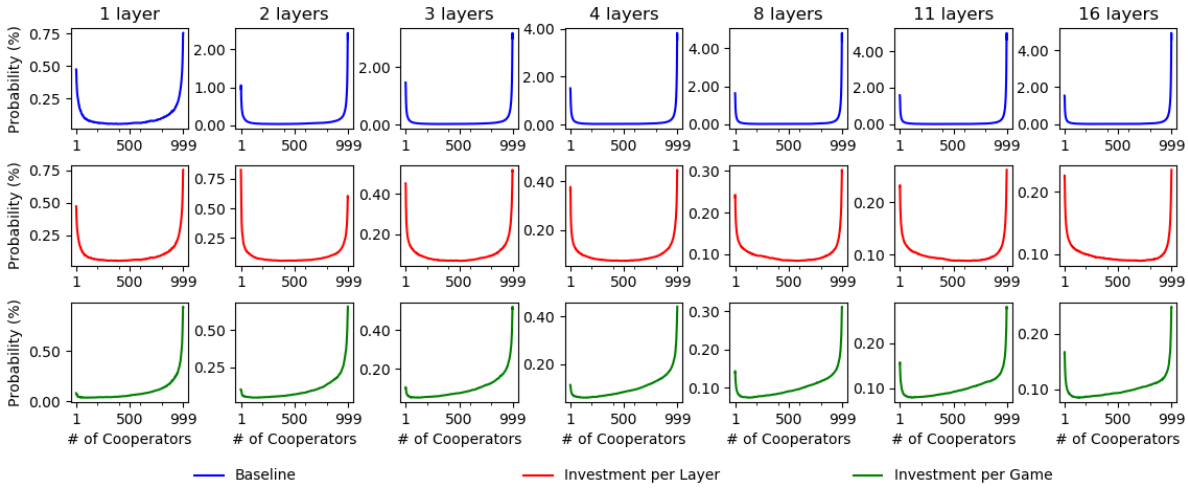

Figure 17- Experimental Quasi-Stationary Distribution for Multilayers averaged across Network Layers. Layers with 1000 individuals (N) are uncorrelated and were independently initialized, each one with a number of Cooperators determined by a uniformly distributed variable with values from 0 to 1000, inclusive

Under topological enslavement, evolution is invariant to changes in the intensity of selection (β) and the enhancement factor (F). Appendix C elaborates analytically on the underlying mechanics of topological enslavement under distributed investment criteria. Appendix B had already pursued the same goal for the baseline case.

The footprint of topological enslavement can be identified when studying the quasi-stationary distributions. Figure 17 considers networks with different number of layers, enhancement factor F of 1.7. Moreover, we consider both Horand networks with intensity of selection $\beta = 1$, and BA networks with $\beta = 0.1$. In order to evaluate multilayer response to different initialization conditions, each layer was independently initialized with a number of Cooperators sampled from an uniform distribution. Quasi-stationary distributions identify the proportion of times the population was observed in a particular number of Cooperators during the simulations.

For Horand networks, the most notorious fact is the perfect match in the bottom right graphic between experimental multilayer quasi-stationary probability and theoretically computed outcome under a random walk (see appendix C). The almost insensitivity of quasi-stationary probability to the number of layers for baseline criteria or the invariance to investment criteria up to 3 layers are other highlights from the figure. Also noticeable is that the quasi-stationary distributions for multilayers with investment distributed per layer tend to follow the ones for multilayers with investment distributed per game but with a gap in the number of applicable layers. For Horand networks, this is as analytically expected, because the investment of an individual per layer is $\langle k \rangle$ times greater in investment per layer criteria case than in investment per game alternative. Now, one of the mechanisms leading to enslavement is that all individuals collect a payoff targeting $F - 1$ with variance tending to zero, inversely proportional to the number of layers. If in investment per layer criteria payoff is $\langle k \rangle$ times higher than in investment per game criteria, the former case has a variance $\langle k \rangle^2$ higher than the latter, requiring a compensation via an increase in the number of layers for the quasi-stationary distribution for both distributed investment criteria to look alike (see appendix C).

On the other hand, BA networks for the baseline criteria have quasi-stationary distributions almost insensitive to the number of layers. Under distributed investment criteria the same trend is observed as on Horand, but less pronounced and with peaks near the absorbing states (ALLC and ALLD). Such peaks, however, gradually fade away as the number of layers increases. For instance, on BA networks with three layers and an investment distributed per layer, the quasi-stationary distribution peaks at both extremes. These results mean that

evolutionary trajectories converge quickly to scenarios where each layer is either ALLC or ALLD. Hence, their relative proportion dictates averaged multilayer level of cooperation. Another example concerns BA networks with 16-layers multilayer and a distributed investment per game criteria. As will be shown in next section, with BA networks, simulations terminate due to all layers saturating. At the end of each simulation at least one layer saturates as ALLC and at least one as ALLD. For the Horand case, it may happen that simulations terminate under the same conditions as with BA networks, although taking a longer time, but it also happens that simulations terminate by reaching the limit of evolutionary steps with layers where Cooperators and Defectors co-exist. These two factors eliminate in Horand case the peaks at absorbing states observed in BA figure.

Similar to both distributed investment criteria is that as either the number of layers increases or the intensity of selection (β) decreases, the variance of accumulated payoff collected by individuals is smashed, resulting in topological and criteria enslavement setting in, expressed as the preservation of the initial proportion of Cooperators in the multilayer along time, irrespective of the tuning of other environment parameters as enhancement factor (F). This phenomenon is experimented with both Horand and BA networks, although former ones do not require so extreme conditions on the number of layers or intensity of selection (β). Thus, at least in extreme conditions, the pair of number of layers and intensity of selection (β) attributes can determine by themselves the cooperative performance of a multilayer.

4.2. Layer and Population Polarization

Stating that evolution on multilayer social networks leads to a particular level of cooperation requires further exploration. That is, multilayer social networks can reach such outcome by various means. An observed level of cooperation, η, can result from the saturation of all layers (a proportion η saturate as ALLC and the remaining $1-\eta$ as ALLD) or all layers can end up in a co-existence characterized by a balance of η Cooperators and $1-\eta$ Defectors. In order to disambiguate such outcomes, we start by comparing the average individual strategy consistency on an 8-layer BA multilayer with intensity of selection of $\beta = 0.1$ for different values of F. See figure 18.

Around F = 1.7 for baseline and investment distributed per layer, there is a minimum in consistency. Until this critical F, individuals are consistently Defectors across all layers. For higher F, they become consistently Cooperators. The decrease in the levels of consistency in the case of investment distributed per layer line is wider and deeper because for this criteria

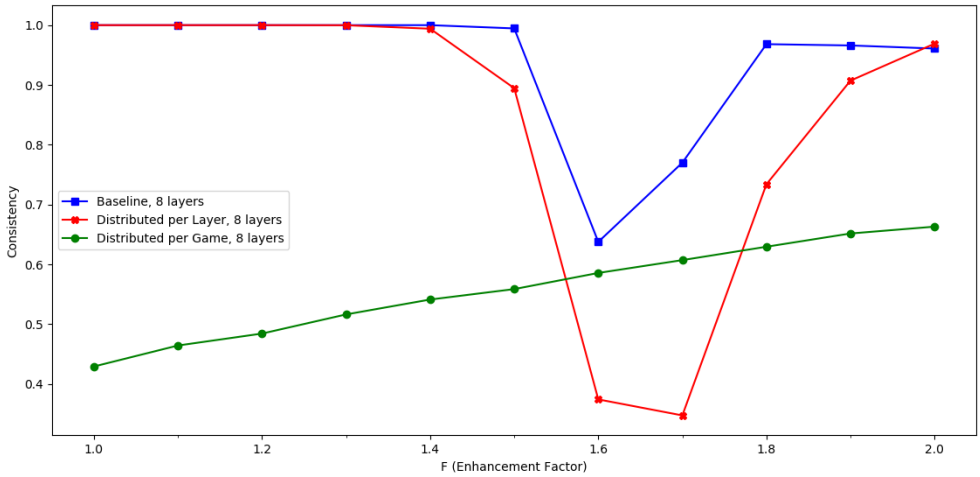

Figure 18- Individual Strategy Consistency across an 8 layer BA multilayer with $\langle k \rangle = 4, \beta = 0.1, N = 1000$. Layers were independently initialized with half individuals as Cooperators

the level of cooperation raises with F not as abruptly as in the baseline case. We conclude that, in the range of parameters associated with cooperative behaviour, on average each individual plays different strategies across layers. Anyway, whether there is any trend for individuals to align their strategies in each layer is still an open question that requires further investigation.

The evolutionary outcome of the multilayer can be characterized by scenarios where all layers always reach a monomorphic state of ALLC or ALLD in all its layers. Another possible outcome is that all layers reach a monomorphic but heterogeneous outcome, that is, some as ALLC while others ALLD. Hence, the relative occurrence of the two outcomes dictates the observed level of cooperation. This is the case when individuals have their strategies aligned per layer. Finally, the evolutionary outcome can be characterized by layers that do not reach a monomorphic state, but instead stay in a co-existence of Cooperators and Defectors. Other alternatives can be identified and even a mix between previous alternatives is possible. As mentioned in Section 3.2, the complementary conditions considered to find at the end of each simulation were reduced to the following set:

1. All layers reach a state of ALLC;
2. All layers reach a state of ALLD;
3. All layers reach a monomorphic state, at least one as ALLC or ALLD, but there is a co-occurrence of both states in the multiple layers;
4. At least one layer did not reach a monomorphic state and stays in a co-existence.

When condition 3 applies we say that there is layer polarization. When condition 4 is observed, polarization happens at population level. Figure 19 illustrates the relative proportions of conditions found at the end of simulations for different combinations of investment criteria,

types of networks, and number of layers and for a fixed network average degree and enhancement factor (F),

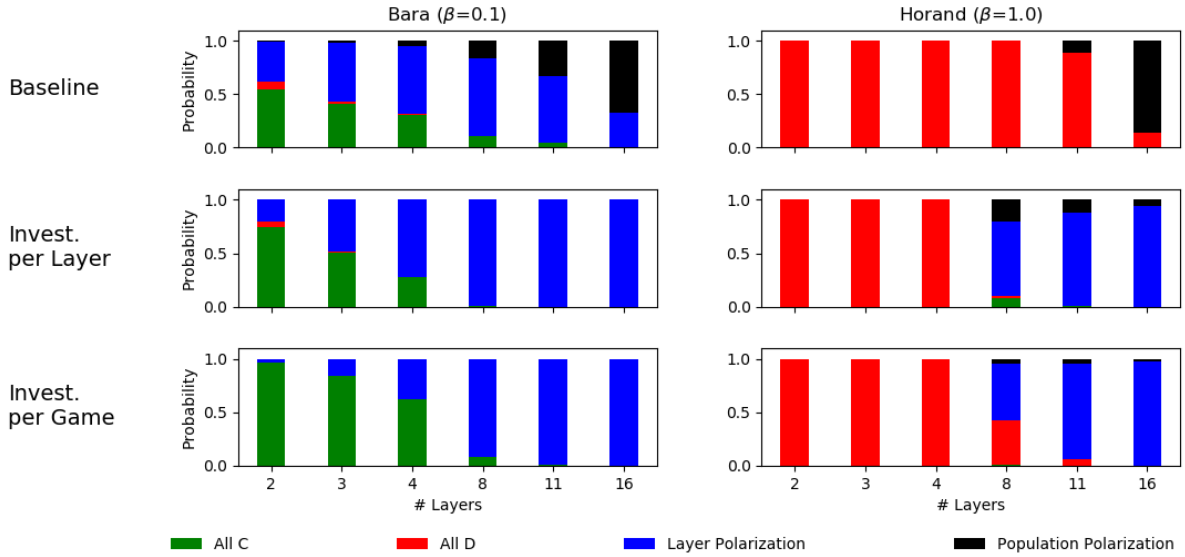

Figure 19- Saturation in Multilayers as the Number of Layers vary. Enhancement factor has value 1.7 and networks have 1000 individuals (N) with $\langle k \rangle$ equal to 4. Layers were initialized with half nodes as Cooperators randomly chosen.

For baseline criteria and BA networks, as the number of layers increases we witnesses a progressive substitution of ALLC layers by layers with Cooperators and Defectors in co-existence. In what concerns scenarios with layer polarization they have a maximum with 8 layers. The same investment criteria with Horand networks has a full defection until 8 layers inclusive. Then, as the number of layers increases, the new condition to emerge is that of population polarization with co-existence in layers.

For investment per layer criteria ALLC and layer polarization scenarios are almost perfectly balanced with minor intrusions of ALLD conditions. As the number of layers increases, some ALLC layers became ALLD and layer polarization steps in. From 8 layers onwards, layer polarization is the rule. The same investment criteria with Horand networks leads to full defection in multilayers with up to 4 layers. From then on layer polarization is the general applicable condition with an increasing relevance as the number of layers increase, an ephemeral minor appearance of ALLC condition for 8 layers and an additional occurrence of population polarization with 8 layers but fading away as the number of layers increases.

With investment per game criteria and BA networks, the trade-off is exclusively between ALLC and layer polarization. ALLC predominance with 2 layers steadily decreases to disappear with 11 layers. As it disappears, it is replaced by layer polarization. For Horand networks defection is the applicable condition until 4 layers. Between 8 and 11 layers ALLD

fades away to make room for layer polarization with occasional appearances of population polarization.

Not surprisingly for the same type of network, distributed investment criteria tend to the same condition as the number of layers increases. Moreover, each distributed investment criteria for different types of networks also tend to the same condition as the number of layers increases. The number of layers plays again the role of a uniforming factor.

As the number of layers increases and mostly for distributed investment criteria, it is common for ALLC or ALLD conditions to open room for layer polarization. The latter is a coarse grained condition spanning scenarios from just one layer as ALLC and remaining ones as ALLD to the reciprocal scenario.

In order to break down layer polarization meaning, the following additional indicators were calculated:

- μ_{AllC} and μ_{AllD} to account for average number of layers saturated as ALLC and ALLD, respectively, at the end of each simulation;
- $\sigma_{AllC-AllD}$ to tackle the standard deviation of the difference between the number of layers saturated as ALLC and ALLD at the end of each simulation;
- Node consistency as defined in 2.1.3 and
- Layers consistency, with the same definition as node consistency, but applied exclusively to saturated layers.

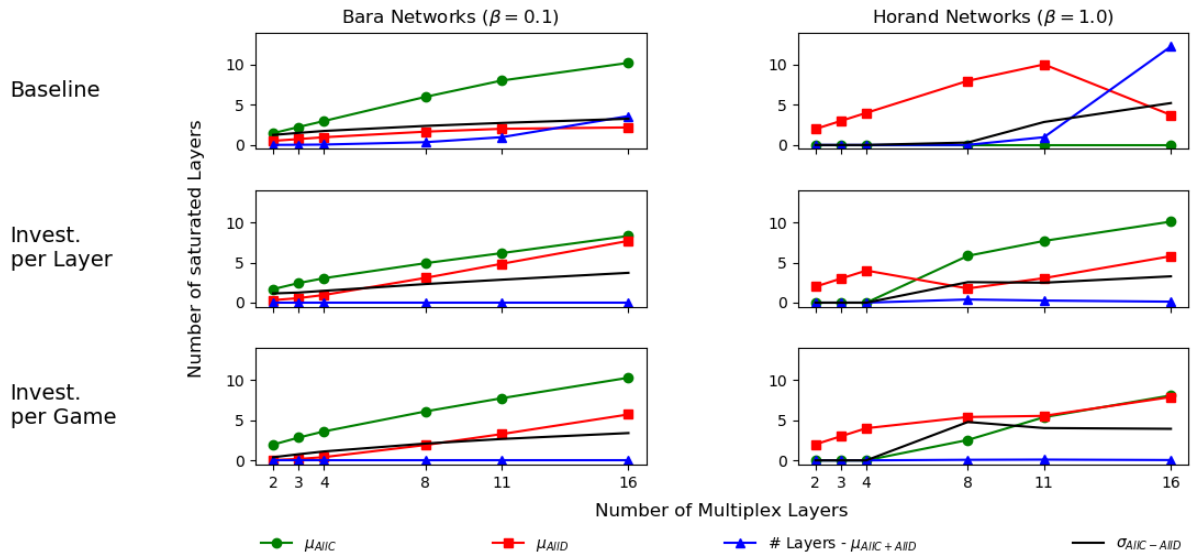

Figure 20- Saturation of Layers in a Multilayer as Investment Criteria and the Number of Layers vary. Enhancement factor (F) has value 1.7 and networks have 1000 individuals (N) with $\langle k \rangle$ equal to 4. Layers were initialized with half nodes as Cooperators randomly chosen

Figure 20 presents first two indicators for the same types of networks and enhancement factors (F) as previous figure. For baseline criteria and BA networks, as the number of layers increases, so does the gap between the number of ALLC and ALLD layers, the number of layers that do not saturate and the standard deviation between the number layers saturating as ALLC and ALLD. For Horand networks and from 11 layers onwards, ALLD layers lose ground to layers where Cooperators and Defectors co-exist. As there are no conditions for ALLC layers $\sigma_{AllC-AllD}$ measures the standard deviation of the number of ALLD layers.

For all distributed investment criteria, all layers always saturate. Noticeable also is that standard deviation of the differential between the number of saturated layers as ALLC and ALLD is significant but does not grow as much as the number of layers. For investment distributed per game and Horand networks, the number of layers as ALLC and ALLD coincide, which means a 50% level of cooperation, precisely the proportion of Cooperators with which the multilayer was initialized.

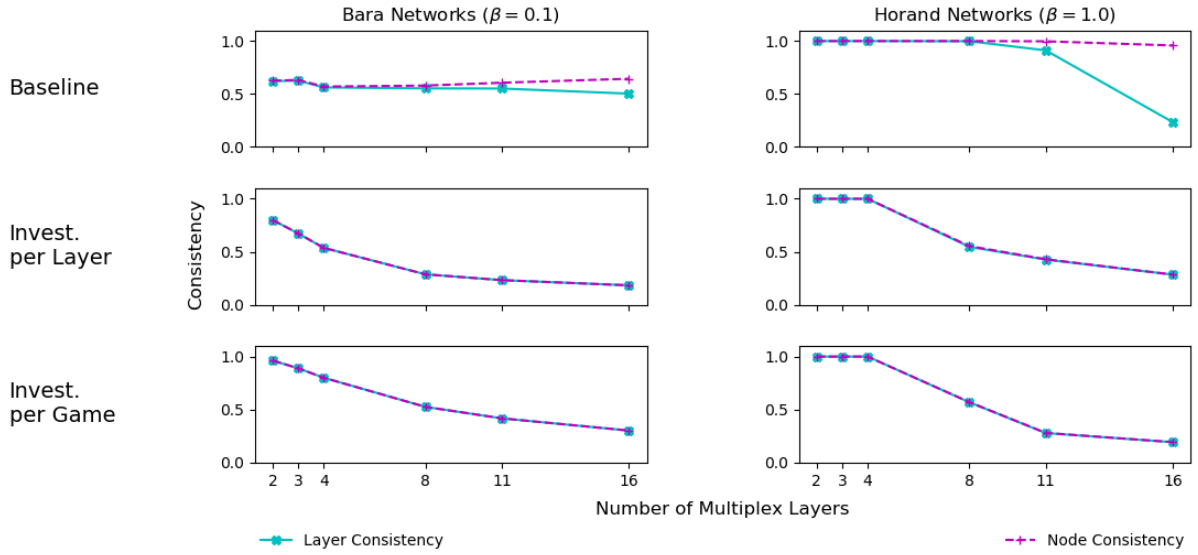

Figure 21- Layer and Node Consistency in a Multilayer as Investment Criteria and the Number of Layers vary. Enhancement factor has value 1.7 and networks have 1000 individuals (N) with $\langle k \rangle$ equal to 4. Layers were initialized with half nodes as Cooperators randomly chosen

Figure 21 presents node and layer consistency for the same types of networks and enhancement factor (F) as in figure 19. More evident in Horand case but also noticeable for BA networks, is that for baseline investment criteria layer and node consistency deviate from each other from 11 layer multilayer onwards, precisely when non saturated layers start appearing.

For both distributed investment criteria and as had already been depicted in figure 20, all layers always saturate, which implies node and layer consistency to coincide.

This section shed light on how the microscopic dynamics locally defined at individual level relates to the resulting global dynamics and allowed to conclude on the inexistence of patterns of "self-similarity" at different scales.

4.3. AGGREGATED AVERAGE GRADIENT OF SELECTION

Up to now, we have analysed the evolutionary dynamics of distributed investments in multilayered social networks on the attained level of cooperation. We now introduce the Aggregated Gradient of Selection (AGoS) tool in order to obtain a more accurate description of the underlying dynamics that leads to the observed outcomes. Hence, we aim at answering what is the population-wide dynamics that characterizes the social-dilemma faced by the population.

In a single layer with finite population, the AGoS is calculated as the difference in the probability to increase of the number of Cooperators by one and the probability to decrease the number of Cooperators by one. The AGoS, which must be computed numerically, aims to estimate these two quantities for all possible state transitions through a large number of computer simulations of the evolutionary process. The AGoS is, by definition, network dependent but context independent, as it recovers the population mean-field character. The AGoS captures dynamical information equivalent to that provided by replicator equation in EGT for infinite well-mixed population presented in 2.1.4.

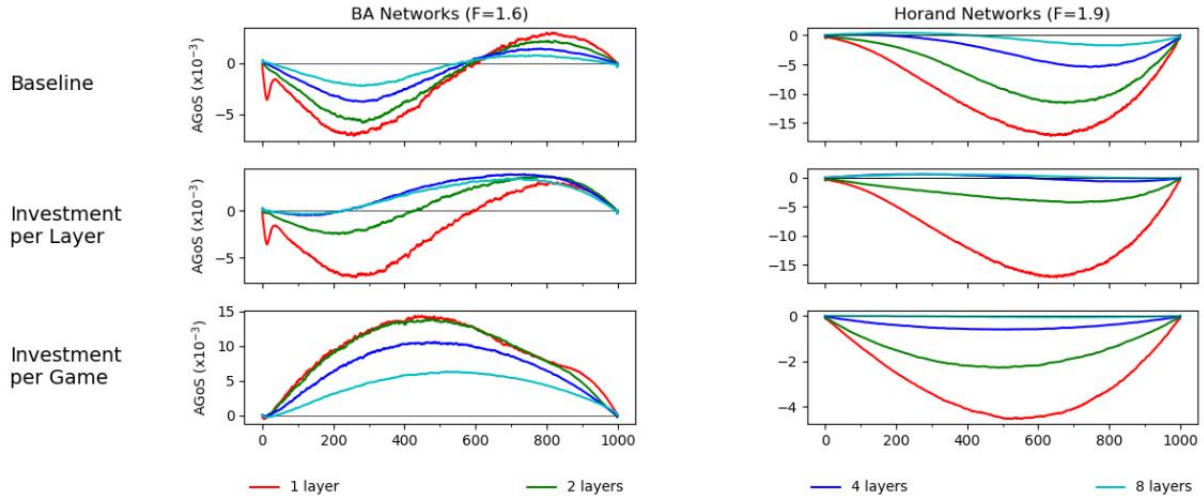

Figure 22- Averaged Aggregated Gradient of Selection (AGoS) averaged across Layers and Time. All networks have 1000 individuals (N) with $\langle k \rangle = 4, \beta = 1$. Layers were independently initialized with a number of Cooperators given by a random variable uniformly distributed between 0 and 1000, inclusive

In order to extend the AGoS to multilayer social networks, we opted to compute the AGoS independently per layer, which is then averaged to obtain a population and layer wide AGoS representation of the dynamics at hand.

Figure 22 shows the average AGoS on multilayers with different number of layers and types of networks. We consider an intensity of selection of 1.0 ($\beta = 1.0$) for both types of networks. The criteria for selecting the enhancement factor (F) follows from the outcomes shown in figure 14 for both network topologies and involves selecting an enhancement factor that is precisely at the transition between ALLD and ALLC outcomes. In that sense, we will be using $F = 1.6$ for BA networks and $F = 1.9$ for Horand networks.

For baseline criteria and BA networks, the multilayer behaviour is one of coordination. In that case, the evolutionary dynamics is characterized by an unstable fixed point. From it results that depending on the initial abundance of Cooperators and the location of the internal fixed point all layers will be driven towards an ALLC or an ALLD outcome. In addition, the location of the fixed point is seemingly invariant with the number of layers. Would the enhancement factor (F) increase (decrease) the fixed point would move to the left (right). The BA type of network is responsible for transforming a defection dominant DPD game in a well-mixed population into a game that is commonly associated with a mild social dilemma for cooperation, a coordination game often known as a Stag Hunt.

Cooperation in Horand multilayers under the baseline criteria is doomed for a small number of layers. However, for 8 layers population evolution is such that the possibility of a co-existence scenario with a stable equilibrium root emerges. The multilayer jointly with the baseline criteria transform a defection dominant DPD game in a well-mixed population into a game with an AGoS typical of a co-existence game. This means that even tough individuals are locally engaged in a DPD, multilayer leads to the emergence of a global population wide dynamics that promotes the co-existence of Cooperators and Defectors.

In the case of a single layer and baseline criteria, results are aligned with those obtained in (Pinheiro, Pacheco, & Santos, 2012). For investment distributed per layer and BA networks, the curves have a similar shape to the baseline case but move leftwards and cease sharing the same equilibrium point. With increasing number of layers, the fixed point moves towards *0*. Moreover, in a case in which the number of layers is very high the AGoS tend to be fully positive, typical of a system evolving to full cooperation. With Horand network and a small number of layers, all defection is multilayer fate as with baseline criteria. However, as the number of layers increase, a stable equilibrium point emerges, and the absolute value of the

averaged AGoS tends to zero. In fact, this reduction of AGoS magnitude was already experienced in the BA case.

With investment distributed per game and BA networks multilayer evolves to full cooperation. It is also noticeable the decrease of the averaged AGoS magnitude as the number of layers increases. In the case of Horand networks, a similar behaviour is observed with the exception that evolution is directed towards full defection in the cases that have been studied.

Common to both distributed investment criteria is that the magnitude of the average AGoS decreases as the number of layers increases, something that had already been anticipated in previous section. Having AGoS with magnitudes close to zero simply means that multilayer trend is to preserve the level of cooperation with which it was initialized. In other words, evolution approaches neutral drift. For distributed investment criteria and Horand networks, appendix D presents a mathematical explanation to why AGoS magnitude tends to zero as the number of layers increases.

Figure 22 shows results for the average AGoS, that is the average AGoS of all layers computed independently. However, as layers are statistically indistinguishable among themselves, individual AGoS concerning each layer are very close between themselves and thus close to their average AGoS. Figure 23 illustrates this result for multilayers with 4 layers and on both types of networks topologies.

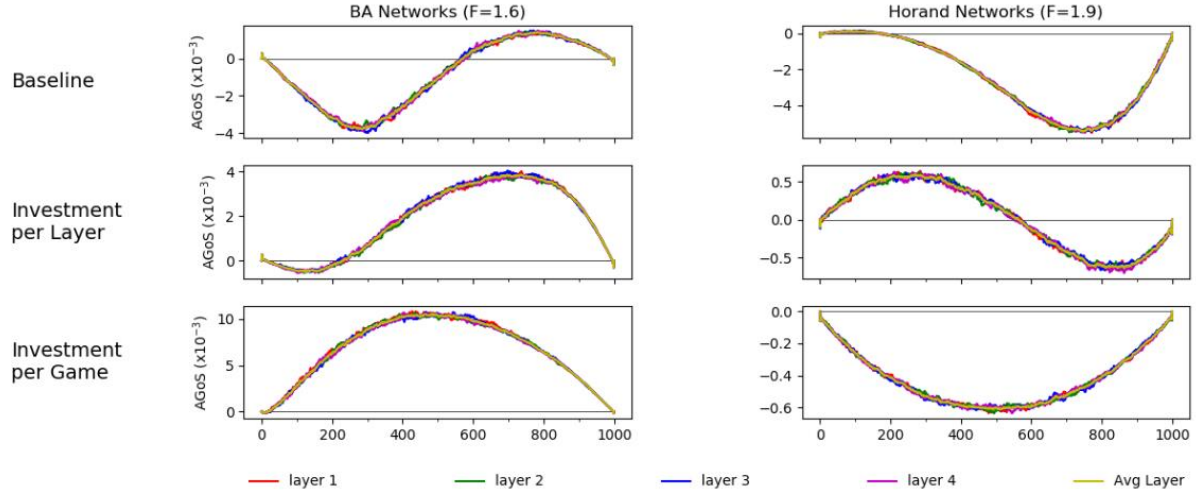

Figure 23- Aggregated Gradient of Selection (AGoS) for 4 Layers Multilayer over Time. All networks have 1000 individuals (N) with $\langle k \rangle = 4,\ \beta = 1$. Layers were independently initialized with a number of Cooperators given by a random variable uniformly distributed between 0 and 1000, inclusive.

Moreover, the computed AGoS presented so far results from a time average that spans over 150 generations. This disposition has the drawback of not capturing the eventual evolution over time that AGoS may experience, thus fails to capture the self-organizing process that

occurs as strategy assortments in the networks build up. In order to report the AGoS temporal dynamics, the time interval was fractioned in 150 intervals of 1 generation each. In each of these intervals, AGoS was calculated independently.

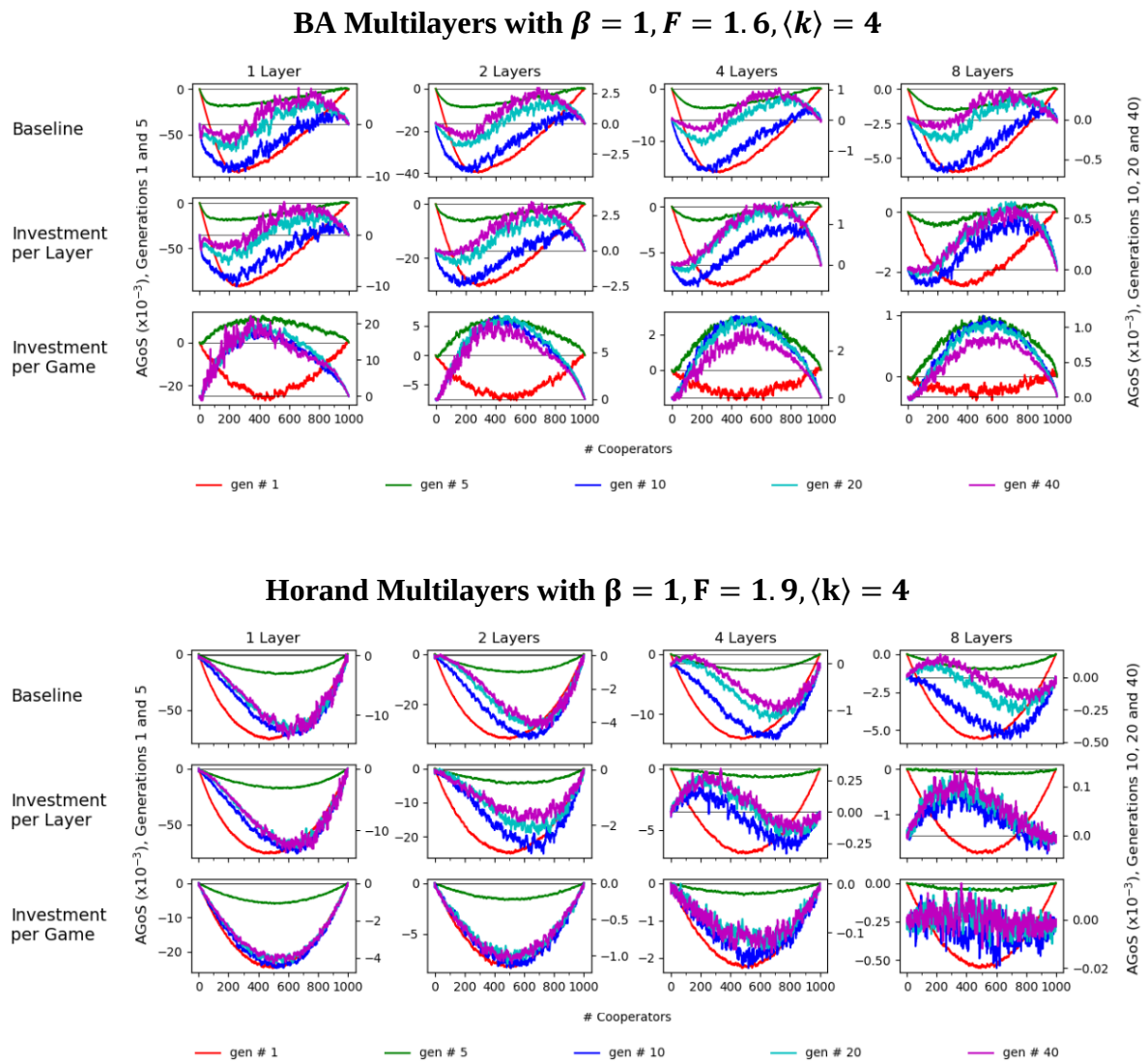

Figure 24- Aggregated Gradient of Selection (AGoS) for Multilayers averaged over Time. Layers with 1000 individuals (N) were independently initialized with a number of Cooperators given by a random variable uniformly distributed between 0 and 1000, inclusive. The noise increases with generation index due to generations having fewer samples. Were the number of 300.000 simulations increased and this noise would be reduced.

Figure 24 exhibits snapshots of the AGoS at different generations for multilayers with different networks and with different number of layers. A common observation to all multilayers considered is that during the first generations AGoS is always negative, which means that multilayers in first evolutionary steps witness an increase in the number of Defectors. Gradually in subsequent generations AGoS changes and results in the emergence of a basin of attraction that favours cooperation. The initial increase in the number of

Defectors results from two motives. First one is related to the fact of Cooperators and Defectors in the initial configuration of the multilayer are randomly positioned in the network making the clustering of nodes with the same strategy extremely improbable. With DPD being played locally, an arguably difficult game for the promotion of cooperation, the AGoS becomes negative. Secondly, may be simply that in the multilayer cooperation is doomed. As population evolve and Cooperators is adopted via the investment they are willing to apply, we witness assortment of strategies with the formation of hubs of cooperation.

For baseline strategy and BA networks, AGoS recovers the unstable fixed point as generations evolve. Around the 10^{th} generation, the fixed point emerges for levels of cooperation close to 1. As generations unfold, the fixed point moves to lower levels of cooperation (decreasing the coordination threshold) until stabilizing at a value with little sensibility to the number of layers. A similar behaviour is depicted on Horand networks.

Here the fixed point is stable, thus promoting a co-existence, and starts emerging with levels of cooperation close to 0. As generations unfold the fixed point moves to higher levels of cooperation until it stabilizes.

For investment per layer criteria and BA networks, AGoS also recovers from negative values to acquire an unstable fixed point that initially also arises close to full cooperation. The difference is that this point moves to lower levels of cooperation faster as generations progress and with greater number of layers. With investment per layer in Horand networks and from four layers onwards an AGoS characterized by a co-existence point emerges. For a given number of layers the co-existence root moves towards larger levels of cooperation for later generations. Additionally, not only the difference in co-existence root between the same generations shrinks as the number of layers increases as the fixed point moves closer to full cooperation.

For investment per game criteria and BA networks, apart from first generations, all subsequent ones have positive AGoS. As the number of layers increases, AGoS magnitudes for the same generations decrease. A similar behaviour is observed on Horand networks, where the AGoS is negative for all generations. As the number of layers increases, the magnitude of AGoS reduces drastically. For 8 layers, AGoS beyond the 10^{th} generation look like white noise with minimum magnitude.

The simple qualitative comparison of successive generations of AGoS concerning the same investment criteria and network combination may be misleading unless we take into account their relative magnitudes. For instance, for one layer the AGoS magnitude for the first generations is much higher than for subsequent ones. If for a given investment criteria and

number of layers combination all generation dependent AGoS are averaged, we recover the AGoS presented in figure 22.

Here, we have focused only in multilayers built from a single type of network. Appendix E addresses the case of a multilayer with heterogeneous layers: half as Horand, another half as BA.

5. CONCLUSIONS

In this thesis we have used methods from Evolutionary Game Theory to study the evolution of cooperation in multilayers made up of distinct and topologically independent networks of a single type, be it homogeneous or heterogeneous. Game dynamics were modelled at microscopic agent level via the Fermi-update dynamics and explored through computer simulations. In each layer, individuals engaged in the simple Public Goods Games in the form of the Distributed Prisoner Dilemma.

Intrinsic to Public Goods Games is a criteria on how much to invest in a game an individual participates as a Cooperator. Three criteria were explored. One scenario of unconstrained resources, the baseline one, considered that individuals contributed a fixed amount of 1 unit per game, irrespective of the number of distinct peers they may interact with. A second one had investment distributed per layer. That is, individuals had to distribute the same unit of investment equally through all layers where he/she participated as a Cooperator. Third criteria of investment was distributed per game, meaning that under that criteria individuals had to split equally a fixed investment across all the games they participated as Cooperators on all layers.

For the baseline investment criteria, we have shown that it has little sensibility to variations in the number of layers. For homogenous networks of Horand type, the parameter domain where cooperation is possible has a minimum enlargement with the number of layers increasing. Adding layers just increases the size of regular space, without breaking its symmetry, as new layers are statistically identical to previous ones with no impact on the investments already applied. If the networks are heterogeneous of BA type, the ones that better map social networks, a slight degradation in cooperation levels is even experienced when the number of layers increases with minimum change of the domain where cooperation is viable.

For distributed investment criteria, as the number of layers increases, we see the emergence of cooperation for lower levels of selection pressure (β). In the case of investment per layer and as the number of layers increases, the promotion of cooperation is more consistent in the homogeneous case than in heterogeneous one. Moreover, the fluctuations of cooperation level in the parameter domain are smaller in the homogeneous case. For investment per game, heterogeneous networks favour cooperation for any number of layers. With homogeneous networks, a higher number of layers is required for Cooperation to succeed.

Similar to both distributed investment criteria is that as either the number of layers increases or the intensity of selection (β) decreases, a topological and criteria enslavement

emerges, causing final level of cooperation to coincide with the initial proportion of Cooperators, irrespective of the values enhancement factor (F) environment. In the parameter space of the number of layers versus intensity of selection (β), a conceptual line with these parameters varying in the direct ratio can be traced such that for any combination of these parameters below the threshold defined by the line enslavement rules.

Moreover, in the distributed investment criteria, as time unfolds layers saturate becoming either ALLC or ALLD for heterogeneous networks and a layer polarization is reached. Thus, the initial proportion of Cooperators reflects in the proportion of layers that saturate as ALLC. For homogeneous cases, we find a mix of polarized layers and polarized populations, i.e., layers where both strategies coexist. However, as the number of layers increases the number of layers with polarized populations fades away until complete disappearance. Because the number of layers is discrete, when it increases also decreases error grain for difference between the proportion of layers saturating as ALLC and initial Cooperator concentration.

This layer polarization is of no surprise, as the increasing number of layers leads the evolutionary dynamics to converge to neutral drift having two absorbing states, ALLC or ALLD, with complementary probabilities of being reached, the probability assigned to former state resulting from the level of cooperation the multilayer was initialized with.

By definition for homogeneous networks cooperation levels attained with investment distributed per game coincide with the ones obtained with investment distributed per game with an higher intensity of selection (β) factor. This behaviour is also experienced with heterogeneous networks.

Another challenge targeted was to understand multilayer global dynamics and how they relate with microscopic dynamics locally defined at agent level. To tackle this, we resorted to AGoS, a numerically computed measure that is network dependent. Initially conceived for a single layer, it was here extended to the case of multilayered social networks. The AGoS measures the balance of probabilities to increase and decrease the number of Cooperators by one at a given strategy configuration.

Firstly, the single layer concept was generalized to a multilayer resulting in an averaged AGoS across layers. What averaged AGoS across layers demonstrates is that for homogeneous networks, regardless of the investment criteria, as the number of layers increases the magnitude of AGoS tends to zero (i.e., to neutral selection). This trend is even emphasized for distributed investment, which explains why the proportion of Cooperators with which a multilayer is initialized is preserved. Still for distributed investment criteria,

AGoS also shows that as the number of layers increases, although with a magnitude tending to zero, AGoS can become positive with an overall dynamics of a co-existence scenario.

For heterogeneous networks, the magnitude of AGoS also tends to zero as the number of layers increases. For baseline and investment per layer criteria, global dynamics is one of coordination. In the former case the root proportion of Cooperators is insensible to the number the layers whereas in latter case it moves leftwards tending to zero. A signal of what is to come for investment distributed by game with an higher number of layers is already verified for investment distributed per game with AGoS always positive and tending to zero as the number of layers increases.

An immediate takeaway from this thesis is that with distributed investment available, which can be time to share among many social networks of interest, in scenarios as the ones explored along the study developed, when the number of layers increases individuals tend to synchronize their strategies and cooperate (defect) in the same layers.

Having this thesis been mostly theoretical in character, with due humility and comparisons apart, the author reminds the anecdotic Hardy example. Hardy was an English mathematician and pacifist who lived during two previous centuries. He claimed to have never done anything useful during his life. By useful he meant applied, that could be used by the army. Because he insisted on only working on pure and abstract mathematics, he never dreamed of it, but much of his work was later on applied in various branches of science as e.g. population genetics.

5.1. FUTURE WORK

As to suggestions for continuing this work, a number of directions can be anticipated. The dependency of cooperation levels on average network degree was not experimented, because although trying different types of networks, all network instances shared the same average degree. When increasing $\langle k \rangle$ no significant changes in the results are expected, although according to equation 15 in appendix C topological enslavement may require an higher number of layers to emerge as $\sigma^2_{C_2} \propto \langle k \rangle$, where $\sigma^2_{C_2}$ accounts for the variance of an individual payoff from neighbours investment. In each multilayer experimented all layers had the same average degree and type of network, no assortiveness. It would be interesting to break this symmetry in three independent directions: cease to have the same average degree across all layers of the same multilayer, allow different types of networks in different layers as it is performed in appendix E and vary assortiveness. A major impact is expected on calculating AGoS in scenarios where symmetry across layers is broken. In terms of characterization, layers share no more a number of indicators or statistical distributions, e.g. $\langle k \rangle$, $Prob(k)$,

assortiveness, etc., which certainly implies AGoS per layer to differ. The challenge is now if and how partial layers AGoS could be combined and summarized in a single one explaining the evolution of cooperation. i.e., if there is a coherent game played across all layers or in opposition if different games are played in different layers such that a summary AGoS ends up reflecting an "average" game played nowhere.

Interesting to find out is also whether asymmetry between layers in a multilayer can break topological and criteria enslavement.

A simple extension to Public Goods Games and to its Distributed Prisoner Dilemma version would be to address voluntary participation, i.e., to allow each player to adopt a third strategy in each interaction, the one of Loner. When an individual abstains from playing by deciding to be Loner, his/her peer in pairwise interaction is compelled to also act as Loner and both players are rewarded by an amount σ, positive but smaller than the typical value corresponding to a cooperation interaction. Because a Loner is better off than a non-Loner playing against a Defector, although with a smaller reward than if playing against a Cooperator, Loner is an attractive strategy for the risk averse players.

Different sets of stochastic rules can be conceived for an individual in a layer to become or cease behaving as a Loner. In the limit when $\sigma = 0$, whenever an individual acts as a Loner in a layer, it is as his/her relationships were temporarily erased from the layer at least during the time interval he/she insists on playing as Loner. An alternative to the game having 3 individual strategies, would be for players to adhere to one of two mixed strategies, Loner plus a base strategy of Cooperation or Defection. Game participation would be probabilistic.

6. BIBLIOGRAPHY

Barabási, A.-L. (1999). Emergence of Scaling in Random Networks. *Science*, 286, 509-512, doi:10.1126/science.286.5439.509.

Barabási, A.-L. (2013). Network Science. *Philosophical Transactions of The Royal Society: Mathematical, Physical and Engineering Sciences*, doi: dx.doi.org/10.1098/rsta.2012.0375.

Barabási, A.-L., & Frangos, J. (2002). *Linked.* Perseus Books Group.

Barabási, A.-L., & Pósfai, M. (2016). *Network Science.* Cambridge: Cambridge University Press.

Battiston, F., Matjaz, P., & Latora, V. (2017). Determinants of public cooperation in multiplex networks. *New Journal of Physics*, 19, doi:10.1088/1367-2630/aa6ea1.

Battiston, F., Nicosia, V., & Latora, V. (2014). Structural measures for multiplex networks. *Physical review. E, Statistical, nonlinear, and soft matter physics*, 89, 032804, doi:10.1103/PhysRevE.89.032804.

Battiston, F., Nicosia, V., & Latora, V. (2016). The new challenges of multiplex networks: measures and models. *The European Physical Journal Special Topics*, 226, doi:10.1140/epjst/e2016-60274-8.

Bianconi, G. (2013). Statistical mechanics of multiplex networks: Entropy and overlap. *Physical review. E, Statistical, nonlinear, and soft matter physics*, 87, 062806, doi:10.1103/PhysRevE.87.062806.

Bogaert, S., Boone, C., & Declerck, C. (2007). Social value orientation and cooperation in social dilemmas: A review and conceptual model. *The British journal of social psychology / the British Psychological Society*, 47, 453-480, doi:10.1348/014466607X244970.

Brandt, H., Hauert, C., & Sigmund, K. (2006). Punishing and abstaining for public goods. *Proceedings of the National Academy of Sciences of the United States of America*, 103, 495-497, doi:10.1073/pnas.0509868103.

Broom, M. (2005). Evolutionary games with variable payoffs. *Comptes rendus biologies*, 328, 403-412, doi:10.1016/j.crvi.2004.12.001.

Buescu, J. (2018). *Curvas Ideais, Relações Desconhecidas.* Gradiva.

Buldyrev, S., Parshani, R., Paul, G., Stanley, H., & Havlin, S. (2010). Catastrophic Cascade of Failures in Interdependent Networks. *Nature*, 464, 1025-1028, doi:10.1038/nature08932.

De Domenico, M., Solè-Ribalta, A., Cozzo, E., Kivelä, M., Moreno, Y., Porter, M., . . . Arenas, A. (2013). Mathematical Formulation of Multi-Layer Networks. *Physical Review X*, 3, doi:10.1103/PhysRevX.3.041022.

Deng, Z.-H., Huang, Y.-J., Gu, Z.-y., Liu, D., & Gao, L. (2018). Multi-games on interdependent networks and the evolution of cooperation. *Physica A: Statistical Mechanics and its Applications*, 510, 83-90, doi:: 10.1016/j.physa.2018.06.120.

Eriksson, K., & Strimling, P. (2012). The Hard Problem of Cooperation. *PLOS ONE*, 7, e40325, doi:10.1371/journal.pone.0040325.

Fehr, E., & Gächter, S. (2002). Altruistic Punishment in Humans. *Nature*, 415, 137-140, doi:10.1038/415137a.

Fowler, J. H., & Harpending, H. C. (2005). Altruistic Punishment and the Origin of Cooperation. *Proceedings of the National Academy of Sciences of the United States of America*, 102, pp 7047-7049, doi:10.1073/pnas.0500938102.

Gintis, H. (2000). Classical Versus Evolutionary Game Theory. *Journal of Consciousness Studies*, 7, 300-304.

Girard, Y., Hett, F., & Schunk, D. (2014). How individual characteristics shape the structure of social networks. *Journal of Economic Behavior & Organization*, 115, doi:10.1016/j.jebo.2014.12.005.

Gómez-Gardeñes, J., Campillo, M., Floría, L., & Moreno, Y. (2007). Dynamical Organization of Cooperation in Complex Topologies. *Physical review letters*, 98, 108103, doi:10.1103/PhysRevLett.98.108103.

Gómez-Gardeñes, J., Reinares, I., Arenas, A., & Floría, L. (2012). Evolution of Cooperation in Multiplex Networks. *Scientific Reports*, 2, 620, doi:10.1038/srep00620.

Grinstead, C. M., & Snell, J. L. (1997). In C. M. Grinstead, & J. L. Snell, *Introduction to Probability* (pp. 405-432). American Mathematical Society.

Grinstead, C. M., & Snell, J. L. (1997). Introduction to Probability. In C. M. Grinstead, & J. L. Snell, *Introduction to Probability* (pp. 405-432). American Mathematical Society.

Hamilton, W. D. (1964). The Genetical Evolution of Social Behaviour. *Journal of Theoretical Biology*, 7, 17-52, doi:10.1016/0022-5193(64)90039-6.

Hardin, G. (1968). The Tragedy of the Commons. *Science*, 162, 1243–1248, doi:10.1126/science.162.3859.1243.

Hauert, C., & Doebeli, M. (2004). Spatial structure often inhibits the evolution of cooperation in the snowdrift game. *Nature*, 428, 643-646, doi:10.1038/nature02360.

Hauertwz, C., De Montewy, S., Hofbauerw, J., & Sigmund, K. (2002). Replicator Dynamics for Optional Public Good Games. *Journal of Theoretical Biology*, 218, 187–194, doi:10.1006/jtbi.2002.3067.

Hayashi, K., Suzuki, R., & Arita, T. (2016). Coevolution of Cooperation and Layer Selection Strategy in Multiplex Networks. *Games*, 7, 34, doi:10.3390/g7040034.

Kim, H., Olave-Rojas, D., Álvarez-Miranda, E., & Seung-Woo, S. (2018). In-depth data on the network structure and hourly activity of the Central Chilean power grid. *Scientific Data*, 5, 180209, doi:10.1038/sdata.2018.209.

Kleineberg, K.-K., & Helbing, D. (2018). Topological enslavement in evolutionary games on correlated multiplex networks. *New Journal of Physics*, 20, doi:10.1088/1367-2630/aac155.

Lehmann, L., Keller, L., West, S., & Roze, D. (2007). Group selection and kin selection: Two concepts but one process. *Proceedings of the National Academy of Sciences of the United States of America*, 104, 6736-6739, doi:10.1073/pnas.0700662104.

Li, Y., Wang, Y., & Sheng, J. (2017). The evolution of cooperation on geographical networks. *Physica A: Statistical Mechanics and its Applications*, 485, 1-10, doi:10.1016/j.physa.2017.05.0.

Li, Z., Shen, B., & Jiang, Y. (2016). The maintenance of cooperation in multiplex networks with limited and partible resources of agents. *Physica A: Statistical Mechanics and its Applications*, 467, doi:10.1016/j.physa.2016.10.040.

Lu, W., Wang, J., & Xia, C. (2018). Role of memory effect in the evolution of cooperation based on spatial prisoner's dilemma game. *Physics Letters A*, 382, doi:10.1016/j.physleta.2018.07.049.

Maciejewski, W., Fu, F., & Hauert, C. (2014). Evolutionary Game Dynamics in Populations with Heterogenous Structures. *PLoS computational biology*, 10, e1003567, doi:10.1371/journal.pcbi.1003567.

Min, B. a.-I. (2014). Multiple resource demands and viability in multiplex networks. *American Physical Society*, 89, 040802, doi:10.1103/PhysRevE.89.040802.

Moran, P. (1958). Random processes in genetics. *Mathematical Proceedings of the Cambridge Philosophical Society*, 54, 60-71. doi:10.1017/S0305004100033193.

Nakamur, Y., Nagashim, Y., & Yasutak, K. (2015, Nov 23-27). Evolutionary Games on Multiplex Networks: Effects of Network Structures on Cooperation. *Proceedings on the 2015 11th International Conference on Signal-Image Technology & Internet-Based Systems*, 444-447, doi:10.1109/SITIS.2015.48.

Newman, M. (2003). The Structure and Function of Complex Networks. *Computer Physics Communications*, 147, 40-45,doi:10.1016/S0010-4655(02)00201-1.

Nicosia, V., & Latora, V. (2015). Measuring and modeling correlations in multiplex networks. *Physical Review E*, 92, 032805, doi:10.1103/PhysRevE.92.032805.

Nowak, M. (2006). *Evolutionary Dynamics.* Cambridge, Massachusetts: The Belknap Press of Harvard University Press.

Nowak, M. (2007). Review Five Rules for the Evolution of Cooperation. *Science (New York, N.Y.)*, 314, 1560-1563, doi:10.1126/science.1133755.

Nowak, M. (2012). Evolving Cooperation. *Journal of Theoretical Biology*, volume 299, pp. 1-8, doi:10.1016/j.jtbi.2012.01.014.

Nowak, M. A., & Sigmund, K. (1992). Tit for tat in heterogeneous populations. *Nature*, 355, 250-253, doi:10.1038/355250a0.

Nowak, M. S. (1998). Evolution of Indirect Reciprocity by Image Scoring. *Nature*, 393, 573-577, doi:10.1038/31225.

Nowak, M., Tarnita, C., & Antal, T. (2010). Evolutionary dynamics in structured populations. *Philosophical transactions of the Royal Society of London. Series B, Biological sciences*, 365, 19-30, doi:10.1098/rstb.2009.0215.

Ohtsuki, H., & Nowak, M. (2006). The Replicator Equation on Graphs. *Journal of theoretical biology*, 243, 86-97, doi:10.1016/j.jtbi.2006.06.004.

Ohtsuki, H., Hauert, C., Lieberman, E., & Nowak, M. (2006). A Simple Rule for the Evolution of Cooperation on Graphs and Social Networks. *Nature*, Volume 441, pp 502-5, doi:10.1038/nature04605.

Ohtsuki, H., Hauert, C., Lieberman, E., & Nowak, M. (2006). A Simple Rule for the Evolution of Cooperation on Graphs and Social Networks. *Nature*, 441, 502-505, doi:10.1038/nature04605.

Ohtsuki, H., Pacheco, J., & Nowak, M. (2007). Evolutionary Graph Theory: Breaking the Symmetry between Interaction and Replacement. *Journal of theoretical biology*, 246, 681-694, doi:10.1016/j.jtbi.2007.01.024.

Oksendal, B. (2003). *Stochastic Differential Equations: An Introduction with Applications.* NY: Springer-Verlag.

Pacheco, J., Pinheiro, J., & Santos, F. (2009). Population Structure Induces a Symmetry Breaking Favoring the Emergence of Cooperation. *PLoS computational biology*, Volume 5, doi:10.1371/journal.pcbi.1000596.

Perc, M. G.-G. (2013). Evolutionary dynamics of group interactions on structured populations: A review. *Journal of the Royal Society, Interface / the Royal Society*, 10, 20120997, doi:10.1098/rsif.2012.0997.

Pinheiro, F. L. (2016). *Characterization of Self-organization Processes in Complex Networks.* Universidade do Minho, Escola de Ciências.

Pinheiro, F. L., Santos, F. C., & Pacheco, J. M. (2016). Linking Individual and Collective Behavior in Adaptive Social Networks. Physical Review Letters. *Physical Review Letters*, 116, doi:10.1103/PhysRevLett.116.128702.

Pinheiro, F., Pacheco, J. M., & Santos, F. C. (2012). From Local to Global Dilemmas in Social Networks. *Physical Review Letters*, 7, e32114, doi:10.1371/journal.pone.0032114.

Pinheiro, F., Pacheco, J., & Santos, F. (2012). How selection pressure changes the nature of social dilemmas in structured populations. *New Journal of Physics*, 14, 073035, doi:10.1088/1367-2630/14/7/073035.

Pinheiro, F., Santos, M., Santos, F., & Pacheco, J. (2014). Origin of Peer Influence in Social Networks. *Physical review letters*, 112, 098702, doi:10.1103/PhysRevLett.112.098702.

Reka, A., Jeong, H., & Barabasi, A.-L. (1999). Diameter of the World-Wide Web. *Nature*, 401, 130-131, doi:10.1038/43601.

Santos, F. C., Pacheco, J. M., & Lenaerts, T. (2006). Evolutionary dynamics of social dilemmas in structured heterogeneous populations. *Proceedings of the National Academy of Sciences*, 103, 3490--3494, doi:10.1073/pnas.0508201103.

Santos, F. C., Pinheiro, F. L., Lenaerts, T., & Pacheco, J. M. (2012). The role of diversity in the evolution of cooperation. *Journal of Theoretical Biology*, 299, 88-96, doi:10.1016/j.jtbi.2011.09.003.

Santos, F. C., Santos, M. D., & Pacheco, M. J. (2008). Social diversity promotes the emergence of cooperation in public goods games. *Nature*, Volume 454, doi:10.1038/nature06940.

Santos, F., & Pacheco, J. (2005). Scale-Free Networks Provide a Unifying Framework for the Emergence of Cooperation. *Physical Review Letters*, 95, 098104, doi:10.1103/PhysRevLett.95.098104.

Santos, F., & Pacheco, J. (2006). A new route to the evolution of cooperation. *Journal of evolutionary biology*, 19, 726-733, doi:10.1111/j.1420-9101.2005.01063.x.

Santos, F., Rodrigues, J., & Pacheco, J. (2005). Epidemic Spreading and Cooperation Dynamics on Homogeneous Small-World Networks. *Physical review. E, Statistical, nonlinear, and soft matter physics*, 72, 056128, doi:10.1103/PhysRevE.72.056128.

Santos, F., Santos, M., & Pacheco, J. (2008). Social diversity promotes the emergence of cooperation in public goods games. *Nature*, 454, 213-216, doi:10.1038/nature06940.

Santos, M., Dorogovtsev, S., & Mendes, J. (2014). Biased imitation in coupled evolutionary games in interdependent networks. *Scientific Reports*, 4, 4436, doi:10.1038/srep04436.

Santos, M., Pinheiro, F., Santos, F., & Pacheco, J. (2012). Dynamics of N-person snowdrift games in structured populations. *Journal of theoretical biology*, 315C, 81-86, doi:10.1016/j.jtbi.2012.09.001.

Sigmund, K. (2010). *The Calculus of Selfishness.* New Jersey: Princeton University Press.

Smith, J. M. (1982). *Evolution and the Theory of Games.* Cambridge University Press.

Szabo, G., & Fath, G. (2007). Evolutionary Games on Graphs. *Physics Report Journal*, 446, doi:10.1016/j.physrep.2007.04.004.

Szabo, G., & Tőke, C. (1998). Evolutionary Prisoner′s Dilemma game on a square lattice. *Physical Review E*, 58, 69-73, doi:10.1103/PhysRevE.58.69.

Szolnoki, A., & Szabo, G. (2007). Cooperation enhanced by inhomogeneous activity of teaching for evolutionary Prisoner's Dilemma games. *EPL (Europhysics Letters)*, 77, 30004, doi:10.1209/0295-5075/77/30004.

Szolnoki, A., Perc, M., & Danku, Z. (2007). Towards effective payoffs in the prisoner's dilemma game on scale-free networks. *Physica A: Statistical Mechanics and its Applications*, 387, 2075-2082, doi:10.1016/j.physa.2007.11.021.

Szolnoki, A., Perc, M., & Szabo, G. (2009). Topology-independent impact of noise on cooperation in spatial public goods games. *Physical review. E, Statistical, nonlinear, and soft matter physics*, 80, 056109, doi:10.1103/PhysRevE.80.056109.

Tanimoto, J. (2015). *Fundamentals of Evolutionary Game Theory and its Applications.* Springer Japan.

Taylor, C., & Nowak, M. (2007). Transforming the Dilemma. *Evolution; international journal of organic evolution*, 387, 2281-2292, doi:10.1111/j.1558-5646.2007.00196.x.

Timbrell, G., Delaney, P., Chan, T., Yue, A., & Gable, G. (2005). A Structurationist Review of Knowledge Management Theories. *International Conference on Information Systems*, Proceedings. 20.

Traulsen, A., & Hauert, C. (2008). Stochastic Evolutionary Game Dynamics. *Reviews of Nonlinear Dynamics and Complexity*, 2, doi:10.1002/9783527628001.ch2.

Traulsen, A., & Nowak, M. A. (2006). Evolution of cooperation by multilevel selection. *National Academy of Sciences*, 103, 10952-10955, doi:10.1073/pnas.0602530103.

Traulsen, A., Claussen, J. C., & Hauert, C. (2006). Coevolutionary Dynamics: From Finite to Infinite Populations. *Physical review letters*, 95, 238701, doi: 10.1103/PhysRevLett.95.238701.

Traulsen, A., Nowak, M., & Pacheco, J. (2006). Stochastic Dynamics of Invasion and Fixation. *Physical review. E, Statistical, nonlinear, and soft matter physics*, 74, 011909, doi:10.1103/PhysRevE.74.011909.

Traulsen, A., Shoresh, N., & Nowak, M. (2008). Analytical Results for Individual and Group Selection of Any Intensity. *Bulletin of mathematical biology*, 70, 1410-24, doi:10.1007/s11538-008-9305-6.

Trivers, R. L. (1971). The Evolution of Reciprocal Altruism. *The Quarterly Review of Biology*, 46, 35-57, doi:doi: 10.1086/406755.

Wang, Z., Perc, M., & Szolnoki, A. (2012). Evolution of public cooperation on interdependent networks: The impact of biased utility functions. *EPL (Europhysics Letters)*, 97, doi:10.1209/0295-5075/97/48001.

Wang, Z., Szolnoki, A., & Perc, M. (2013). Optimal interdependence between networks for the evolution of cooperation. *Scientific reports*, 3, 2470, doi:10.1038/srep02470.

Wang, Z., Wang, L., Szolnoki, A., & Perc, M. (2015). Evolutionary games on multilayer networks: A colloquium. *The European Physical Journal B*, 88, 124-138, doi:10.1038/srep02470.

Watts, D. J., & Strogatz, S. H. (1998). Collective dynamics of 'small-world' networks. *Nature*, 393, 440–442, doi:10.1038/30918.

Zaggi, M. (2013). Eleven mechanisms for the evolution of cooperation. *Journal of Institutional Economics*, 10, 197-230, doi:10.1017/S1744137413000374.

Zukewich, J., Kurella, V., Doebeli, M., & Hauert, C. (2013). Consolidating Birth-Death and Death-Birth Processes in Structured Populations. *PloS one*, 8, e54639, doi:10.1371/journal.pone.0054639.

Appendix A. Algorithm for Payoff and AGoS Calculation

The numeric optimization considered in order to make the simulations less demanding on CPU requires more variables (memory) as a trade-off. The relevant set of variables considered for the optimization of the simulations' duration is as follows:

Variable		Meaning
n	-	Chosen node which strategy is to be updated in…
l_n	-	… layer l_n
F	-	Enhancement factor
M	-	Number of layers
β	-	Intensity of selection
N^l	-	Number of nodes in layer l with $N^l = N$
S_i^l	-	Strategy of node i in layer l It can value C (Cooperator) or D (Defector)
Invest_i^l	-	Investment of node i in layer l per game
Payoff_i^l	-	Payoff collected by node i in layer l
Payoff_i	-	Accumulated payoff of node i across all layers $\text{Payoff}_i = \sum_{l=1}^{M} \text{Payoff}_i^l$
Neigh_{1i}^l	-	Set of nodes with direct links to node i in layer l The distance between nodes i and x in layer l with $x \in Neigh_{1i}^l$ values 1.
Neigh_{2i}^l	-	Set defined as $\{x: \exists j \in \text{Neigh}_{1i}^l, x \in Neigh_{1j}^l, x \neq i, x \notin \text{Neigh}_{1i}^l\}$, it implies that $\text{Neigh}_{2i}^l \cap \text{Neigh}_{1i}^l = \emptyset$. The distance between nodes i and x in layer l with $x \in Neigh_{2i}^l$ values 2.
k_i^l	-	Number of neighbours of node i in layer l. k_i^l equals the cardinality of Neigh_{1i}^l set.

AGoS_i^l - Contribution of node i to AGoS of layer l

$$AGoS_i^l = \begin{cases} \frac{1}{k_i^l} \sum_{j \in \text{Neigh}_{1i}^l, S_j^l = C} \frac{1}{1 + e^{-\beta(\text{Payoff}_j^l - \text{Payoff}_i^l)}}, if\ S_i^l = D \\ -\frac{1}{k_i^l} \sum_{j \in \text{Neigh}_{1i}^l, S_j^l = D} \frac{1}{1 + e^{-\beta(\text{Payoff}_j^l - \text{Payoff}_i^l)}}, if\ S_i^l = C \end{cases}$$

AGoS^l - AGoS in layer l

$$\text{AGoS}^l = \frac{1}{N^l} \sum_{j=1}^{N^l} \text{AGoS}_j^l$$

The AGoS variables are stored in an IEEE 754 double format with 8 bytes, 52 bits (plus 1 more implicit bit) for the significant digits of a number in binary format. This means a precision of at least $floor(log_{10}(2^{53})) = 15$ decimal digits, more than enough to accommodate the cumulative effects of rounding errors resulting from the iterations of each simulation.

In each iteration of the stochastic process modelling the evolution of cooperation on a multilayer with M layers of networks, after focal node n in layer l_n has been selected, pairwise comparison of its payoff with the one of its neighbour with a distinct strategy in the same layer may dictate with a Fermi-like probability that strategy $S_n^{l_n}$ is to be updated. In case it is and before it is, the following steps are taken in order to incrementally update individual and global payoffs and AGoS with minimum CPU consumption:

1. At every layer, delete (i) contribution of node n to AGoS of the layer, (ii) contribution of direct neighbours of node n to AGoS of the layer and contributions of nodes at distance 1 from node n to (iii) the partial AGoS of nodes at distance 2 of node n and (iv) to the AGoS of the layer:

   For every $l \in \{1, \dots, M\}$ do

   $\text{AGoS}^l \leftarrow \text{AGoS}^l - \text{AGoS}_n^l$ -- (i)

   For every $x \in \text{Neigh}_{1n}^l$ do

   $\text{AGoS}^l \leftarrow \text{AGoS}^l - \text{AGoS}_x^l$ -- (ii)

   For every $y \in \text{Neigh}_{2n}^l$ do

   IF $S_x^l \neq S_y^l$ THEN

   aux $\leftarrow$ contribution to $AGOS_y^l$ from node x in layer l

$\text{AGoS}_y^l \leftarrow \text{AGoS}_y^l - \text{aux}$ -- (iii)

$\text{AGoS}^l \leftarrow \text{AGoS}^l - \text{aux}$ -- (iv)

END IF

2. Delete contributions of node n to its neighbours' payoffs at (i) layer and (ii) multilayer level:

   Set $LS = \{l_n\}$ or $LS = \{1, \dots, M\}$, depending on investment distribution criteria being baseline or other, respectively.

   For every $l \in LS$ do

   IF $S_n^l == C$ THEN

   For every $x \in \text{Neigh}_{1n}^l$ do

   $\text{aux} \leftarrow \frac{F}{2} Invest_n^l$

   $\text{Payoff}_x^l \leftarrow \text{Payoff}_x^l - \text{aux}$ -- (i)

   $\text{Payoff}_x \leftarrow \text{Payoff}_x - \text{aux}$ -- (ii)

   END IF

3. Update focal node n strategy in layer l_n

   $S_n^{l_n} \leftarrow S_n^{l_n} == C \ ? D : C$[4]

With strategy $S_n^{l_n}$ updated, following steps close current iteration of stochastic process:

4. In case of distributed investment, i.e. not baseline, update investment Invest_n^l across all l layers.

5. Update contributions of node n to its neighbours' payoffs at (i) layer and (ii) multilayer level:

   Set $LS = \{l_n\}$ or $LS = \{1, \dots, M\}$, depending on investment distribution criteria being baseline or other, respectively.

[4] $cond \ ? \ val1 : \ val2$ values $val1$ or $val2$ depending on Boolean condition $cond$ being $true$ or $false$, respectively.

For every $l \in LS$ do

IF $S_n^l == C$ THEN

For every $x \in \text{Neigh}_{1n}^l$ do

aux $\leftarrow \frac{F}{2} Invest_n^l$

$\text{Payoff}_x^l \leftarrow \text{Payoff}_x^l + \text{aux}$ -- (i)

$\text{Payoff}_x \leftarrow \text{Payoff}_x + \text{aux}$ -- (ii)

6. Calculate new node n payoffs (i) per layer and (ii) multilayer:

$\text{Payoff}_n \leftarrow 0$

For every $l \in \{1, \dots, M\}$ do

$\text{Payoff}_n^l \leftarrow 0$

For every $x \in \text{Neigh}_n^l$ do

$\text{Payoff}_n^l \leftarrow \text{Payoff}_n^l + \left(S_x^l == C \; ? \; \frac{F}{2} \text{Invest}_x^l : \; 0\right)$

$\text{Payoff}_n^l \leftarrow \text{Payoff}_n^l + \left(S_n^l == C \; ? \; (\frac{F}{2}\text{-}1)\text{Invest}_n^l k_n^l : \; 0\right)$ -- (i)

$\text{Payoff}_n \leftarrow \sum_{l=1}^{M} \text{Payoff}_n^l$ -- (ii)

7. Update (i) node n AGoS in every layer and impact it on (ii) AGoS of the layer:

For every $l \in \{1, \dots, M\}$ do

Calculate $AGoS_n^l$ -- (i)

$\text{AGoS}^l \leftarrow \text{AGoS}^l + \text{AGoS}_n^l$ -- (ii)

8. At every layer, (i) calculate AGoS for neighbours of node n, (ii) impact it on the AGoS of the layer, add contributions of nodes at distance 1 from node n (iii) to the partial AGoS of nodes at distance 2 of node n and (iv) to the AGoS of the layer:

For every $l \in \{1, \dots, M\}$ do

For every $x \in \text{Neigh}_{1n}^l$ do

Calculate $AGoS_x^l$ -- (i)

$\text{AGoS}^l \leftarrow \text{AGoS}^l + \text{AGoS}_x^l$ -- (ii)

For every $y \in \text{Neigh}_{2n}^l$ do

IF $S_x^l \neq S_y^l$ THEN

aux ← contribution to $AGOS_y^l$ from node x in layer l

$\text{AGoS}_y^l \leftarrow \text{AGoS}_y^l + \text{aux}$ -- (iii)

$\text{AGoS}^l \leftarrow \text{AGoS}^l + \text{aux}$ -- (iv)

END IF

Model variables are ready for subsequent stochastic process iteration.

Appendix B. Degree-Degree Correlation and Overlapping

Degree-degree correlation in a multilayer is only meaningful for its multiplex subtype with the same set of nodes present in all layers, no inter-layer links, and in case these are supported on heterogeneous networks.

Pearson correlation index is used to estimate the degree correlation between two layers. It varies between -1 (when individuals have the same degrees but in different network layers), passing by 0 (meaning layer networks with uncorrelated individual degrees) to 1 (when individuals have coinciding degrees in both layer networks). A methodology for correlation tuning was developed, based on a simulated annealing method proposed in (Nicosia & Latora, 2015). The starting point is a set of two layers, second one replicated from first one. Then iteratively, one randomly selects a pair of individuals, N_1 and N_2, in second layer and switches their names in that layer. Implicitly, in second layer N_1's neighbours swap with N_2's and vice-versa. If the individual switching moves degree-degree correlation towards intended target it is accepted; otherwise, it is accepted conditioned on a certain probability. This allowed deviation from the path towards target correlation is essential, in order to avoid getting stuck on local minima and to keep the parameter space of exploitation open. This logic is applied in cascade to the $M-1$ consecutive pairs of an M-layers multilayer.

As in (Nicosia & Latora, 2015), a M-layers multilayer having a particular degree-degree correlation means that layers l and $l+1$, whatever $l \epsilon \{1, \dots, M-1\}$ have that degree-degree correlation. As correlation between layers is non-transitive, the pairs of layers $\{l-1, l\}$ and $\{l, l+1\}$ having the same correlation does not imply the same value applies to $\{l-1, l+1\}$ pair of layers. Additionally and due to the inexistence of inter-layer links, the notion of consecutive layers is purely arbitrary, depends on labelling, as layers are statistically

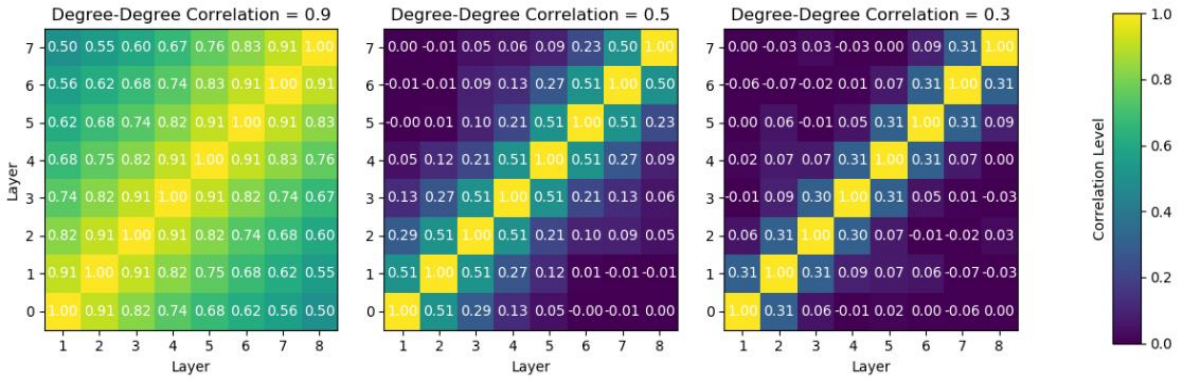

Figure B-1- Example of a Degree-Degree Correlation Matrix

indistinguishable from each other. If degree-degree correlation MxM matrix is to be plotted for a M-layer multilayer resulting from the application of this algorithm, main diagonal values 1 and diagonals next to main one assume multilayer degree-degree correlation. The matrix is symmetric. Values for other entries are not anticipated. An example of a correlation MxM matrix is depicted in Figure B-1.

Overlapping is a different concept from degree-degree correlation, although not independent. Overlapping between two layers α and α' provide an indicator on how probable it is for an arbitrary pair of nodes to be linked in both layers. It is defined as

$$overlapping^{\alpha\alpha'} = \frac{\sum_{i<j} a_{ij}^{\alpha} a_{ij}^{\alpha'}}{\sum_{i<j} a_{ij}^{\alpha} + \sum_{i<j} a_{ij}^{\alpha'} - \sum_{i<j} a_{ij}^{\alpha} a_{ij}^{\alpha'}} \quad (1)$$

with

$$a_{ij}^{\alpha} = \begin{cases} 1, & if\ nodes\ i\ and\ j\ are\ linked\ in\ layer\ \alpha \\ 0, & otherwise \end{cases} \quad (2)$$

Although overlap concept applies to multilayers both with heterogeneous networks as with Horand networks, former case is the only one addressed because of its increased relevance due to degree heterogeneity. Overlapping between two layers was tuned by copying randomly links from one BA layer to the other, until reaching the pretended number of replicated links. Then, in the layer in construction new links are added such that (i) they are absent from reference layer, (ii) each node needs to have at least $m\ (= \frac{<k>}{2})$ connections and (iii) preferential attachment principle is taken into account when deciding on the nodes to be connected next by new links. The steps have been conducted ensuring that networks remain fully connected.

Degree-degree correlation and overlapping are not independent variables, because one cannot be totally controlled without impacting the other, e.g. a perfect 1 overlapping implies a degree-degree correlation of 1.

If layers α and α' have not a single link in common connecting the same pair of nodes, overlapping is null. If any pair of nodes linked in one layer is also linked in the other, overlapping is total.

Along this appendix, the influence of degree-degree correlation and overlapping on multilayer behaviour is taken into account. Here we will conclude that in general degree-degree correlation refrains cooperation and in particular for unconstrained (baseline) criteria favours topology enslavement, a phenomenon in which the system gets insensitive to system

parameters as enhancement factor (F) or intensity of selection (β) in the case of Public Goods Games or alike, S or T in original pairwise games as Prisoner's Dilemma. No matter the value of this parameter, the level of cooperation achieved coincides with the one the multilayer was initialized with. Overlapping also leads to topology enslavement because it implies degree-degree correlation. For the constrained case, topology enslavement is also observed but driven by a chain of mechanisms of different sort described in appendix C.

In an attempt to shed light on degree-degree correlation influence on cooperation evolution, average level of cooperation across layers was calculated as a function of degree-degree correlation and intensity of selection β for 8-layers multilayer with BA networks and an enhancement factor of 1.7, a value for which cooperation is viable for any investment criteria. The results discriminated by investment distribution criteria are presented in figure B-2.

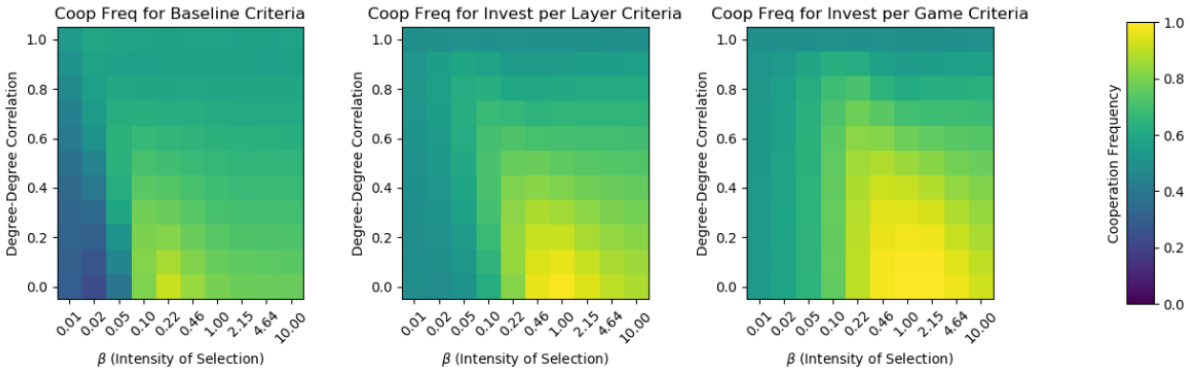

Figure B-2- Average Level of Cooperation for Degree-Degree Correlation versus Intensity of Selection (β). Multilayer have 8 layers, 1000 (N) individuals per layer, ⟨k⟩ equals to 4 and F values 1.7 and BA networks. In each layer, nodes were randomly initialized with half as Cooperators.

The figure highlights two facts. The most notorious one is that, apart from baseline criteria for very low intensity of selections, level of cooperation decreases when degree-degree correlation gets stronger, a behaviour due to cumulative payoff. When degree-degree correlation is maximum, the cooperation level for all criteria reaching the value of 50%, precisely the proportion of Cooperators the multilayer was initialized with, is the second fact to highlight in the figure. This multilayer inertia in changing initial level of cooperation had already been noticed by (Kleineberg & Helbing, 2018) for the baseline case.

The way a multilayer is constructed, it having a high degree-degree (Pearson) correlation means that the number of neighbours any node has in any layer with a high probability is similar to the set of neighbours the same node has across all layers in the multilayer. Thus, odds of a hub in a layer being also a hub in another layer increase with degree-degree

correlation. Let us now consider a hub node and a high degree-degree correlation between the layers in the multilayer. Because of this correlation factor, hubs are aligned across layers. The payoff collected in layers in which the node cooperates, because of it being cumulative, impacts all layers. This means that a hub can defect in a layer l_0 with a high payoff collected in other layers where the hub cooperates. The Defector strategy of this hub in layer l_0 because of its high payoff functions as a reference and tends to, if not to saturate the all layer as ALLD, at least to dry out cooperation in the neighbourhood. The initial strategy of bigger nodes in a layer, randomly determined, dictates the direction of saturation, ALLC or ALLD, of the layer or at least the neighbourhood. Moreover, when degree-degree correlation is high, a node tends to have the same neighbours in all layers, which means that if it has k degree it tends of have a total of distinct k neighbours across all M layers of the multilayer.

Now let us consider a multilayer with maximum degree-degree correlation, investment per layer criteria, an arbitrary focal node and any one of its neighbours. These two nodes will share a link across all layers. If the neighbour is cooperative in N_C layers, it will contribute to focal node payoff with $\frac{F}{2N_C}$ per link in $N_C$links resulting in an aggregated contribution of $\frac{F}{2}$. If this neighbour now switches strategy from cooperation to defection in one of the layers its contribution to focal node payoff will be updated to $\frac{F}{2(N_C-1)}(N_C-1)$, i.e., in spite of strategy update neighbour contribution to focal node payoff was preserved, as long as the neighbour kept cooperating in at least 1 layer, a condition with probability tending to 1 as the number of layers tends to infinity. This rational is easily extended to focal node change of strategy and the other distributed investment criteria. The bottom line is that degree-degree correlation tends to make individuals' accumulated payoffs invariant in time. Additionally, having Cooperators been randomly positioned, the chances of an individual A switching strategy under influence of a neighbour B in a layer is equal to chances of symmetrical strategy switch between the same pair of individuals. This leads to the preservation of initial level of cooperation.

On the other hand, for unconstrained baseline criteria, contributions of a neighbour in different layers are independent and an exclusive function of neighbour' strategy in that layer. This suggests baseline not to be so dependent on degree-degree correlation as figure B-2 illustrates. For a fixed intensity of selection, the variation of the level of cooperation versus degree-degree correlation replicates findings in (Kleineberg & Helbing, 2018). Still for baseline criteria and maximum degree-degree cooperation, topological enslavement derives from hub alignment across layers, which provides them a considerable strategy inertia,

minimizing the odds of a hub changing its strategy. Thus, the initial proportion of Cooperators in a multilayer coincides with the expected proportion of hubs functioning as sources of strategy spreading, leading to a final level of cooperation equal to the initial one.

Common to all criteria and apart from baseline case with minimum intensity of selection is that degree-degree correlation reduction favours cooperation. By not having hubs aligned across layers, the number of individuals being hubs in at least one layer increases, its global basin of attraction widens, i.e., the set of hub distinct neighbours across all layers increases, diversity settles in and cooperation levels raise.

With no surprise, heat map concerning investment distributed per layer is similar to the one distributed per game one for $\beta \langle k \rangle$ times bigger, $\langle k \rangle$ being the average degree of the network.

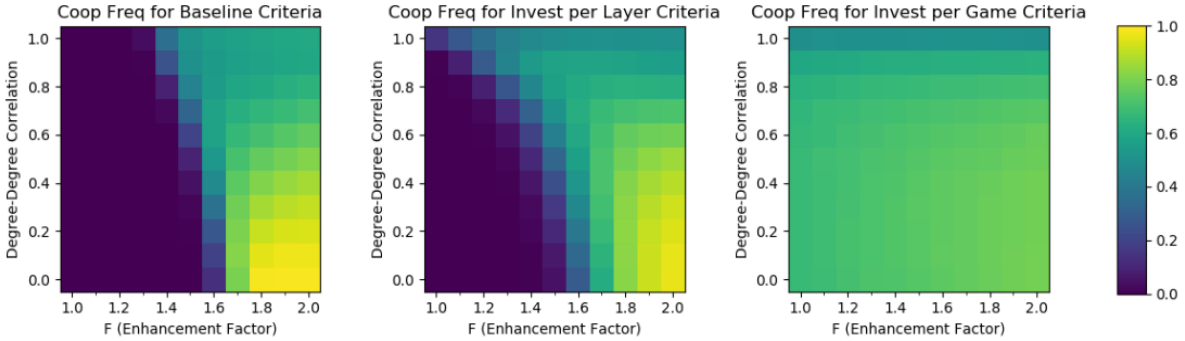

Figure B-3- Average Level of Cooperation for Degree-Degree Correlation versus Enhancement Factor. Multilayer has 8 layers, 1000 (N) individuals per layer, $\langle k \rangle$ equals to 4, β values 0.1 and BA networks. In each layer nodes were randomly initialized with half as Cooperators

Another perspective of analysis is to fix intensity of selection β to 0.1 and make the enhancement factor F and the degree-degree correlation vary. Results are depicted in figure B-3. Thin horizontal stripes taken from the bottom of the heat maps with minimum degree-degree correlation reproduces the results already achieved in the right panels of figure 14. For higher values of F, as 1.7, cooperation decreases while correlation increases as it had already been explained. The other way around happens with lower values of F. For baseline and investment per layer criteria, the critical F beyond which cooperation fires decreases when degree-degree correlation increases. This is not totally surprising if one takes into account that for no degree-degree correlation this is a territory of defection. When correlation is added, nodes that are hubs in one layer tend to also be hubs in other layers with the same degree, as Pearson variation of correlation is used, and with the same neighbours considering how the multilayer is built. If these hubs are initialized as Cooperators in some layers degree-degree correlation reinforces their payload which make them a reference for neighbours to copy their

strategy spreading cooperation along these layers. It is this phenomenon that causes the defection region to recede in the heat maps for baseline and investment per layer criteria as degree-degree correlation increases.

For investment distributed per game criteria, topological enslavement sets in. As it had already been identified in figure 14 and figure 16 from main body, cooperation levels tend to be independent of enhancement factor. Additionally, cooperation level exhibits almost no sensitivity to degree-degree correlation. This has to do with the fact that unless a node defects

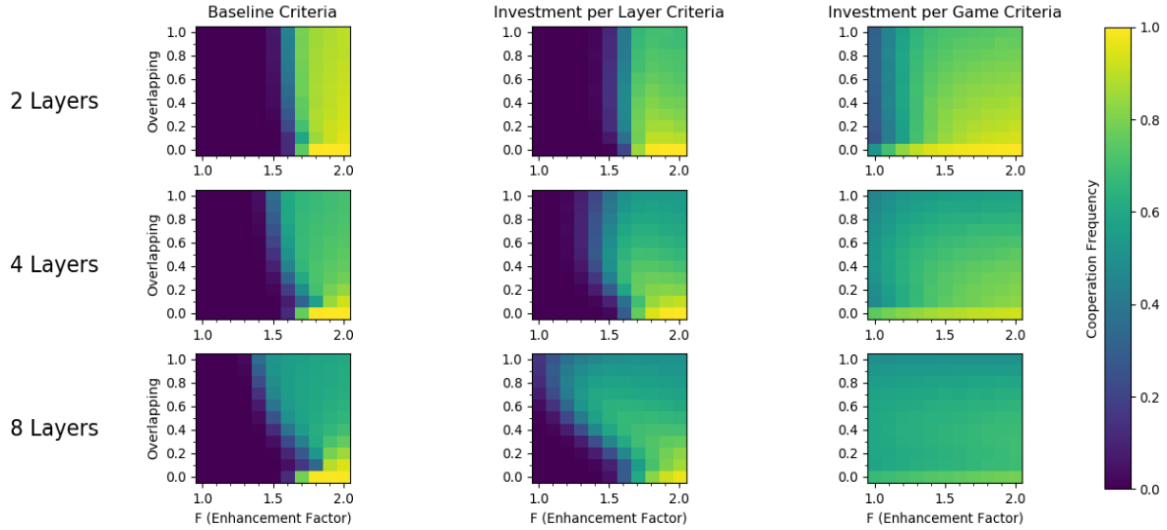

Figure B-4- Average Level of Cooperation in BA Multilayers as a function of Link Overlapping and Enhancement Factor. Multilayer has 8 layers, 1000 (N) individuals per layer, ⟨k⟩ equals to 4, β equals to 0.1 and BA networks. In each layer nodes were randomly initialized with half as Cooperators

in all layers, the total amount it is committed to invest across all layers is fixed to 1 unit. So in opposition to what happens with other criteria, with investment distributed per game a node by being a hub does not experiment a change in its overall investment and in corresponding payoff impact.

Analogously, the payoff contributions collected from neighbours does not change statistically by the fact of these neighbours having or having not their degrees (and neighbours) aligned across layers. Had the multilayer more layers, the heat map relative to investment distributed per game would be more uniform and the heat map for investment distributed per layer would get closer to former one.

Overlapping measures how repetitive links are across layers. In the limit a multilayer having full overlapping means all its layers being equal. Figure B-4 plots for BA multilayers accomplished level of cooperation averaged across all layers as a function of overlapping and enhancement factor. Heat maps are not too different from previous figure, something aligned

with (Kleineberg & Helbing, 2018) observation that cooperation in multilayers is much more sensitive to degree-degree cooperation than to link overlapping, this having to do with the fact that overlapping cannot be introduced without degree-degree correlation. What is new in this heat map is dependency on the number of layers. For baseline, the critical F value beyond which cooperation triggers recedes as the number of layers increases but at expenses of cooperation where it is achieved to reach lower marks. With a higher number of layers and overlapping, hubs get aligned across layers and increase their payoff. Thus on the layers they cooperate the trend is for cooperation to spread. This explains why critical F backs off when the number of layers increase. In the parameter domain where cooperation succeeds and for higher degree-degree correlation, average cooperation scores less because topological enslavement sets in.

Heat maps concerning investment per layer criteria are similar to the ones concerning baseline, sharing the same trends although with a larger cooperation domain.

Topological enslavement and insensitiveness on enhancement factor F evolution with the increase in the number of layers is best portrayed in the heat maps concerning investment per game criteria.

Appendix C. Criteria and Topological Enslavement

A multilayer of the multiplex subtype, i.e., with the same set of nodes present in al layers and no inter-layer links, with constrained investment criteria, be it investment distributed per layer or game, exhibits the characteristic that as the number of layers increases the accumulated payoff from individual's interactions tends to converge to a constant value for all individuals in the population. In other words, the number of layers is inversely proportional to the observed variance of accumulated payoffs among nodes or individuals. A consequence of this disposition is that the multilayer gets trapped in its initial conditions and insensitive to game parameters as S, T or F, meaning that the level of cooperation reached at the end of simulation is no different from the one multilayer was initialized with. This applies to both pairwise games as Prisoner's Dilemma and Public Goods Games, no matter the payoffs being averaged or accumulated. (Kleineberg & Helbing, 2018) had already noticed this phenomenon in an unconstrained (baseline) multilayer with heterogeneous networks but this fate was reached via a chain of mechanisms completely different from the ones in place with distributed investment, requiring a high degree-degree correlation to tight together individual payoffs in different layers in order to boost global hubs' payoff.

Here one presents a mathematical explication to why distributed investment criteria and topology lead to multilayer enslavement even in the absence of degree-degree correlation. The arguments to follow apply to homogeneous networks, but experimentation show that they are extensible to heterogeneous ones.

Let us consider a multilayer with M layers and where each layer corresponds to an independently generated network from the same type. For instance, all layers correspond to Horand or BA that are generated with the same parameters but independently. Let $\langle k \rangle$ be the average degree of each layer. Moreover, strategies are initialized at random. In each layer, the strategy of each individual is to cooperate with probability p and to defect with probability $1 - p$.

The payoff of a randomly chosen focal individual N_f results from the sum of two independent contributions:

- C_1: Contribution of node N_f investment across all layers of the multilayer and
- C_2 : Contribution of each neighbour investment across all layers.

C_1 is a Bernoulli variable with distribution

$$\text{Prob}\left(\text{C}_1 = \left(\frac{F}{2} - 1\right)\right) = \text{Prob}(\text{N}_\text{f} \text{ is Cooperator in at least 1 layer}) = \quad (1)$$

$$1 - (1 - \text{p})^{\text{M}}$$

$$\text{Prob}(\text{C}_1 = 0) = \text{Prob}(\text{N}_\text{f} \text{ defects in all M layer}) = (1 - \text{p})^{\text{M}} \quad (2)$$

Contribution C_1 depends exclusively on individual N_f strategy across layers, being independent of his/her neighbours' strategy. First moments of C_1 are:

$$\mu_{C_1} = \text{E}(C_1) = (\frac{F}{2} - 1)\,(1 - (1 - \text{p})^M) \quad (3)$$

$$\sigma^2_{C_1} = (\frac{F}{2} - 1)^2 (1 - \text{p})^M (1 - (1 - \text{p})^M) \quad (4)$$

As long as the multilayer layers are independent and Cooperators are assorted at random along the nodes of the network, then all individual share a payoff first component that tends to $(\frac{F}{2} - 1)$ with a decreasing variance towards zero as the number of layers increase.

Contribution C_2 has no dependency on individual N_f strategy and is given by

$$\text{C}_2 = \frac{F}{2} * [(P_{11} + \cdots + P_{1K_1}) + \cdots + (P_{L1} + \cdots + P_{LK_L}) \quad (5)$$

where k_l represents the degree (number of links) of individual N_f in layer l and P_{li} the contribution of neighbour i in layer l.

Let us know assume the particular case where all the layers are Horand networks. Then $k_1 = k_2 = \cdots = k_L = \langle k \rangle$ and individual N_f will have $\langle k \rangle * M$ neighbours from all the layers in the multilayer. From a game played with each of the neighbours in a generic layer M_0, neighbours' contribution will equal

$$P_{M_0 i} = \begin{cases} \dfrac{1}{< k > (\delta_{S_1,C} + \cdots + \delta_{S_{M_0-1},C} + 1 + \delta_{S_{M_0+1},C} + \cdots + \delta_{S_M,C})} & , if\ (i) \\ 0 & , \text{if (ii)} \end{cases} \quad (6)$$

where condition (i) applies if neighbour i of individual N_f in layer M_0 cooperates, otherwise condition (ii) applies. Moreover, in equation 6, $\delta_{S_i C}$ denotes the Kronecker delta, which is one if an individual in layer l Cooperates, being zero otherwise. Under these assumptions, the contribution C_2 can be simplified to a sum of random variables

$$C_2 = \frac{F}{2} \sum_{layer\ l=1}^{M} \sum_{neighbor\ n=1}^{<k>} P_{ln} \quad (7)$$

where P_{in} can be considered independent when networks are sparse, i.e., $\langle k \rangle \ll N$. The first moments of C_2 are:

$$E(C_2) = \frac{F}{2}\mathrm{M}\langle \mathrm{k} \rangle \sum_{l=0, l\neq M_0}^{M-1} \frac{1}{<k>(l+1)}$$

Prob (Neighbour is Cooperator in l layers besides M_0)

$$= \frac{F}{2}\ \mathrm{M}\ \sum_{l=0}^{M-1} \frac{1}{l+1} p\ C_l^{M-1} p^l (1-p)^{M-1-l} \tag{8}$$

$$\sigma_{C_2}^2 = \left(\frac{F}{2}\right)^2 \sum_{layer\ l=1}^{M} \sum_{neighbor\ n=1}^{<k>} \sigma_{P_{in}}^2 = M\langle k \rangle \left(\frac{F}{2}\right)^2 * \sigma_{P_{in}}^2 \tag{9}$$

Considering the binomial distribution approximation to the Poisson one when $\lambda = Mp \gg 1$, $E(C_2)$ the above expression further simplifies to

$$\mu_{C_2} = E(C_2) = \frac{F}{2}\mathrm{Mp}\sum_{l=0}^{+\infty} \frac{e^{-\lambda}\lambda^l}{(l+1) * l!} = \frac{F}{2} * \mathrm{M} * \frac{p}{\lambda} * \sum_{l=1}^{+\infty} \frac{e^{-\lambda}\lambda^l}{l!} = \frac{F}{2}\ e^{-\lambda}\ (e^{\lambda} - 1) \approx \frac{F}{2} \tag{10}$$

Hence, as the number of layers increases, i.e., when λ increases, the payoff of any node tends to $\mu_{C_1} + \mu_{C_2} = \left(\frac{F}{2} - 1\right) + \frac{F}{2} = F - 1$. Concerning, the variance of the payoff distribution ($\sigma_{C_2}^2$), it can be calculated based on the variance of the contribution of a generic neighbour n in a generic layer l as follows:

$$\sigma_{P_{in}}^2 = E(P_{in}^2) - E(P_{in})^2 \tag{11}$$

$$E(P_{in}^2) = \sum_{layer\ l=0}^{M-1} \frac{1}{(l+1)^2} p C_l^{M-1-l} p^l (1-p)^{M-1-l} \tag{12}$$

where, we again consider the binomial distribution approximation to the Poisson distribution with $\lambda = Mp \gg 1$,

$$E(P_{in}^2) = \sum_{layer\ l=0}^{+\infty} \frac{p}{(l+1)^2} \frac{e^{-\lambda}\lambda^l}{l!} = p\frac{e^{-\lambda}}{\lambda^2} \sum_{layer\ l=0}^{+\infty} \frac{l+2}{l+1} \frac{\lambda^{l+2}}{(l+2)!} \tag{13}$$

As $\frac{l+2}{l+1} < 2$ for positive l,

$$E(P_{in}^2) < 2p\ * \frac{e^{-\lambda}}{\lambda^2} \sum_{layer\ l=2}^{+\infty} \frac{\lambda^l}{l!} = 2p\ * \frac{e^{-\lambda}}{\lambda^2}\ (e^{\lambda} - 1 - \lambda) \tag{14}$$

Now, $\sigma_{P_{in}}^2$ is positive by definition and is topped by $E(P_{ln}^2)$ with is an $O(\lambda^{-2})$. Thus, $\sigma_{P_{in}}^2$ tends to zero with λ^{-2}. This implies that

$$\sigma_{C_2}^2 = M * \langle k \rangle * \left(\frac{F}{2}\right)^2 * \sigma_{P_{in}}^2 = \frac{\lambda}{p} * \langle k \rangle * \left(\frac{F}{2}\right)^2 * \sigma_{P_{in}}^2 = O(\lambda^{-1}) \tag{15}$$

If we consider equations 4 and 15, the corollary that follows is that in Horand multilayers accumulated payoff variance tends to zero as the number of layers increase. Experimental evidences on first moments of accumulated payoff across a Horand multilayer are depicted

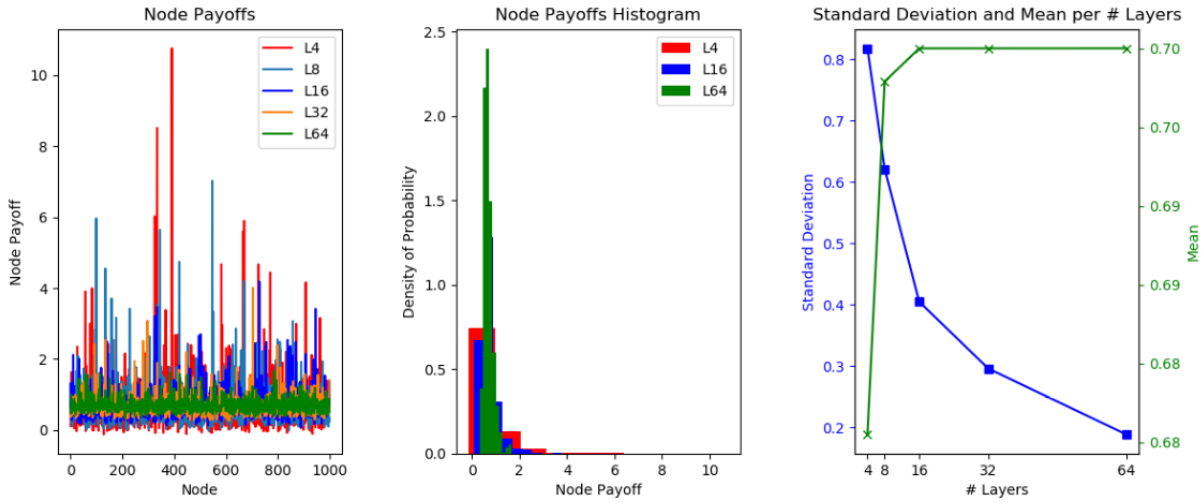

Figure C-1- Payoffs Distribution for Horand Multilayer with Investment per Game versus Number of Layers. Networks are built with uncorrelated layers with $\beta = 1, \langle k \rangle = 4, F = 1.7$, 1000 nodes ($N$) per layer. . Layers were initialized with half nodes as Cooperators randomly chosen. Results were collected after 100 generations, one generation being equal to number of layers ties 1000 iterations.
Two facts are highlighted in the figure: payoff average tends to $F-1$ and its variation to zero as the number of layers increase. Although not presented, the extension of this phenomenon to BA multilayers was also noticed.

in figure C-1.

Having node payoff variance tending to zero has an additional consequence when it comes for a node to consider imitating a neighbour in a given layer with a different strategy: the argument of the exponential in Fermi distribution tends to zero, which allows its expression to be simplified to

$$Prob(\mathrm{S_A} \rightarrow \mathrm{S_B}) = \frac{1}{1 + e^{-\beta(\pi_B - \pi_A)}} \cong \frac{1}{2} + \frac{\beta}{4}(\pi_B - \pi_A) \qquad (16)$$

meaning that with equal probability the strategy of a node is maintained or updated.

The probability of a node updating its strategy on a layer depends now only on it and one of its neighbours randomly chosen having different strategies, which depends on the level of cooperation on the layer. Dependency on nodes relative payoff vanishes as the number of layers increases.

Up to now homogeneous networks with investment per game criteria were considered, but arguments are extensible to investment per layer criteria as a multilayer with homogeneous

networks with degree $\langle k \rangle$, β_0 intensity of selection and investment per game criteria behaves exactly the same as if it had investment per layer and $\beta_0/\langle k \rangle$ intensity of selection.

As all nodes tend to have a similar accumulated payoff and all layers look and behave alike, i.e., they are replicas from the same stochastic model, each generic layer can be mapped to a one dimension random walk alike model with dynamic probabilities of moving either way or staying in the same spot. Figure C-2 plots samples of time series on the evolution of the number of Cooperators for both the average number of Cooperators across a Horand multilayer and the number of Cooperators in individual layers.

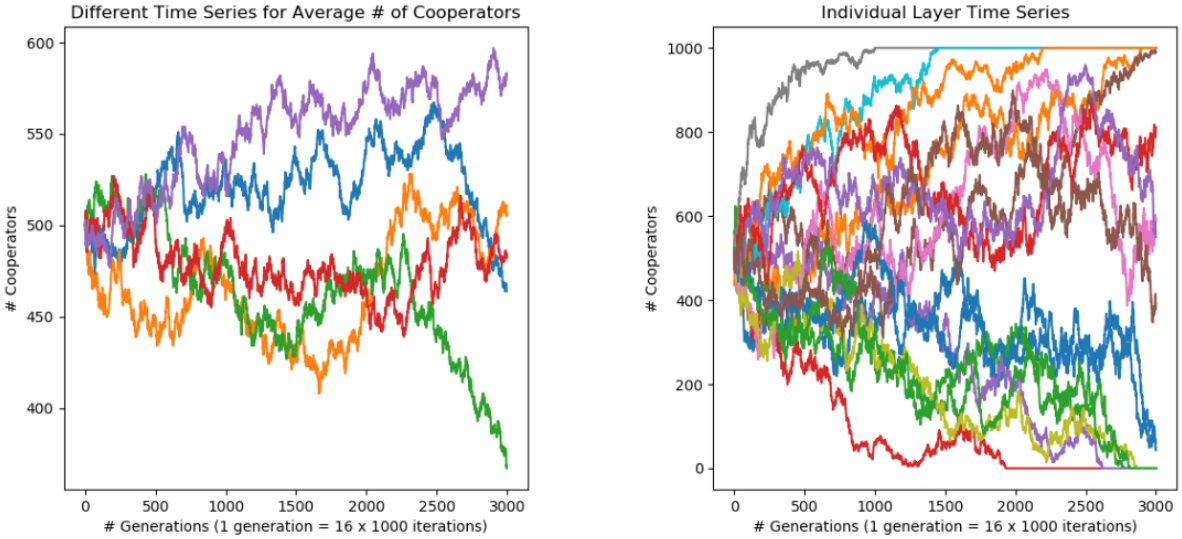

Figure C-2- Time Series of Evolution of Cooperation Level in 16 Layer Horand Multilayer with Investment distributed per Game. Networks are built with $\beta = 1, \langle k \rangle = 4, F = 1.7$, 1000 nodes ($N$) per layer. Layers were initialized with half nodes as Cooperators. On the right side multilayer average number of Cooperators is plot for 5 different runs. On the right side, for a single run, the evolution of the number of Cooperators per layer is plot. Saturation of some layers is noticeable.

Once a multilayer is characterized at a particular point in time, its evolution depends exclusively on its status at that point in time being irrelevant the path leading to that status. This fact makes the evolution of the multilayer suitable to be studied as a Markov process in which the past has no influence on the future once the present is specified. Thus, in a Markov process x(t)

$$Prob(x(t_n) \leq x_n \mid x(t), t \leq t_{n-1}) = Prob(x(t_n) \leq x_n \mid x(t_{n-1})) \quad (17)$$

$x(t)$ is generically an array with one position per layer. A special sort of Markov process is the Markov chain when the system can be described by a finite or countably infinite set of states such that the future evolution of the process, once it is in a given state, depends only on the present state and not on how it arrived at that state. A Markov chain is a stochastic model that can be described as a set of states, $S = \{s_1, \ldots, s_n\}$ and a set of events implying transitions

between states. The process starts in one of these states and moves successively from one state to another with a probability that is an exclusively function of the former and latter states irrespectively of eventual states visited before. Each move is called a step. If the chain is currently in state s_i, then the probability of moving to state s_j is given by p_{ij}. Naturally, $\sum_j p_{ij}$ = 1. A single layer with N nodes can be modelled by a Markov chain where each state is assigned a particular combination of strategies followed by nodes. For a system with N nodes and S strategies there are potentially N^S different states. A multilayer with M layers can also be represented by a Markov chain, but the number of states skyrockets to N^{SM}.

In order to tackle this complexity and with no loss of generality, a single layer will be addressed instead as representative of the set of all multilayer layers, as all layers are replicas from a single agent-level dynamics reference. Moreover, a mean-field approximation will be used in which the identity of the individual nodes following a particular strategy will not be addressed, but instead only the number of nodes following each strategy will be accounted.

With mean field approximation, a scenario where the layer can be divided by a frontier such that on each side of the line all nodes have the same strategy in terms of state representation cannot be distinguished from another one where nodes with different strategies are all randomly mixed.

With mean-field representation, because reproduction is modelled via an imitation process, at each step of the process in the layer where imitation happens the number of Cooperators is altered by at most 1 unit. This implies p_{ij} = 0 for $|i - j| > 1$.

A state i is called absorbing if p_{ij}=δ_{ij}, i.e., once state i is entered it is exited with probability zero. ALLC and ALLD, i.e., state 1000 and state 0 will be absorbing states. Non-absorbing states are qualified as transient.

The graphical representation of the Markov chain derived from mean-field evolution of a single layer is as in figure C-3. This Markov chain corresponds to the one describing the classical stochastic Drunkard's walk process (or Gambler's Ruin) (Grinstead & Snell, 1997)

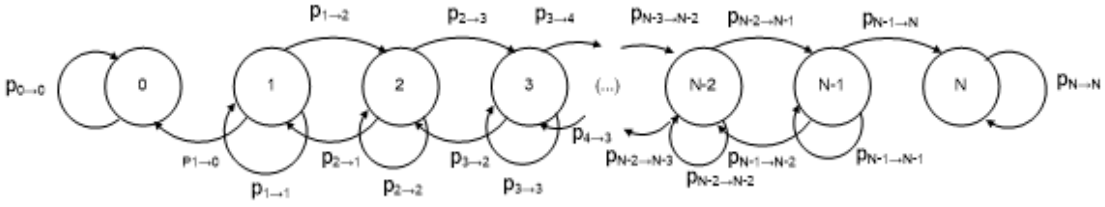

Figure C-3- Markov Chain corresponding to Drunkard's Walk Process

with the following differences: the probability of preserving the state is not zero ($p_{ii} \neq 0$) and the probabilities of changing state depends on present state. The two absorbing states map to home and bar states in Drunkard's walk.

Corresponding Markov transition matrix as described in 2.1.3 for finite populations, is given by the following expressions:

$$p_{ij} = \begin{cases} 1 & , i = j = 0 \\ 1 & , i = j = N \\ \frac{N-i}{N} * \frac{i}{N-1} * \mathrm{Prob_{Fermi}}(\mathrm{S_j} \rightarrow \mathrm{S_i}) & , j = i + 1 \; AND \; 0 < i < N \\ \frac{i}{N} * \frac{N-i}{N-1} * \mathrm{Prob_{Fermi}}(\mathrm{S_j} \rightarrow \mathrm{S_i}) & , j = i - 1 \; AND \; 0 < i < N \\ 1 - \mathrm{p}_{i,i-1} - \mathrm{p}_{i,i+1} & , 0 < i < N \\ 0 & , i = 0 \; AND \; j > 0 \\ & , i = N \; AND \; j < N \\ & , |j - i| > 1 \end{cases} \quad (18)$$

with $Prob_{Fermi}(S_j \rightarrow S_i)$ representing the Fermi probability of node i with strategy S_i copying S_j strategy from node j. $Prob_{Fermi}(S_j \rightarrow S_i)$ is a function of both node i and node j payoffs. As the number of layers increases, all nodes tend to share the same payoff and $Prob_{Fermi}(S_j \rightarrow S_i)$ tend to $\frac{1}{2}$. Let us focus on the content of $p_{i,i+1}$, the probability of increasing the number of Cooperators. First factor, $\frac{N-i}{N}$, reflects the probability of first chosen node being a Defector. Second factor, $\frac{i}{N-1}$, accounts for the probability of, given that a Defector has already been chosen, from N – 1 nodes to choose from, next node to select is 1 of i Cooperators available. Clearly here mean-field approach is followed, as the concrete underlying network is not taken into account. Now that nodes selected are suitable for a strategy imitation, all it is lacking is a favourable probability from Fermi distribution.

Markov transition matrix mixes absorbing and transient states. For an absorbing Markov chain P and after canonicalization is performed as in 2.1.3, one obtains the fundamental matrix N = $\sum_{k=0}^{+\infty} Q^k = (I - Q)^{-1}$ for P. The entry n_{ij} of N gives the expected number of times that the process reaches the transient state s_j if it is started in the transient state s_i. This implies that the expected number of steps before the chain is absorbed, given that the chain starts in

state s_i, is given by t_i, the i-th element of t column vector t, with $t = Nc$, where c is a column vector all of whose entries are 1 (Grinstead & Snell, 1997).

The probability that Markov chain will evolve to absorbing state s_j starting from transient sate s_i is given by b_{ij} entry of matrix B resulting from $B = NR$.

In what follows, Markov chain is applied to a single multilayer average layer with 1000 nodes whose level of cooperation results from the average of Cooperators across all layers.

Figure C-4 plots on its left panel the theoretical quasi-stationary distribution for the mean-field approximation of single layer pretending to represent a multilayer with investment distributed per game and a number of layers tending to infinity. This quasi-stationary distribution reflects the probability of each transient state being visited until the multilayer saturates in any of the absorbing states. Considering all states equally probable for multilayer initialization and the ergodicity of the Markov chain, what is plot in left side panel is just $\frac{\sum_i n_{ij}}{\sum_{ij} n_{ij}}$, where the denominator is just a normalization factor to transform the number of visits in a state into a probability. This corresponds to equally weight each line of the fundamental N matrix, i.e., each possible starting state. The equal probability for all transient states is the highlighting result.

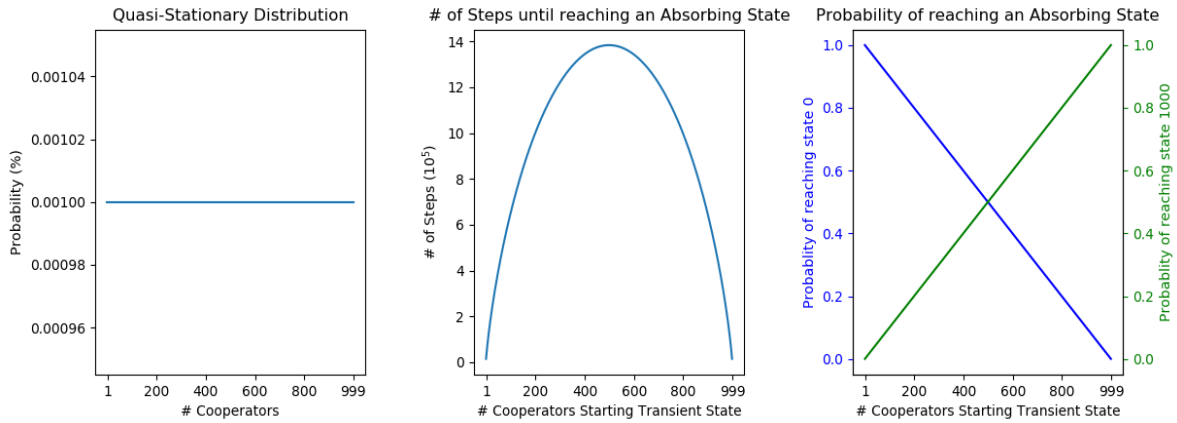

Figure C-4- Theoretical results for a Mean-Field approximation of a Layer with Nodes with equal Payoff. Quasi-stationary distribution, number of steps until reaching an absorbing state and probability of reaching each absorbing state are plot for a mean-field approximation of a generic layer pretending to represent a multilayer with investment distributed per game and number of layers tending to infinity

Vector t, with fields calculated as $t_i = \sum_j n_{ij}$ is depicted in central panel. As expected, the number of steps increases further away from absorbing state initial state is located. Symmetry of the line results from problem symmetry, $p_{i,j} = p_{N-i,N-j}$.

Finally the right panel depicts normalized b_{ij} for final absorbing state j equal to 0 or 1000, i.e., the probability of the system ending up in each of the two absorbing state as a function of starting state. Lines in graph are complementary because in an absorbing Markov chain $Q^n \to 0$ as the number of steps (n) increases, thus the probability that the process will be absorbed is 1, and 0 and 1000 are the only possible absorbing states.

This quasi-stationary distribution uniformity of a generic layer implies an AGoS tending to zero which forces a multilayer to preserve the proportion of Cooperators with which it was initialized. On the other hand, as time unfolds the natural trend is for individual layers to saturate either as ALLC or ALLD. Thus, the initial proportion of Cooperators is reflected in the proportion of layers saturated as ALLC.

This layer polarization is of no surprise, because this overall multilayer Drunkard's walk alike process, having absorbing states of ALLC or ALLD, is doomed to converge to one of them. In this stochastic process, the probability of convergence to ALLC final state equals the proportion of initial Cooperators with which the system was initialized, which justifies why the initial proportion of Cooperators is preserved and why quasi-stationary distribution of states is uniform.

In order to compare theoretical and experimentally the influence of initial Cooperator probability in multilayer evolution, a multilayer with 16 layers of BA and Horand networks with investment criteria distributed per game was independently initialized with a variable concentration of Cooperators. Usual enhancement factors were applied. The evaluation was performed both until and at saturation time. The results are depicted in Figure C-5.

Focusing on BA multilayer, until saturation, final level of cooperation depends on initial one with almost no dependency on enhancement factor. Would the number of layers increase and this dependency would completely fade away. Additionally, for extreme initial probabilities, a sharp transition in final level of cooperation is noticeable. Considering again a single layer with equal payoffs representative of the multilayer, theoretical value for final level of cooperation results from plotting $E(N_{C_f}|N_{C_i})$, with N_{C_i} and N_{C_f} representing, recpectively, initial and final number of Cooperators. Taking into account that generic n_{ij} entry from Markov chain fundamental N matrix represents the expected number of times the multilayer will be in state j , given that it starts in state i, one has

$$\text{Prob}(N_{C_f} = j | N_{C_i} = \text{i}) = \frac{n_{ij}}{\sum_x n_{ix}} \tag{19}$$

$$E(N_{C_f}|N_{C_i} = i) = \sum_j j \frac{n_{ij}}{\sum_x n_{ix}} \tag{20}$$

The theoretical result of $E(N_{C_f}|N_{C_i} = i)$ is precisely what is plot on the top right panel of the figure. The matching is perfect particularly for extreme initial levels of cooperation.

At saturation time the heat map is analogous apart from the fact that final level of cooperation varies linearly with initial one. Against this is as expected and already depicted in right panel of figure C-4. What happens for this BA multilayer as will be illustrated in appendix D when studying its AGoS is that all layers of the multilayer will saturate, some as ALLC; others as ALLD. Moreover, because the naming of the layers is arbitrary and layers are independent, the same layer saturates either as ALLD or ALLC across experiences.

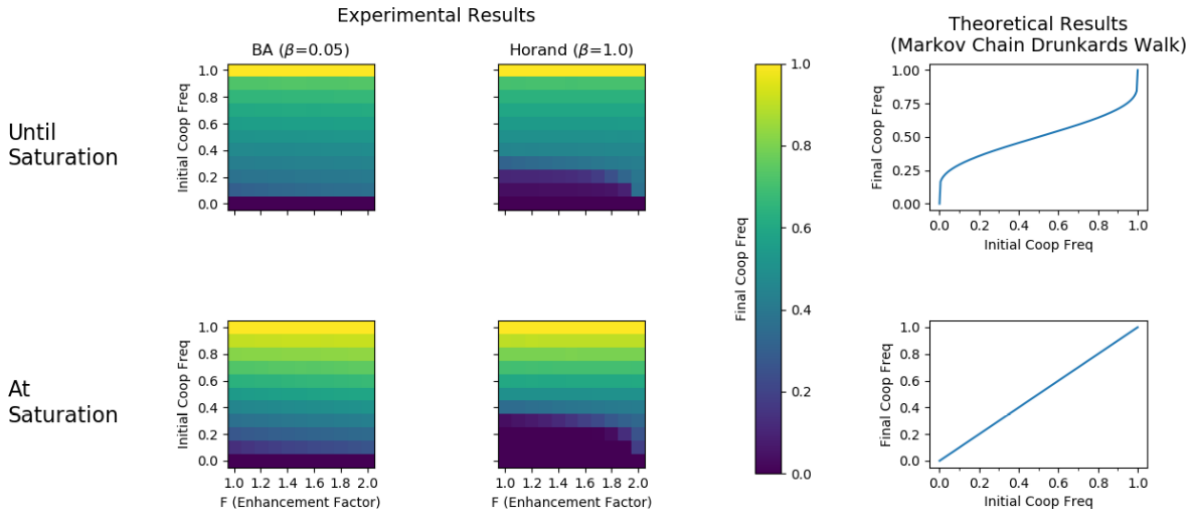

Figure C-5- Topological and Criteria Enslavement in Multilayers with 16 Layers, Investment distributed per Game. Both BA and Horand multilayers have 1000 nodes (N) and $\langle k \rangle = 4$. Former one has $\beta = 0.05$ and $\langle k \rangle = 4$, latter one $\beta = 1.0$. Multilayer layers are independent and randomly initialized with a number of Cooperators taken from a discrete random variable in the set 0 to 1000, inclusive.

The proportion between the number of layers in different conditions will be such as dictated by initial level of cooperation. Topology and investment criteria enslave the multilayer because its evolution cannot be steered by acting upon enhancement factor.

Reasoning on the basis of the Markov chain corresponding to a Drunkard's walk stochastic process, the single layer the multilayer is mapped to is doomed to end up as either ALLC $\left(N_{C_f} = N\right)$ or ALLD $\left(N_{C_f} = 0\right)$, The probability of ending up as ALLC is given by the initial proportion of Cooperators in the layer as from the right panel from figure C-4, i.e.,

$$Prob(N_{C_f} = N) = \frac{N_{C_i}}{N} \tag{21}$$

As there are only two outcomes possible, ALLC or ALLD,

$$\mathrm{E}(N_{C_f}) = NProb\left(N_{C_f} = N\right) + 0Prob\left(N_{C_f} = 0\right) = N_{C_i} \tag{22}$$

which leads one to conclude that final level of cooperation equals initial one.

As in fact one has a multilayer instead of a single layer and as all layers saturate, the initial proportion of Cooperator population in the multilayer dictates the percentage of layers that saturate as ALLC, i.e., the final proportion as Cooperators in the system as all the other layers will saturate as ALLD.

The Horand multilayer exhibits the same trends as described for BA multilayer but with deviations for small initial levels of cooperation, particularly for small values of enhancement factors. This deviation from the theoretical expectations is not surprising and will be experienced in following figures where it will be explained. Were the number of layers greater or the intensity of selection lower and the agreement between theoretical and experimental results would be better.

Considering exclusively multilayers with investment per game criteria, the lines reflecting the way the number of layers, intensity of selection, type of network or enhancement factor modulate the final level of cooperation versus initial are depicted in Figure C-6. The higher

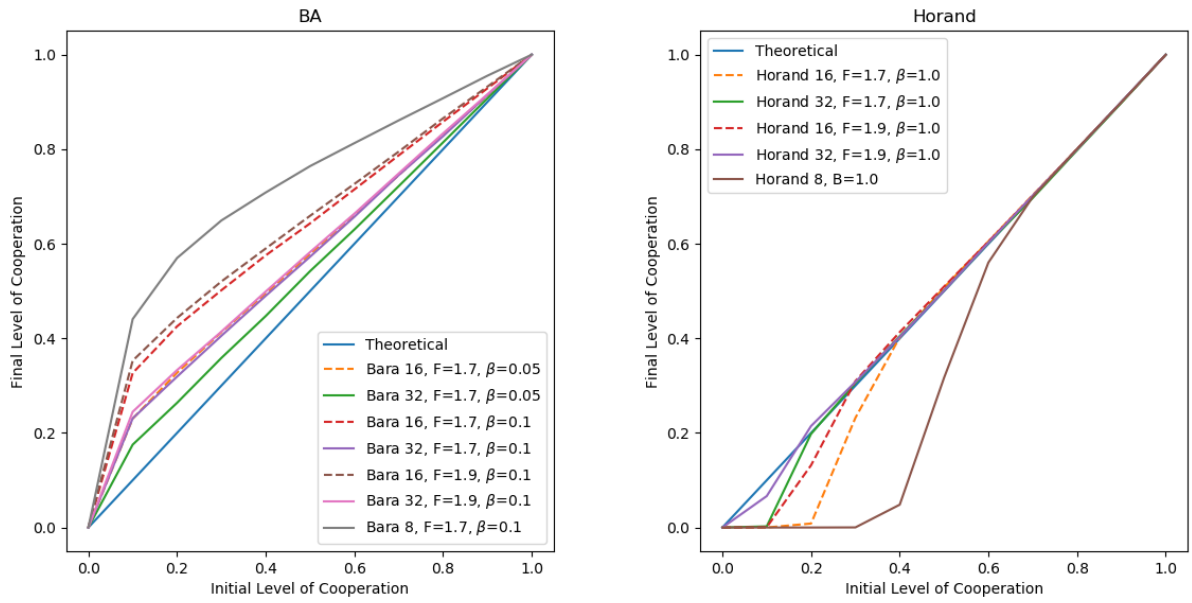

Figure C-6- Final Level of Cooperation as a Function of initial One. Each network has 1000 nodes (N), $\langle k \rangle = 4$. Investment is distributed per game and layers in the multilayer were initialized with half nodes as Cooperators.

the number of layers for a fixed intensity of selection, the closer experimental curve fits theoretical one. Higher values for intensity of selection require high number of levels for experimental lines to better fit theoretical ones. This makes sense because in the exponential argument controlled of the Fermi distribution controlling the probability of strategy imitation an increase in the β value is compensated by a lower payoff variance resulting from a higher number of layers and vice-versa. Higher values of enhancement factors are particularly useful for low initial level of cooperation. Something also expectable as it is essential for the few Cooperators to hold their ground.

Theoretical and experimental lines share the same shape but the deviation between them is higher for smaller initial levels of cooperation. This is not surprising because the theoretical model is based on the approximation of a binomial distribution to a Poisson one, which is only valid for great values of $\lambda\,(=Np)$. For smaller values of initial level of cooperation, theoretical model loses validity and so it is senseless to expect an exact match between these lines.

Taking as a reference investment distribution per game criteria, for a given type of network, Bara or Horand, the number of layers determines de variance of accumulated payoff between nodes, which dictate the level of topological and criteria enslavement..

For investment distributed per game, Figure C-7 depicts the fact that for a given number of layers, 16 in this particular case, a maximum intensity of selection can be identified below which multilayer evolution is stuck to initial conditions and insensitive to variations in enhancement factor. For Horand networks, the figure shows that up to intensity factors valuing 1 and irrespective of enhancement factor, average level of cooperation does not change from initial values. Were the multilayer initialized with a different value and that same value would

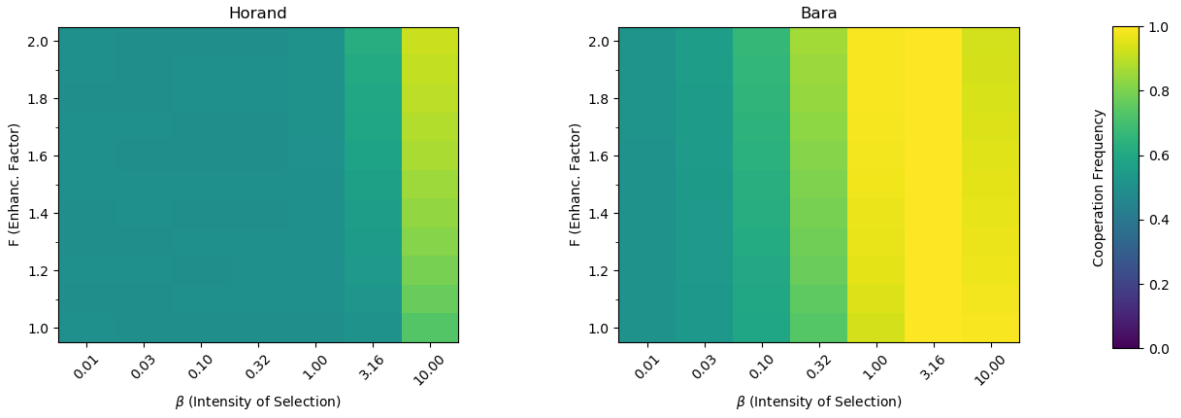

Figure C-7- Topological and Criteria Enslavement for 16-layers Multilayer, 1000 nodes (N) per layer. Multilayers are initialized with half Cooperators per layer random and independently selected.

be preserved. Moreover, if heat maps corresponding to a different number of layers are depicted, it will be noticeable that the wave front of the colour code corresponding to the initial level of cooperation with which the multilayer was initialized moves rightwards as the number of layers increase.

For a distributed investment criteria, heterogeneous networks tend to have a behaviour similar to homogeneous one, but requiring more layers to achieve the same behaviour with the same intensity of selection. For a given network type, investment per layer criteria tends to experience the same behaviour as its investment per layers counterpart, but with a higher number of layers and/or lower intensity of selection.

Defining enslavement as the condition of final level of cooperation in a multilayer with investment per game criteria differing in less than 20% from the initial level of 50% with which a multilayer was initialized, whatever the value of enhancement factor $F \in [1,2]$, Figure C-8 displays the domain of the number of layers versus intensity of selection β where enslavement rules. Were the enslavement criteria more demanding against acceptable fluctuation on the final level of cooperation, for the same number of layers a lower intensity of selection would be required.

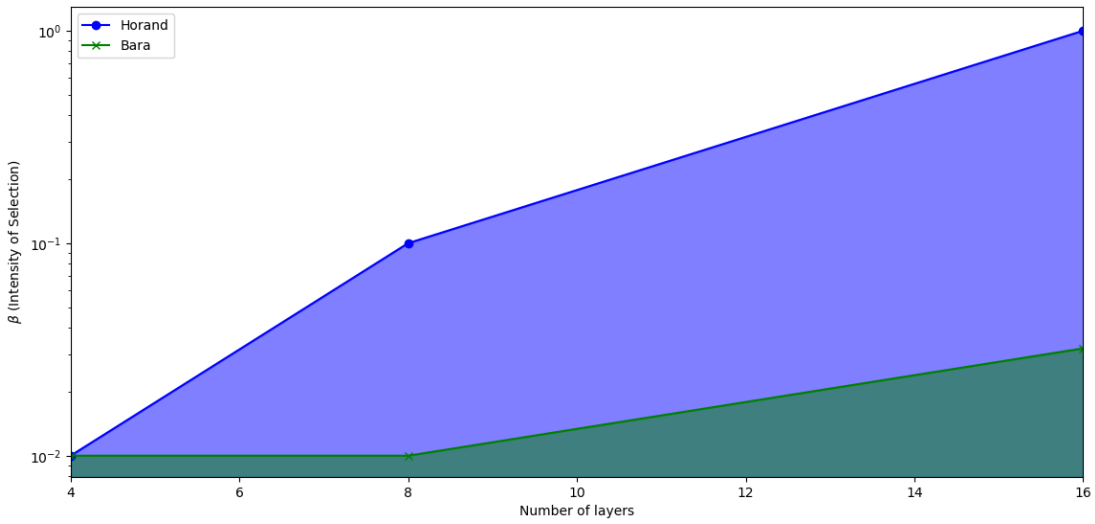

Figure C-8 - Domain of Topological Enslavement for Investment distributed per Game. Shaded areas represent the locus of number of layers l and intensity of selection β parameters such that heat map $hm_l(\beta, F)$ displaying the level of cooperation achieved in a multilayer with l layers, initialized with half nodes as Cooperators, investment distributed per game, intensity of selection β and enhancement factor F, for a given number of layer $\beta = \max_x |hm_l(x, F) - 0.5| < 0.1, \mathrm{x} \in [10^{-2}, 10], \forall\, F \in [1,2]$

Node consistency is another possible comparison perspective of confrontation between experimental and theoretical results as depicted in figure C-9. Due to the finite number of layers it must be stressed that experimental consistency evolves by *quanta* that amount to

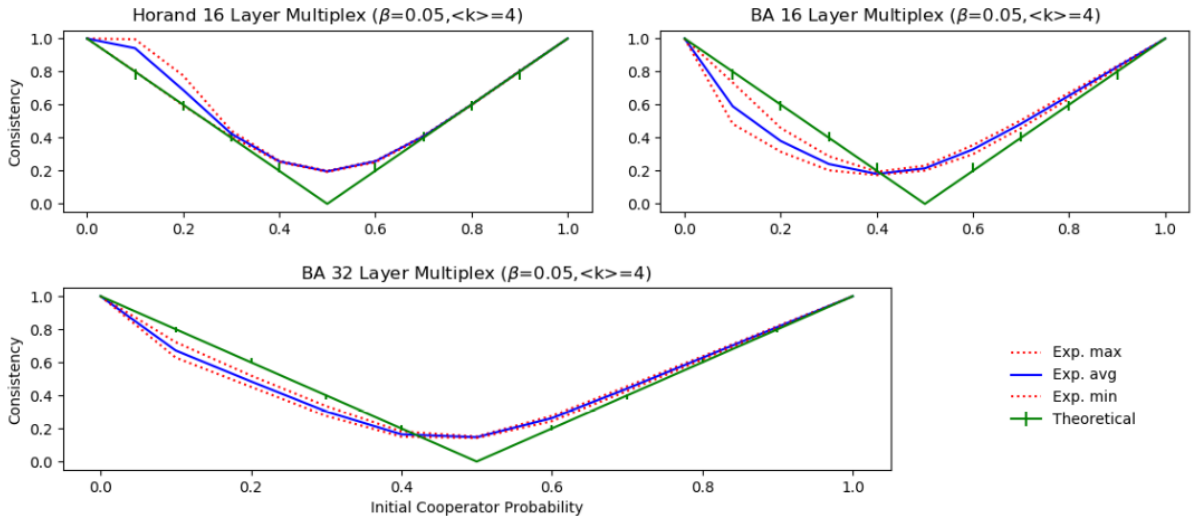

Figure C-9 - Consistency Trend in Multilayers with Investment distributed per Game. For each initial level of cooperation the usual set of enhancement factors from 1 to 2, 0.1 apart was experienced. Error bars in the theoretical green line account for the discrete jumps in consistency due to the finite number of multilayer layers, each one with 1000 (N) nodes. Experimental maximum, average and minimum consistencies due to variations of enhancement factor are plot for each initial level of cooperation.

multiples of $\frac{2}{<Number-of-Layers>}$. The error bars affecting theoretical line in the figure mark the closest possible values of consistency taking into account that the multilayers have 16 or 32 layers. For each initial level of cooperation all enhancement factors (F) multiples of 0.1 within $[1, 2]$ interval were experimented and maximum and minimum levels of cooperation were measured. As the number of layers increases, the experimental maximum, minimum and

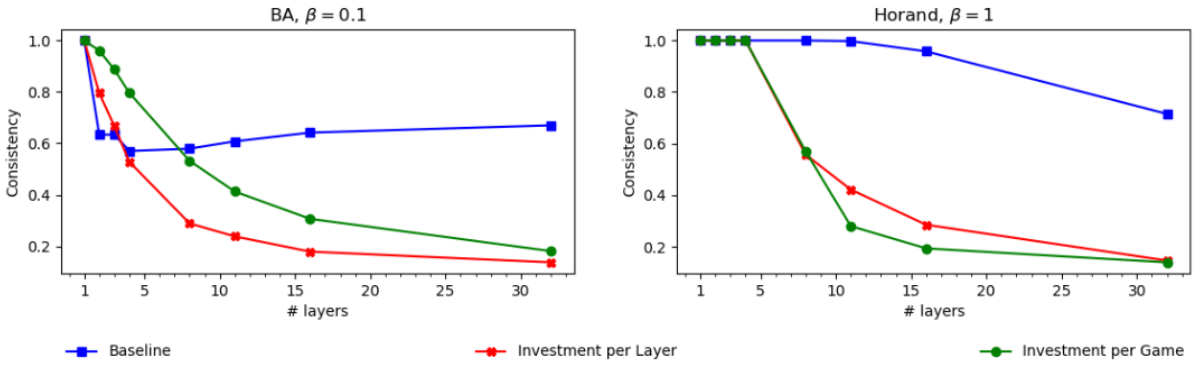

Figure C-10- Consistency in Horand Multilayers as the Number of Layers varies. F values 1.7, $\langle k \rangle$ equals 4 and all layers with 1000 (N) nodes were initialized with half of its nodes random and independently chosen as Cooperators

average lines close up, the *quanta* in two discrete consecutive possible consistency values get smaller, which means shrinking the size of error bars assigned to theoretical line, and the experimental curve gets closer to the theoretical one. The matching between experimental and theoretical curves is weaker for low initial levels of cooperation for the reasons already mentioned.

With an initial level of cooperation of 0.5 theoretical and experimental consistency lines mismatch. In order to evaluate how this mismatch evolves as the number of layers increase consistency for different network types was traced versus number of layers in the multilayer. The result is presented in figure C-10, which highlights the downward trend of consistency as the number of layers increases for distributed investment criteria, even for more unfavourable intensity of selections as the ones used.

Appendix D. Theoretical Aggregated Gradient of Selection with Distributed Investment

Aggregated Gradient of Selection (AGoS) is defined as a time-dependent indicator that captures single layer network reciprocity and reflects the expected increase in the number of Cooperators to result from next evolutionary step (Pinheiro, Pacheco, & Santos, 2012). This capture is averaged across all nodes on a large number of network instances. For a multilayer scenario, there is an AGoS per layer. If the multilayer is of type multiplex with the same set of nodes present in all layers all layers are statistically indistinguishable, it is reasonable to also consider a multilayer AGoS resulting from the average of individual layer AGoS.

Along this appendix, one derives a mathematical expression for the AGoS of a multilayer with independent instances of the same type of homogeneous network type in each layer, where Distributed Prisoner´s Dilemma is played subject to a distributed investment criteria.

The expected variation in the number of Cooperators in the multilayer to occur during next evolutionary step can result both from a Defector copying a Cooperator's strategy or vice-versa. Let us start by focusing on the first possibility. In a multilayer with M layers, a layer M_0 is randomly selected. Within this layer node n_1 is chosen. Then, a n_1's neighbour, n_2, is randomly chosen. n_1 and n_2 follow Defector and Cooperator strategies, respectively. P_1 and P_2 are n_1's and n_2's payoff, respectively.

If p represents the probability of finding a Cooperator in the multilayer, the probability of n_1 copying n_2's strategy, is given by

$$Prob(S_D \rightarrow S_C | P_1, P_2) = p\,(1-p)\frac{1}{1+\,e^{-\beta(P_2-P_1)}} \tag{1}$$

If analysis is constrained exclusively to investment per game criteria, P_1, a random variable corresponding to the accumulated payoff of n_1, a Defector node, results from the sum of two components:

$$P_1 = A_1 + \frac{F}{2}\Big(\sum_{layer\ l=1}^{M}\ \sum_{node\ i=1,\{l,i\}\neq\{M_0,n_2\}}^{<k>_l} B_i + C_1\Big) \tag{2}$$

A_1 represents the payoff n_1 receives from its own investment. It is a random variable characterized by

$$A_1 = \begin{cases} \frac{F}{2}-1 & ,with\ probability\ 1-\ (1-p)^{M-1} \\ 0 & ,with\ probability\ \ (1-p)^{M-1} \end{cases} \tag{3}$$

Last branch applies if n_1 node defects in all layers.

Bi represent the contribution for the payoff of n_1 from each of the $\langle k \rangle_l$ neighbours of n_1 in layer l with layer l = 1, …, M, excluding node n_2 in layer M_0. It is given by

$$B_i = \begin{cases} \dfrac{1}{\sum_{layer\ l=1}^{M} \langle k \rangle_{il} \delta_{CS_{il}}} & , if \sum_{layer\ l=1}^{M} \delta_{CS_{il}} > 0 \\ 0 & , otherwise \end{cases} \quad (4)$$

$\delta_{CS_{il}}$ values 1 only if node i cooperates in layer l. $\langle k \rangle_{il}$ stands for the number of neighbours of node i in layer l.

The contribution from n_2 is C_1, very similar, apart from fact that it is known beforehand that n_2 cooperates with n_1 in layer M_0:

$$C_1 = \frac{1}{\langle k \rangle_{2M_0} + \sum_{layer\ l=1, l \neq M_0}^{M} \langle k \rangle_{2l} \delta_{CS_{2l}}} \quad (5)$$

If one considers the constraint that networks are homogeneous, which means $\langle k \rangle_l = \langle k \rangle =$ k whatever the node, B_i and C_1 can be simplified to:

$$B_i = \begin{cases} \dfrac{1}{kl} & , with\ probability\ C_l^M p^l (1-p)^{M-l} \\ 0 & , with\ probability\ (1-p)^M \end{cases} \quad , l = 1, \dots, M \quad (6)$$

$$C_1 = \frac{1}{k(1+l)}\ , with\ probability\ C_l^{M-1} p^l (1-p)^{M-1-l}, l = 1, \dots, M-1 \quad (7)$$

The binomial distribution emerges because nodes are random and independently initialized across and within layers. There are in total $kM - 1$ distinct B_i variables contributing to P_1.

Taking into account that the density of the network is very small, because the average degree in each layer is much smaller than the number of nodes, B_i variables can be considered independent. Additionally, for a large number of layers, C_1 can be replaced by another B_i. So P_1 ends up being equal to

$$P_1 = A_1 + \frac{F}{2} \sum_{i=1}^{kM} B_i \quad (8)$$

As M is considered large and B_i variables are independent, its sum tends to a Gaussian distribution $N_1 = N(\mu = kM\mu\sigma_{B_i}, \sigma = \sqrt{kM}\sigma_{B_i})$ and one gets

$$P_1 = A_1 + \frac{F}{2} N_1 \quad (9)$$

B_i is well characterized so its two first moments can easy and numerically be calculated.

In what concerns P_2, the rational applied is similar

$$P_2 = \left(\frac{F}{2} - 1\right) + \frac{F}{2}\sum_{i=1}^{kM-1} B_i \tag{10}$$

There is no contribution of node n_2 to n_1 payoff in layer M_0 because n_2 defects in this layer. B_i variables in P_2 are independent between them besides being independent on the ones from P_1. Thus the variables B_i in P_2 tend to a Gaussian distribution $N_2 = N(\mu = (kM - 1)\mu_{B_i}, \sigma = \sqrt{(kM-1}\sigma_{B_i})$. Because a linear combination of independent Gaussian variables is also Gaussian, from payoffs subtraction it results

$$P_2 - P_1 = (\tfrac{F}{2} - 1 - A_1 + \tfrac{F}{2}N_3) \tag{11}$$

with $N_3 = N(\mu = -\mu_{B_i}, \sigma = \sqrt{(kM-1) + kM}\sigma_{B_i}) \approx N(\mu = -\mu_{B_i}, \sigma = \sqrt{2kM}\sigma_{B_i})$

One is now in conditions to express the expected increase in the number of Cooperators, given level of cooperation p:

$$E(Increase\ of\ 1\ cooperator) = \sum_{Prob(P_1)Prob(P_2)} Prob(S_D \to S_C|P_1, P_2) \tag{12}$$

with

$$Prob(S_D \to S_c|P_1, P_2) = p\,(1-p)\frac{1}{1 + e^{-\beta(P_2 - P_1)}} \tag{13}$$

By simply exchanging variables,

$$E(Increase\ of\ 1\ cooperator) = \sum_{Prob(A_1)Prob(N_3)} Prob(S_D \to S_C|A_1, N_3) \tag{14}$$

Reciprocally to what was performed here above, the probability of Cooperator n_x with P_x payoff copying Defector n_y's strategy with P_y payoff, is given by

$$Prob\big(S_C \to S_D|P_x, P_y\big) = p\,(1-p)\frac{1}{1 + e^{-\beta(P_y - P_x)}} \tag{15}$$

Although independent, P_x has the same distribution than P_2. Moreover, being also independent, P_y has the same distribution than P_1.

Thus, the expected decrease in the number of Cooperators, given level of cooperation p, is:

$$E(Decrease\ of\ 1\ cooperator) = \sum_{Prob(\overline{A_1})Prob(\overline{N_3})} Prob(S_C \to S_D|\overline{A_1 N_3}) \tag{16}$$

The bar on top of the variable is just to stress that variable is independent than the one without bar, but sharing the same distribution of probability.

Finally the theoretical AGoS is given by

$$AGoS = E(Increase\ in\ 1\ cooperator - E(Decrease\ in\ 1\ cooperator) \quad (17)$$

The numerical calculation of the expression just obtained leads to figure D-1, applicable to networks with $\langle k \rangle$ equal to 4.

It must be stressed that in order to reach these results a number of assumptions were considered. They were: (i) number of layers must be high, such that the probability of a node initialized with defection in all layers is minimum and the number of B_i variables is high enough to be approximated by a Gaussian distribution; (ii) the network must have a low density of edges so that B_i become independent; (iii) degree of the nodes must fixed and (iv) investment be distributed by game.

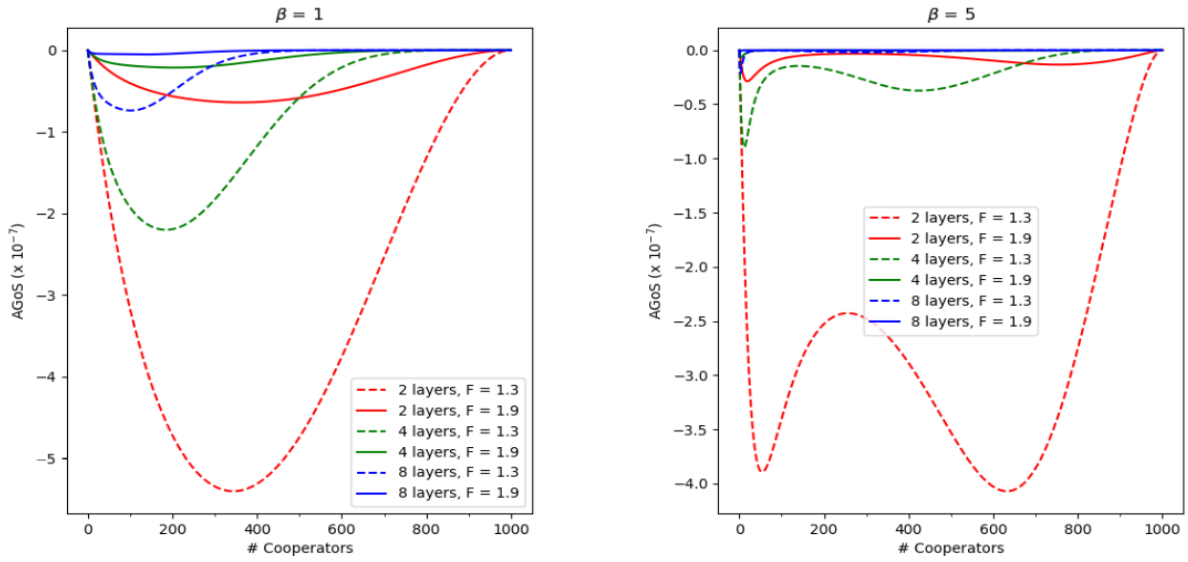

Figure D-1- Theoretical AGoS for Horand Networks in Multilayers with Investment per Game Criteria
Every single layer has 1000 (N) nodes

What theoretical AGoS highlights with its minimum magnitude is that for multilayer in these conditions the number of Cooperators in the multilayer is not expected to change over time, whatever the initial conditions. This is what explains the topological and investment criteria enslavement.

The conclusions reached for investment distributed per game are obviously extended to investment distributed per layer in homogeneous case. It is just a matter of intensity of selection scaling. Experimental results show that conclusions can also be extended to heterogeneous networks.

Appendix E. Multilayers with different Types of Networks

In the main body of the document, multilayers were considered of independent layers supported on network instances of a single type. Here we drop second constrain: layers are still independent but need to more to share network type. Figure E-1 presents results collected from a multilayer with half layers as Horand, another half as BA.

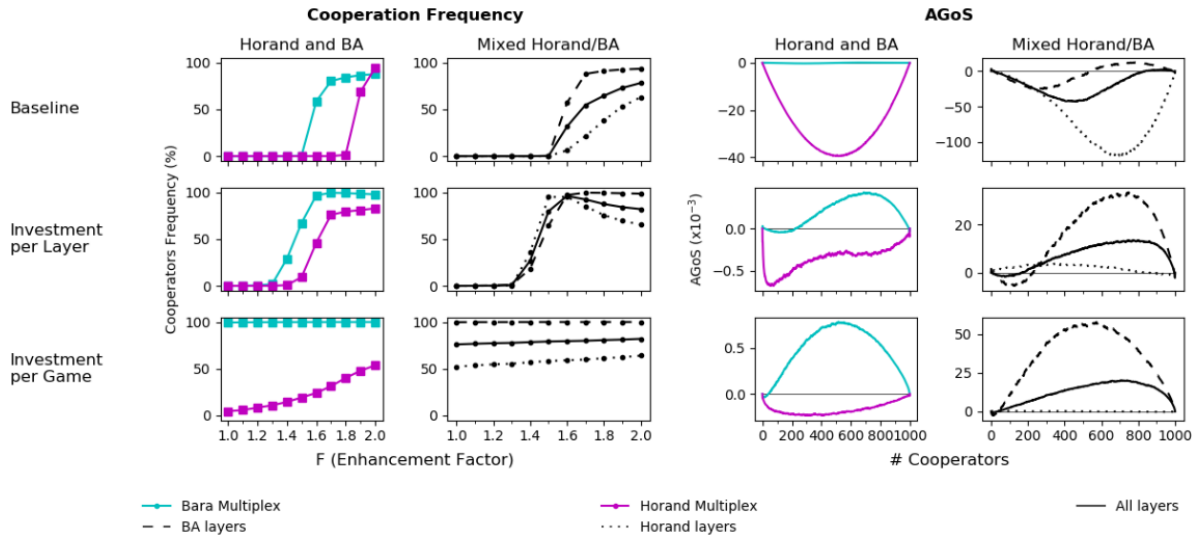

Figure E-1- Multilayer with 8 layers BA or Horand vs. Mixed Multilayer with 4 layers Horand plus 4 layers BA. Level of cooperation and AGoS for pure 8-layer Horand and BA multilayer are compared with a mixed multilayer with half layers with Horand networks and the other half with BA networks. AGoS lines were calculated for intensity of selection $\beta = 1$, enhancement factor $F = 1.6$ and 1000 (N) nodes per layer. Layers were independently initialized with half individuals as Cooperators or a number of Cooperators given by a random variable uniformly distributed between 0 and 1000, inclusive, depending on the level of cooperation or AGoS being calculated, respectively.

Lines for single network type multilayers were recovered from graphics previously traced on document main body. Pure BA multilayers are more cooperative than Horand ones. In particular for enhancement factor $F = 1.6$ and baseline criteria, Horand only 8-layer multilayer is defective. However, in the mixed scenario and due to contributions to accumulated payoff received from of some BA layers cooperation becomes feasible. As a general rule, the behaviour of the mixed multilayer is positioned somewhere between behaviours of pure ones.